Alma Mater Studiorum - Università di Bologna

DOTTORATO DI RICERCA IN

Biologia Cellulare e Molecolare

Ciclo XXX

Settore concorsuale di afferenza: 06/A2

Settore scientifico disciplinare: MED/04

"The Impact of MYC Modulation on Epithelial Cancer Evolution"

Presentata da:

Dott.ssa Manuela Sollazzo

Coordinatore del Dottorato

Prof. Giovanni Capranico

Relatrice

Prof.ssa Annalisa Pession

Correlatrice

Dott.ssa Daniela Grifoni

Esame Finale Anno 2018

CONTENTS

GENERAL INTRODUCTION

The ability to proliferate and participate in several cellular processes, such as morphogenesis, wound healing and adult tissue maintenance, can make cells gain access to a level of genomic information that is normally denied, allowing them to subvert the functions of normal tissues [1]. During carcinogenesis, deregulation of several cellular and enzymatic processes is observed, and specific alterations have been characterised for many types of cancer [2]. It is now largely accepted that cancer onset and progression are the result of genetic and epigenetic changes in a subset of cells that acquire advantageous phenotypes, leading to unrestrained clonal expansion. Such as it happens with Darwinian evolution, frankly neoplastic cells develop from such kinds of mutant clones [3]. Therefore, tumour-forming cells are the result of a development gone awry[1]. Two classes of genes, essential to fundamental physiological processes (cell cycle regulation, DNA damage repair, control of cell polarity, endocytic pathways), are involved in tumourigenesis: **oncogenes** and **tumour suppressor genes** (TSGs). Dominant, gain-of-function (GOF) mutations lead to high protein production or increased protein activity, while TSGs are generally inactivated by loss-of-function (LOF) mutations [4]. About 90% of human cancers have an epithelial origin, and the first genetic alterations usually cause local hyperplasia, dysplastic growth and subsequent evolution to an *in-situ* carcinoma, whose cells are confined within the basement membrane (BM). Subsequently, tumour mass starts to suffer from hypoxia and secretes soluble factors that activate the stromal endothelial cells. In time, tumour cells secrete molecules able to degrade the basement membrane (BM) and begin to spread in the underlying compartment, where they can enter lymphatic or blood vessels and move away from the primary site. Finally, cancer cells can seed micro-metastases that in time may develop into secondary lesions [1]. This multi-step process, in which a series of subsequent mutations guides cell transformation, is complicated by the involvement of the microenvironment (Fig. INTRO 1) [5–7]. Furthermore, studies performed in murine tumour models showed intra-tumour functional and phenotypic heterogeneity: different sections of the same tumour displayed cells with distinct growth rates, metabolism and metastatic potential [8].

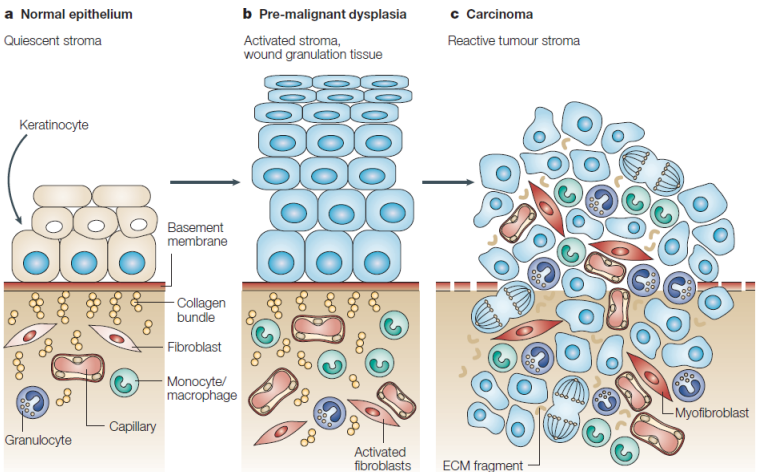

Figure INTRO 1 | Stromal contribution during tumour progression [7].

THE HALLMARKS OF CANCER

To better define the complex biology of cancer, Hanahan and Weinberg classified and described the main characteristics of cancer cells (Fig. INTRO 2).

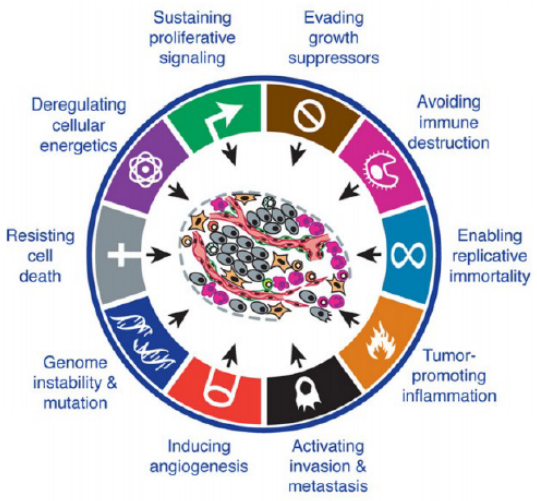

Figure INTRO 2 | Phenotypic traits of cancer cells [9].

The phenotypic traits of cancer cells include six main biological abilities acquired during tumourigenesis. They represent the first level of tumour complexity [9].

Sustaining Proliferative Signalling

The most obvious capacity of a cancer cell is an uncontrolled proliferation. Normal tissues release and control production of growth-promoting signals, which promote access and progression into the cell cycle, ensuring the maintenance of cell homeostasis and the normal architecture and function of tissues. Due to deregulation of these signals, tumour cells cater for their own sustenance. Growth factors (GFs) are essential molecules in signal activation; they bind their receptors at the cell surface, turning on intracellular signalling pathways involved in cell cycle control (an increase of cell size and cell survival) and metabolic reprogramming [4,9]. Tumour cells acquire the ability to sustain proliferative signals through some alternative ways: they can produce GFs by themselves and may respond by expressing related receptors, resulting in the stimulation of an autocrine proliferation [10]; otherwise, cancer cells can stimulate tumour-associated stromal cells to supply them with GFs [11]. Several studies have shown an active role of normal stromal cells in tumour growth and cancer cell dissemination [12]. The signalling pathways can also be deregulated by receptor hyper-expression on the tumour cell's surface or by structural aberration of receptor proteins, leading to a constitutively activated signalling [9]; activation of downstream cytoplasmic circuits is also responsible for sustained proliferation: a central role is played by the RAS/RAF/MAPK cascade, altered in 25% of human tumours [13].

Evading Growth Suppressors

To be completely independent of cell's regulatory systems, cancer cells must also circumvent the anti-proliferative signals dedicated to cell quiescence and tissue homeostasis. The anti-proliferative signals can act on cell cycle in two ways: they may allow cells to enter a reversible quiescent state in which they cannot divide (G0), or they may induce cells to differentiate [4]. Many TSGs are involved in the regulation of cell growth and proliferation. The *RB* (retinoblastoma-associated) and *TP53* genes are the two most important TSGs, which act as key regulators of cell proliferation or, alternatively, activate senescence/apoptotic death programmes. The pRb protein integrates anti-proliferative signals from the extracellular environment, while the TP53 protein operates as a stress sensor, detecting intracellular dysfunction. In a normal condition, when the TP53 circuit is active, the cell cycle is stopped; cells try to repair the damage but, if they fail, apoptotic mechanisms are triggered. *TP53* is often mutated in cancer cells: stress signals are not adequately transmitted and cells continue to divide [14]. Therefore,

mutations in these two genes have deep consequences in cell's capacity to respond to alarm signals, ultimately resulting in uncontrolled growth induction [9].

Resisting Cell Death

Apoptosis represents an important biological phenomenon in homeostasis regulation. It is activated by intracellular physiological stress (irreversible DNA damage, low oxygen levels, proliferative signal shortage) or by extracellular signals (loss of cell-cell or cell-matrix interactions, unbalance between pro-apoptotic and proliferative factors in the surrounding environment) [15]. In the '70s, massive apoptotic phenomena were observed in overgrown cells, and this led to the hypothesis that programmed cell death may be used by tissues as a barrier against tumour development [16]. Cancer cells have developed a number of strategies to overcome apoptosis, such as LOF of *TP53*, that is mutated in about 50% of human tumours [14]. Alternatively, tumour cells can increase anti-apoptotic (Bcl-2, Bcl-xL, Bcl-w) and pro-survival (Igf-1, Igf-2) gene activity and/or they can down-regulate pro-apoptotic genes (Bax, Puma, Bin) [4,9].

Enabling Replicative Immortality

The traits so far described are not sufficient to explain uncontrolled cell proliferation, as the replicative potential of a cell is limited: cells divide a definite number of times, after that, they stop growing and enter irreversible senescence [17]. In cancer, *TP53* or *Rb* inactivation permits cells to proliferate until they undergo massive cell death, along with a random acquisition of replicative immortality [4,9]. In physiology, the replicative cycles are not endless, due to telomere shortening and attrition. Telomeres represent the chromosome ends and play a protective role on DNA. A ribonucleoprotein enzyme, the telomerase, is able to extend telomeres but, in normal cells, its activation is not sufficient and at each cell cycle a part of the telomeric sequences is lost. When telomere reaches a minimum length, cells enter senescence. Tumour cells gain the ability to replicate unlimitedly by maintaining high levels of telomerase: about 90% of tumour cell lines indeed express high rates of this enzyme [17–19].

Inducing Angiogenesis

Due to cancer cell hyper-proliferation, oxygen and nutrients become insufficient to sustain the growing mass. This condition triggers an angiogenic switch: normally, quiescent vascularisation proliferates and spreads new vessels, penetrating the tumour and

supplying it with oxygen and nutrients. A sustained angiogenesis allows tumour cells to access the bloodstream and metastasise at distant sites, an essential characteristic of cancer progression. Vessel formation is usually activated by tumour cells through the secretion of pro-angiogenic factors: VEGF (*Vascular Endothelial Growth Factor*) and FGF (*Fibroblast Growth Factor*), responsible for regulating vascular growth even during development and wound healing. VEGF plays an essential role in cancer for its ability to change endothelial permeability, by activating the MAP kinase signalling pathway (MAPK) [4,9]. In addition to canonical angiogenesis, also known as "sprouting angiogenesis"**,** at least four other mechanisms are known, still poorly studied: a pre-existing vessel can split into two or more minor calibre vessels due to mechanical forces resulting from the invagination of neo-formed capillaries, a phenomenon known as "intussusception"; in "vascular co-option", tumour cells grow wrapped around the resident vessels instead, thus benefiting from direct oxygen and nutrient release; cancer cells can also form vessel-like structures in a process called "vascular mimicry"; finally, tumour cells can trans-differentiate into endothelial-like cells and contribute to the formation of vascular structures, a process called "trans-differentiation". The last three vessel formation strategies are typical of cancer and are found in particularly aggressive tumours and/or in those undergone anti-angiogenic therapies [20,21].

Activating Invasion and Metastasis

The distinctive trait of malignancies is the ability to spread from the primary site to other districts through blood or lymphatic vessels. A metastatic disease considers the acquisition by cells of invasive and migratory capabilities. A typical alteration of the invading cells is the decrease of E-cadherin expression, a key molecule in cell-cell contact and in proper formation and maintenance of the epithelium. In human carcinomas, E-cadherin down-regulation has often been associated with invasion. In addition to this, molecules that are normally expressed during organogenesis and cell migration have been found up-regulated in tumour cells (as an example N-cadherin, physiologically essential in neurons and mesenchymal cells during organogenesis) [22,23]. Essential to cancer cells is the "epithelial-to-mesenchymal transition" (EMT) programme, through which cells change their structure and acquire invasive abilities. The EMT process is normally activated in response to a proliferative signal linked to migration capacity, such as during wound healing. The junctional and structural collapse, the release of lytic enzymes, especially the metalloproteases (MMP), dedicated to the extracellular matrix (ECM)

degradation, and the motility increase, allow cancer cells to invade, enter circulation and colonise other organs and tissues. In the new site, these cells can be eliminated by intrinsic tumour suppression or reside in a quiescent state, known as "dormancy", until the conditions are favourable to proliferate again [4,9].

The analysed traits represent specific capabilities that cancer cells acquire to proliferate, survive and disseminate. In the last decade, many studies suggested that two emerging traits are also involved in tumour progression: the ability of cells to reprogramme their metabolism and the escape from the immune system. The acquisition of every characteristic is finally helped by two additional promoting features: genomic instability and inflammation (Fig. INTRO 3) [9].

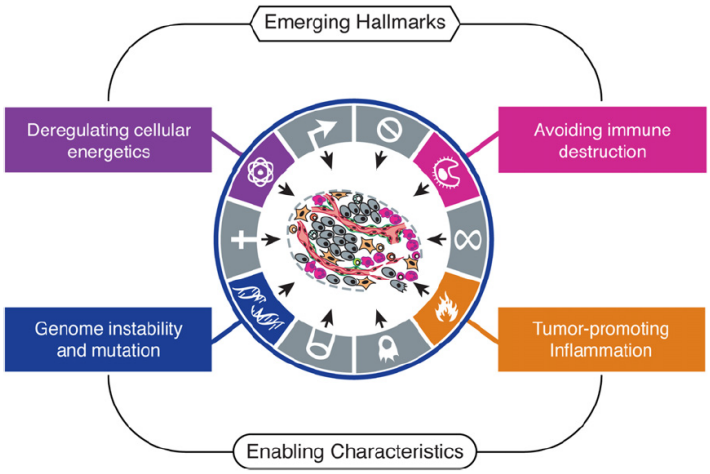

Figure INTRO 3 | Emerging hallmarks and enabling characteristics of cancer cells [9].

Deregulating Cellular Energetics

In aerobic conditions, normal cells process glucose in the cytoplasm through glycolysis (glucose is transformed into pyruvate) and, subsequently, in the mitochondria through the oxidative phosphorylation (pyruvate is released as a carbon dioxide molecule and this process leads to the production of 36 ATP molecules). In anaerobic conditions instead, mitochondrial oxidation cannot occur, and pyruvate is partially oxidised and transformed into lactate with the production of 2 ATP molecules. In 1956, Warburg observed that tumour cells reprogrammed their metabolism towards the use of glycolysis even in the presence of oxygen. This phenomenon is known as aerobic glycolysis or "Warburg effect" [24]. In cancer, this metabolic switch is partly provoked by the glucose transporter (GLUT1) up-regulation, that increases the intra-cytoplasmic glucose afflux. Moreover,

the most typical cell alterations (such as RAS oncogenic activation, MYC up-regulation and *TP53* LOF mutation) support glycolysis: MYC and TP53 regulate glycolysis and oxidative phosphorylation respectively; in addition, RAS constitutive activation can increase the Hypoxia Inducible Factor (HIF) levels that, together with cancer cell's peculiar hypoxia, up-regulate the glycolytic process [25]. It is now asserted that tumour mass is a complex tissue, constituted by non-cancer and cancer cells interacting with each other. With the increase in mass, some internal cells, more distant from the vascular system, suffer from hypoxia and are subject to the Warburg effect. They release lactate as a waste product, which is used by the most peripheral cells as the main source of energy. The two cell populations cooperate in a symbiotic manner to support cell proliferation. The basis of this phenomenon, known as "metabolic commensalism", are still poorly characterised [9,26,27].

Avoiding Immune Destruction

During cancer formation, a still unclear aspect is the role of the immune system. The immune surveillance theory proposes that it checks and eliminates the most part of the rising tumour cells. According to this concept, the succeeding solid tumours should have managed to limit the immune response control, eventually avoiding suppression. The immune evasion seems to be confirmed by the increasing of virus-induced tumours in immunocompromised individuals [9,28]. Besides, experiments conducted in genetically modified mice and epidemiological studies suggest that the immune system operates as a barrier also during formation and progression of some non-viral cancers. Furthermore, it was observed that highly immunogenic cancer cells were usually eliminated in immunocompetent hosts, a phenomenon called "immunoediting". Less immunogenic tumour cells persist in the tissue and can successively colonise both immunocompetent and immunodeficient hosts. Contrariwise, when immunogenic cancer cells are transplanted in an immunodeficient host, they can undertake unimpeded proliferation. Tumour cells are thus eliminated from the tissues when confronted with the immune system of the host for the first time [29–31]. Clinical epidemiology supports the existence of anti-tumour immune responses in some forms of human cancers [32,33]. All these argumentations try to elucidate the strategies that tumour cell use to evade the immune system components, but the evidence is still rudimentary and, for this reason, it is considered an emerging trait [9].

Genome Instability and Mutation

Tumour progression is often represented as a succession of mutations conferring growth and expansion capabilities to cells. Damage detection and repair ensures proper maintenance of tissue homeostasis, and the spontaneous mutation rates are usually very low during cell division. Tumour cells often increase the mutation rates to trigger tumour processes [9,34]. Cells must segregate their intact genetic material into daughters. When this process goes awry, genic and genomic alterations such as chromosomal translocations and/or aneuploidies occur. Genomic instability can initiate cancer in different ways: telomere attrition, centrosome amplification, epigenetic modifications and DNA alterations [35,36]. In the last twenty years, substantial progress has increased the understanding of gene functions involved in genome integrity maintenance (for example, *TP53*). The behaviour of these genes is like that of TSGs, so, during tumour progression, their function can be lost through both inactivating mutations and epigenetic silencing [37]. Moreover, telomeric DNA damage generates karyotypic alterations such as amplification and/or deletion of chromosomal segments [38]. In cancer cells, the rate of DNA damage is high, and damaged cells are more susceptible to the onset of new mutations. Genomic instability can confer a selective benefit to pre-cancerous cells: some mutations can help cells proliferate, expand and adapt to different microenvironments; for this reason, DNA damage is considered an enabling characteristic [9].

Tumour-Promoting Inflammation

It is well known that tumours are composed of different cell types, including the immune system cells [33]. This picture reminds the inflammatory state of non-tumour tissues. Already in the '80s, Dvorak defined cancer as "a wound that never heals" [39]. The inflammatory response was attributed to the attempt of the immune system to eradicate tumours, but it has successively been recognised as an enabling trait providing cells with growth, survival and angiogenic properties, and with signal molecules that trigger EMT, invasion and metastasis [40,41]. Furthermore, inflammation cells can contribute to genomic instability by releasing Reactive Oxygen Species (ROS) [9,40].

DROSOPHILA CANCER MODELS

As previously described, cancer is a complex disease affecting many organs, and its onset is driven by the accumulation of mutations and epigenetic changes. The complicated pathological picture reveals the need to use simple animal models to study the many alterations that contribute to cancer progression. The signalling pathways and regulatory system conservation between humans and flies have made *Drosophila melanogaster* a suitable model for cancer studies [42,43]. Since the beginning of the XX century, *Drosophila* has been used to study biological complex processes, thanks to the simple use and breeding in the laboratory (its life cycle is completed in 10 days at 25°C) (Fig. INTRO 4), and to the availability of genetic manipulation techniques that allow the induction of cancer in a normal organ *in vivo* [44]. In the '70s, the first tumour-related mutation has been found in *Drosophila* [45] in a sub-telomeric *locus* on the second chromosome left arm, subsequently associated with the *lethal giant larvae* (*lgl*) gene [46].

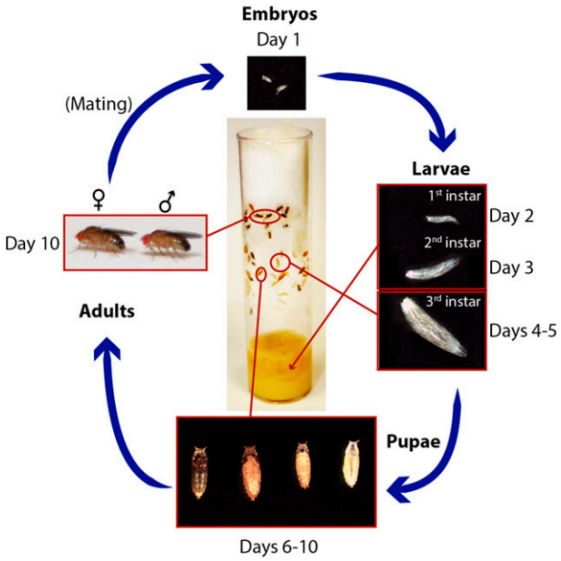

Figure INTRO 4 | **The life cycle of *Drosophila melanogaster***. At 25°C the cycle is completed in 10 days. The progeny is very abundant. Embryogenesis happens inside the egg shells, and 24 hours after egg laying (AEL) three larval stages follow (L1, L2, L3) during which larvae increase their size. Finally, metamorphosis occurs during the pupal stage and the adult, or *imago*, emerges at day 10 [47].

Later, other TSGs functionally conserved in mammals have been identified. Fundamental developmental processes are highly preserved, such as organogenesis, nervous system formation, cell proliferation control, vessel formation and oxygen transport; this has allowed the identification of the mechanisms that govern tumour biology [42,48].

The *Drosophila* Nervous System as a Model for Brain Cancer

Although the clear anatomic divergence between humans and flies, the nervous system development and its cellular lineages show many similarities. In the adult fly, many mature neural cells, such as the motor neurons and the interneurons, have an embryonic origin [49]. During the larval and pupal stages, a large number of neurons and mature glia are specified. The central nervous system (CNS) of L3 larvae develops from progenitor cells, the **neuroblasts** (NBs), comparable to the human neural stem cells, and is formed by two brain hemispheres connected by the **ventral ganglion** (VG). Each hemisphere is divided into two regions: a medial area contiguous to the VG, called **central brain** (CB), and a lateral region, the **optic lobe** (OL), dedicated to the vision (Fig. INTRO 5) [50].

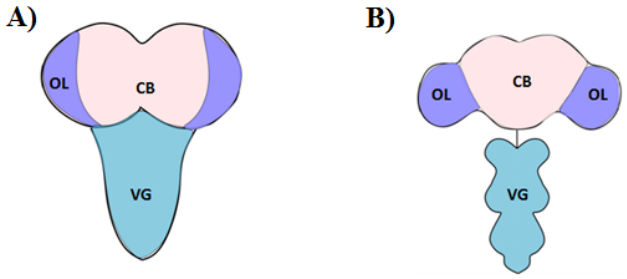

Figure INTRO 5 | Larval (A) and adult (B) CNSs schematic representation. Optic Lobe (OL), Central Brain (CB) and Ventral Ganglion (VG) are highlighted (original drawings by Simona Paglia).

The NBs, progenitors of the mature neurons and glia, originate from the embryo neuroepithelium. The neuroepithelial (NE) cells divide symmetrically expanding the progenitor pool. Successively, some cells begin a differentiation programme and delaminate, becoming NBs [51]. The NBs divide asymmetrically at any stage, and each of them originates two daughter cells: apically, a cell that preserves NB's identity and self-renewal capacity, and basally a small cell, named Ganglion Mather Cell (GMC) which, following a single division, differentiates into two neurons or two glial cells. Each hemisphere of the *Drosophila* CB contains about 100 NBs, subdivided into type I and II, differing in gene expression and lineages [52,53]. Type II NBs are an attractive model to study the molecular networks involved in cell fate determination because their lineage resembles that of mammalian stem cells [54]. Type II NBs constitute a small population (only 8 NBs/hemisphere) and divide asymmetrically into a NB and a smaller daughter cell, called Intermediate Neural Progenitor (INP). Successively, the immature INP becomes mature through a process dependent on Brat and Numb activity; after an

additional division cycle, the mature INP generates a new INP, with self-renewal ability, and a GMC (Fig. INTRO 6) [55].

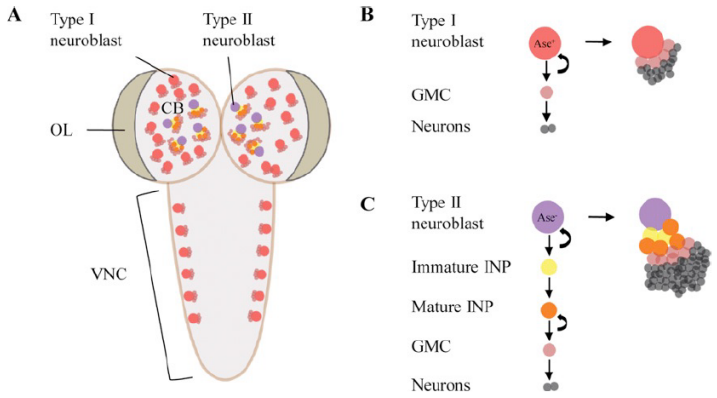

Figure INTRO 6 | Neuroblast lineages in the *Drosophila* larval brain [56].

Mammalian neural stem cells generate *transit-amplifying cells*, that divide transiently and exist for a short period before terminal differentiation [54,57]. Many genes, implicated in neuronal development and cancer, are evolutionarily conserved between humans and *Drosophila.*

The multiple analogies with the human CNS make the fruit fly an excellent model to study both neurodegenerative pathologies (such as Alzheimer's, Parkinson's and SLA) and brain tumours [58]. A fly model of glioblastoma (GBM) was built by Renée Read and colleagues [59]. The authors focused on the signalling pathways altered in humans: the EGFR (*Epidermal Growth Factor Receptor*) and the PI3K (*Phosphatidylinositol-4,5-bisphosphate 3-kinase*) cascades. They simultaneously expressed the constitutively active form of PI3K and EGFR in glial cells, using a pan-glial promoter called *repo* (*reverse polarity*). This co-activation in larval glia caused neoplasia, neurological defects and lethality [59,60]. Even though this may be a good model for brain tumours, it has to be taken into account that several regions in the mammalian adult brain contain immature precursors and that brain tumours such as GBM are thought to originate from cell populations with stem properties. Alterations in the PTEN/aPKC/Lgl network have recently been associated with the GBM tumour-initiating cells [61,62]. The same axis is preserved in the *Drosophila* brain. Very recently, our laboratory showed that *PTEN* loss of function induces aPKC cortical increase and Lgl inhibition in the fly brain and, in addition, they found that the tumourigenic potential is promoted by aPKC increase

specifically in the type II NBs [63]. The genetic manipulation of this network can thus represent a good starting point for tracing GBM origin.

Drosophila Imaginal Discs as a Model for Epithelial Tumours

The *Drosophila* larval tissues are composed of larval and imaginal cells. During metamorphosis, larval tissues undergo histolysis, while imaginal tissues differentiate into the adult structures [64]. Imaginal cells are highly proliferating epithelial cells organised in structures called "imaginal discs" [65] (Fig. INTRO 7). In particular, the imaginal wing disc is composed of a pseudo-stratified columnar epithelium (disc proper) and a squamous epithelium (peripodial membrane) [66] (Fig. INTRO 8).

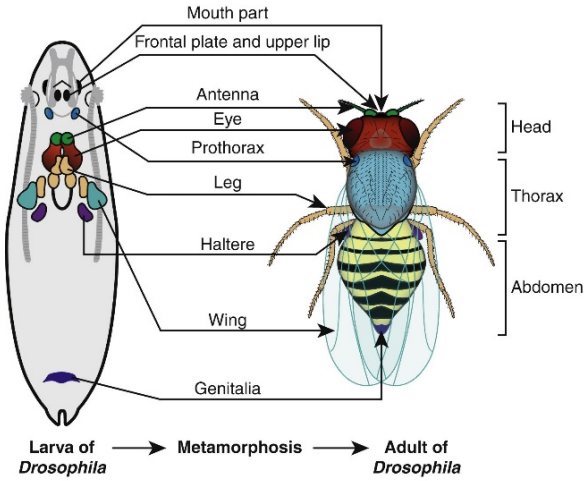

Figure INTRO 7 | Schematic representation of the *Drosophila* imaginal discs with the corresponding adult structures [67].

Imaginal wing disc structure is morphologically and biochemically comparable to mammalian epithelia, and represents a good model for growth and proliferation studies [68]. During embryogenesis, the wing disc consists of about thirty cells, known as founder cells, which proliferate throughout larval development; at the end of the larval life, about 50.000 cells compose the wing disc. The imaginal tissue differentiation into adult structures occurs by eversion [69]. To assure that imaginal wing disc development occurs properly, positional signals are needed, including the Wingless (Wg) protein, belonging to the Wnt glycoprotein family. These proteins can activate several intracellular pathways responsible for the imaginal disc formation [70]. In embryos, the wing disc starts to assemble from a group of Distalles (Dll)-expressing cells. It originates in the intersection zone between the ectodermic cells secreting Wg and the ones that release

Decapentaplegic (Dpp), the fly orthologue of the human TGF-β (*Transforming Growth Factor β*). Cells destined to become wing disc migrate dorsally and start to express Vestigial (Vg) [70]. At the end of the larval life, wing discs show a distal region, the "wing pouch", which originates the adult wing, and more proximal regions: the "hinge" will originate the structure connecting wing and thorax, and the "pleura" and the "notum" will contribute to thorax formation [71]. The wing disc is subdivided by the anterior-posterior border (A/P) into an anterior (A) and a posterior (P) compartment and, orthogonally to this, the dorsal-ventral border divides the disc into a dorsal and a ventral compartment. At the basal side of the disc, it is also possible to observe the stromal components of the wing disc: the "myoblasts", that differentiate into the adult flight muscles, and a branch of the tracheal system, the "transverse connective", which conveys oxygen to the organ (Fig. INTRO 8) [72].

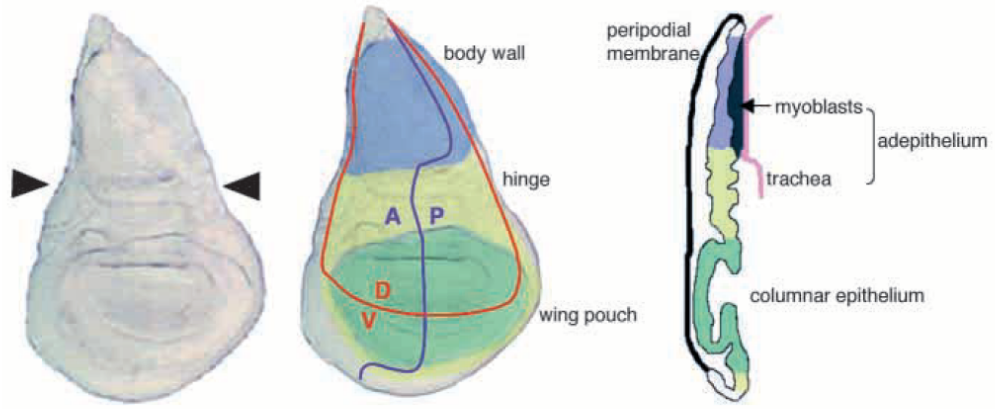

Figure INTRO 8 | Graphic representation of the territories, compartments and cell populations of the *Drosophila* larval wing disc [72].

The development of the A/P boundary is defined by the *engrailed* (*en*) gene [73], which is precociously expressed in the P compartment. Successively, En induces Hedgehog (Hh) expression, a morphogen that spreads towards the A compartment and induces *dpp* activation, encoding another morphogen which leads to the A/P border determination. At the beginning of the second larval instar, determination of the dorsal and ventral compartments occur [74] thanks to Apterous (Ap) activity, which is only expressed in the dorsal compartment. Ap activates *fringe (fg)*, which in turn induces the expression of *Serrate (Ser)*, which encodes a ligand for the Notch receptor (Fig. INTRO 9) [75].

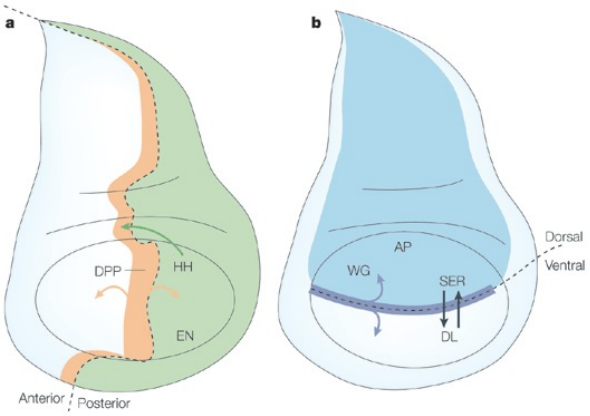

Figure INTRO 9 | Positional signals and compartment formation during *Drosophila* wing disc development [76].

To exploit their function correctly, epithelia need a close association of the cells that compose them. Cell junctions, and a correct apical-basal cell polarity, are fundamental traits that maintain epithelial architecture and function. During tumourigenesis, the tissues lose these characteristics and overturn the normal biological processes of growth and tissue organisation. The cells change their normal architecture and acquire invasive and migratory traits. For the first time in *Drosophila*, Bilder found a correlation between loss of apical-basal polarity and proliferation dysregulation [77].

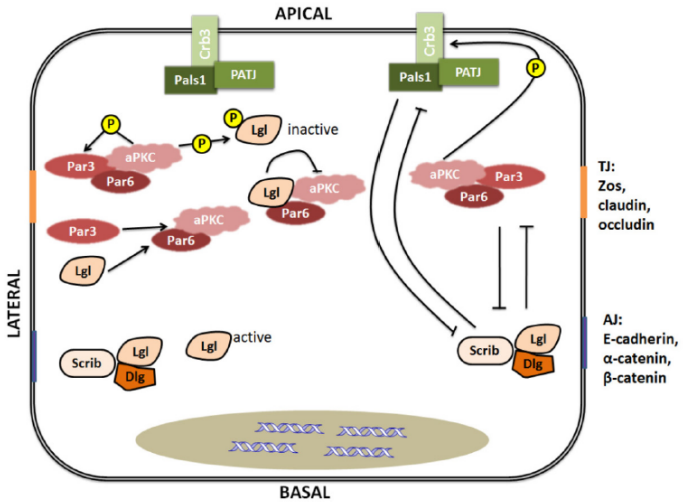

Figure INTRO 10 | The Apical-basal polarity regulation in *Drosophila* epithelial cells [84].

Three large complexes establish and maintain the epithelial polarity in the fruit fly: the **Crumbs/Stardust/PATJ/Bazooka**, the **Par6/aPKC** and the **Scribble/Discs large/Lethal giant larvae** complexes, which are respectively located at the apical, sub-apical and basal-lateral membrane (Fig. INTRO 10). Alterations in any component of these complexes cause hyper-proliferation of the epithelial cells and alterations of the imaginal tissues [46,78]. In epithelial tumours, the LOF of several genes involved in apical-basal polarity regulation has been described in both flies and mammals [79–81].

lethal giant larvae: Cell Polarity and Cancer Development

Loss of cell polarity is a distinct trait of cancer cells, as it regulates many biological processes such as proliferation, migration and transformation [82,83]. The Lethal giant larvae (Lgl) protein plays an essential role in cell polarity regulation, asymmetric division and tumourigenesis by interacting with other polarity proteins, regulating exocytosis, being involved in maintaining cytoskeleton and in several signalling pathways [84]. *lgl* is the first TSG found in *Drosophila*, and it owes its name to the fact that mutant larvae show an amazing growth of the imaginal discs and brain. Therefore, these larvae do not enter metamorphosis and die as giant, bloated animals at the end of an extremely long larval stage [85]. *lgl* encodes a 127 kDa protein, rich in WD40 domains involved in cell-cell interactions [46,86]. Lgl localisation depends on its phosphorylation state: when aPKC is at the membrane, Lgl is phosphorylated and released into the cytosol [87]. It is also known that Lgl inhibits aPKC recruitment at the basal-lateral membrane domain. Therefore, the two proteins are mutually exclusive, contributing to apical-basal polarity maintenance (Fig. INTRO 10) [77,88]. Lgl protein function is also important in neural tissues: it indeed plays a key role in the asymmetric division of the NBs. The protein is necessary for a correct localisation of cell fate determinants: *lgl* LOF provokes NBs' inability to divide asymmetrically, resulting in an accumulation of highly proliferative precursors [89]. *lgl* mutant phenotype is partially masked by a strong maternal contribution of the wild-type product, sufficient as to ensure the development of homozygous mutant individuals until the last larval stage. *lgl* mutant individuals are commonly used to study the molecular basis of epithelial transformation [46,77,78,90]: imaginal wing discs indeed display a severely altered morphology and show a considerably larger size than *wild-type* (*wt*) organs (Fig. INTRO 11) [46]. Those neoplastic tissues transplanted in *wt* flies overgrow and acquire metastatic potential [91]. Loss of cell polarity impacts on cell proliferation through deregulation of the "Hippo (Hpo) pathway", an important signalling cascade that controls organ size through proliferation and apoptosis regulation [92]. *lgl* LOF upregulates cell cycle inducers (such as Cyclin E and E2F1) and triggers nuclear translocation of Yorkie (Yki), the downstream effector of the Hpo pathway, with a consequent activation of its targets, mainly involved in growth, proliferation and resistance to apoptosis [78,93].

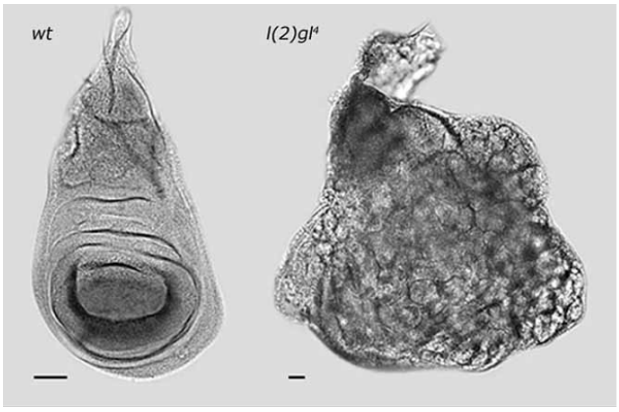

Figure INTRO 11 | Effects of *lgl* LOF: a *wild-type* imaginal wing disc (on the left) and an *lgl* mutant wing disc (on the right) [94].

The clonal behaviour of *lgl* mutation is quite different. *lgl* mutant clones induced through X-rays in *wt* individuals do not show aberrant growth and/or morphological anomalies in the adult wing [95] and they are smaller than the neighbouring *wt* twin clones. Our laboratory found that MYC oncoprotein is involved in $lgl^{-/-}$ clonal phenotype. When MYC is overexpressed in $lgl^{-/-}$ clones, it supports their growth and enables them to develop into a tumour, while *lgl* mutant cells are not able to grow in a *wt* epithelium and undergo apoptosis [96] as the result of a phenomenon known as **cell competition** (see after) [97,98].

In humans, two *lgl* orthologues have been found: *HUGL-1* and *HUGL-2* [79,80], whose LOF has been associated with many human cancers [80,99,100].

Oncogenic Cooperation

In cancer, different mutations can accumulate in the same cell and cooperate to promote neoplastic growth. In fact, in mammalian tumours, we can often observe the contemporary LOF of TSGs and aberrant activation of oncogenes. The *Drosophila* imaginal wing discs provide an excellent model for studying oncogenic cooperation, thanks to the advanced genetic tools able to mimic the onset of human cancer [42,101]. Simultaneous induction of both TSGs LOF (for example mutations in cell polarity genes such as *lgl, scrib* and *dlg*) and oncogenic activating mutations (such as constitutively active forms of Ras) in single cells is indeed possible in the fly [101,102]. Many well-characterised TSGs such as *PTEN* or Hpo pathway components and interactors, and many cancer drivers (such as EGFR, Ras, MYC, Notch, Yki) control cell proliferation and

growth during development, and are also deregulated in cancer. Surprisingly, their single activation in imaginal discs is not sufficient to trigger malignant tumours, although in some cases it causes hyperplasia [42]. By clone induction, with a combined activation of Ras signalling and LOF mutations of cell polarity genes, the Richardson and Xu laboratories showed neoplastic overgrowth of epithelial and brain tissues [101,103]. These pivotal studies demonstrated that, as it happens in mammals, TSG mutations and oncogene activation cooperate in transforming cells into malignant derivatives. Cells expressing the constitutively active form of Ras (Ras^{V12}) grow in a hyperplastic manner due to Ras ability to increase at the post-transcriptional level both MYC and Cyclin E (CycE) [104], and mutations in cell polarity genes activate Yki, the final effector of the Hpo pathway, provoking tissue overgrowth [93,105–107] and alterations in tissue architecture [46]. Also in human epithelial cancers, these mechanisms are deregulated and loss of cell polarity is frequently observed [108-110].

Activation of the PI3K signalling pathway is not sufficient to promote malignant transformation instead [101,103,111].

Drosophila Cancer Hallmarks

Thanks to the high preservation of genes and signalling pathways involved in physiology and cancer between humans and fruit flies, it is possible to describe distinct traits of *Drosophila* cancers (Fig. INTRO 12) in order to clarify and highlight new molecular aspects of cancer, and to suggest new and innovative therapeutic strategies.

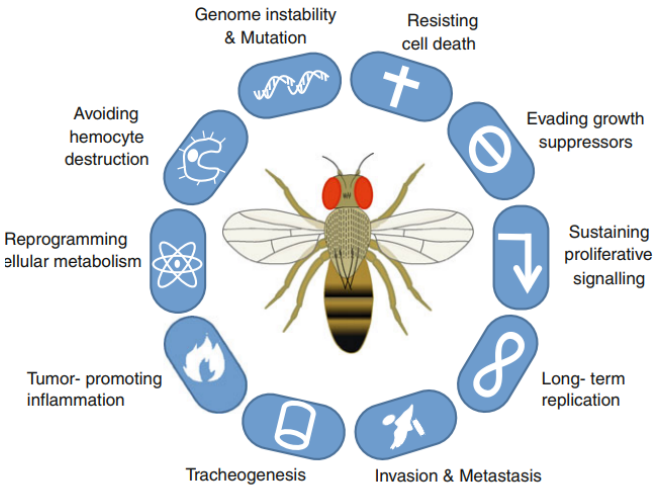

Figure INTRO 12 | *Drosophila* cancer traits [112].

Sustained Proliferative Signals, Anti-Proliferative Stimuli Evasion and Cell Death Resistance

In *Drosophila,* mutations in the Hpo signalling cascade promote growth and proliferation and also inhibit cell death by CycE and DIAP1 (*Death-associated inhibitor of apoptosis 1)* hyper-expression respectively [113]. The constitutive activation of signalling pathways such as Ras/Raf/MAPK, PI3K, JAK (*Janus Kinase*)-Stat and Dpp, and MYC up-regulation, induce growth and uncontrolled cell proliferation [48] but also trigger apoptosis in epithelial models. Apoptosis evasion is an essential requirement of tumours both in mammals and in *Drosophila*. Different signals can allow limiting cell death: in addition to the Hpo pathway, Dpp was found involved in apoptosis control by modulation of *bantam* miRNA [114]. *bantam* limits *hid* (one of the three pro-apoptotic genes in *Drosophila*) activation: when overexpressed, Hid protein levels result very low [115]. *bantam* also promotes proliferation by stimulating cell growth and cell division [116]. Moreover, the EGFR/Ras/MAPK pathway limits apoptosis [104]: Hid is directly inhibited by Ras signalling [117] and, indirectly, through EGFR-dependent *bantam* expression [118]. *Drosophila* development studies have revealed that cell growth and cell death are strictly interconnected: during tissue growth, unfit, stressed and damaged cells are eliminated, and apoptosis-induced proliferation occurs to compensate for cell loss. Dying cells secrete mitogenic signals that induce cell proliferation [114]. These cells also activate JNK (c-Jun N-terminal Kinase) signalling, which induces MMP1 expression and EMT, supporting cancer formation [42].

Invasion and Metastasis

During cancer progression, cells acquire the capability to migrate and invade surrounding tissues. Several models recapitulate these traits in *Drosophila*. Transplantation of brain and epithelial cancer fragments (*lgl, dlg* and *scrib* mutants as an example) in the abdomen of adult flies results in the formation of secondary tumours in thorax, brain, wings, muscles, intestine and ovaries [91]. The oncogenic cooperation between mutations of polarity genes and Ras^{V12} triggers invasive and metastatic tumours [101] through JNK signalling induction. The JNK cascade triggers apoptosis (blocked by Ras activation) and MMP1 secretion, crucial to matrix degradation and to provide cancer cells with invasive potential [103,119]. The same properties have been observed in intestinal cells [120].

Genomic Instability

Genomic instability is a common trait of cancers. In *Drosophila*, defects in the cell cycle, exposure to DNA damaging agents, telomere loss and centrosome alterations can provoke genomic aberrations (such as aneuploidies) which sometimes allow cells to escape apoptosis, resulting in tumour formation [121-123]. Moreover, in *Drosophila* tissues, genomic instability triggers the JNK cascade that addresses cells to apoptosis programmes [122]. This mechanism may suggest new hints on tumour suppression [42]. Moreover, epigenetic studies indicate that histone modifications may drive cancer onset in the fly [124,125].

Tumour Metabolism

In *Drosophila*, the energetic metabolism is regulated by the TOR protein kinase and Insulin pathways [126]. Hyper-activation of the Insulin signalling provokes nutrient accumulation in the fat body [127], where TOR controls the release of Insulin-like peptides from the Insulin-producing cells of the brain, working as a sensor for the amino acid concentration in the haemolymph [128]. Tumour risk increases in patients with metabolic syndrome, and *Drosophila* is used as a model to study diet effect on cancer progression: high levels of glucose increased malignant tumour formation, accompanied by insulin resistance [129]. Also, Ras/SRC-dependent tumours evaded the effects of ImpL2 (homologue of Insulin Growth Factor Binding Protein, IGFBP, in mammals), an antagonist of the PI3K/AKT/TOR cascade, by Insulin signalling activation. Finally, models of oncogenic cooperation begin to identify enzymes involved in other metabolic cascades, suggesting an important cooperation between cancer and metabolism also in *Drosophila* [42].

Tumour-Stroma Interactions

In the host organs, the tumour is a new entity that competes with the normal tissue to grow and expand. Generally, this process leads to tumour suppression, but when something goes wrong, cancer cells recruit several components of the microenvironment to support their growth, resulting in a very complex picture [130]. *Drosophila* models developed in our (unpublished data) and other laboratories [131] showed that the induction of cancer cells in epithelial tissues triggers an abnormal proliferation of the mesenchymal population. Herranz and colleagues found the malignant transformation depends on the interactions between cancer cells and the surrounding normal stromal cells [131]. Despite these preliminary findings, a stromal signature has not been defined in *Drosophila* yet.

Inflammation

Depending on the tissue context, the inflammatory process can promote or limit tumour onset. Usually, cancer cells secrete chemokines and cytokines recruiting the immune system cells [42]. In the fruit fly, tumour formation activates the JNK cascade that leads to cytokine secretion and subsequent JAK/STAT signalling activation [102,132]. The inflammation signals recruit the haemocytes (the *Drosophila* immune cells) that express Eiger (the orthologue of the Tumour Necrosis Factor, TNF, in mammals) [133]. *Drosophila* haemocytes, such as macrophages in mammals, show functional plasticity and it is supposed that, even in *Drosophila* epithelia, their activation induces proliferation and tumour growth [134].

Tumour Tracheogenesis

In the fruit flies, the circulatory system is open: the haemolymph (blood in mammals) is pumped by the heart in the body cavity and the exchanges occur directly with the internal organs [112]. An intricate network of branched and interconnected tubes conveys oxygen to the organs: the "tracheal system". This system is particularly studied for its similarities with the mammalian circulatory system [135]. We have found that the *Drosophila* tumour cells express Branchless (Bnl), the mammalian FGF, normally involved in branch morphogenesis, and suffer from oxygen shortage, as it is for mammalian tumours. This condition leads to the formation of new tumour vessels to provide cancer cells with gas exchange and nutrients. In addition, we have identified alternative strategies tumours undertake to replenish their supply of oxygen: the co-option of pre-existing tracheal branches, trans-differentiation of cancer cells into pseudo-tracheal cells and new vessel formation by cancer cells. These complex mechanisms of tumour tracheogenesis perfectly recapitulate what happens in mammalian tumours [136,137]. These new *Drosophila* cancer traits can further help the study of these complex phenomena.

MYC AND CELL COMPETITION

During normal tissue development, and in cancer, a phenomenon known as "cell competition" (CC) controls cell selection through combined proliferation and death. During normal development, MYC oncoprotein is mainly involved in cell growth and in cell death, and it has been shown to play an essential role in CC [138].

Principal Functions of MYC Oncoprotein

c-MYC is the principal member of a mammalian transcription factor family of the basic-helix-loop-helix-leucine zipper class (BHLH-LZ), with a number of functions in cell growth, metabolism and cell death. Three family members (c-, L-, N-Myc) exist [139] and the most part of MYC's transcriptional activity happens following dimerisation with its partner MAX [140]. The only *Drosophila* homologue is *diminutive* (*dm*), identified in the '30s as a spontaneous mutation, but associated with *Drosophila* MYC protein only in 1996 [141,142]. MYC/MAX dimerisation and its antagonists MAD/MXI/MNT are conserved in *Drosophila* but, as for *dm* (also called *dmyc*), only an isoform exists [142,143]. Like in vertebrates, the MYC/MAX complex binds the E-box sequence CACGTG [142]. *Drosophila* MYC protein is poorly conserved in sequence respect to its counterpart in mammals, but studies in experimental models have demonstrated its functional conservation [142,144]. *dm* mutations show growth defects: mutant embryos hatch but do not complete larval development, and die at the second larval instar [145]; the $dmyc^{P0,P1}$ hypomorphic alleles cause developmental delay, smaller fly size and a reduced cell number [146,147]. On the other hand, overexpression of MYC increases cell size accelerating the G1/S transition [98,146]. In fact, a correct MYC activity is required for an efficient cell transit from G1 into the S phase of cell cycle [145]. Also in mice, MYC protein regulates growth: *MYC* mutant mice show small body size and, unlike flies, they display differences in cell number and not in cell size [144]. Many growth defects caused by MYC down-regulation are similar to those provoked by mutations of genes encoding ribosomal proteins [148]. MYC regulates growth also through the Insulin/TOR [149–151] and ecdysone signalling [152], and its expression is in turn regulated by several pathways involved in tissue morphogenesis and regeneration, such as the Wg/WNT and Dpp cascades [139], but an important role in MYC regulation is played by the Hpo pathway [153,154]. Following Hpo signalling deregulation, Yki, the homologue of human YAP (Yes-Associated-Protein), moves into the nucleus and transcribes, in addition to *dm*, other genes involved in growth, proliferation and survival

such as *CycE*, *dIAP1* and *bantam* [155]. While an increase in MYC levels stimulates cell growth, excessive MYC production can induce autonomous cell death [156]: a really high MYC activity indeed triggers cell death in the eye and wing imaginal discs [98,157]. In *Drosophila*, the autonomous cell death depends on the activation of the three pro-apoptotic genes *hid, reaper* and *grim*, the expression of which can be directly induced by MYC [157]. Their genic products negatively regulate dIAP1 that, in turn, inhibits the Caspase cascade [158,159]. MYC pro-apoptotic function is conserved in mammals, both in development and during tumourigenesis [160–162].

Studies in *Drosophila* have revealed a pivotal role of MYC in a fundamental process involved in tissue homeostasis, repair and development of adult tissues, and also in tumour modulation: cell competition.

Cell Competition

CC is a phenomenon by which cells compare their fitness, resulting in the elimination of the unfit cells and a compensatory proliferation of the fittest. CC has been observed for the first time in the '70s: Morata and Ripoll, while studying the growth rate of cells with mutations in ribosomal genes (*Minute, M*) [97,163] in *Drosophila* imaginal wing discs, noticed that *wt* clones induced in *Minute* heterozygous (*M*/+) flies (*Minute* heterozygous flies show a normal morphology, vitality and fertility while displaying slow development and a lower cell proliferation rate than the *wt* flies) triggered the apoptotic death of *M*/+ cells and over-proliferated colonising the whole organ [97]. On this basis, CC has been proposed as a surveillance mechanism in which the fittest cells (called *winners*) kill the unfit cells (called *losers*) that undergo JNK-mediated apoptosis [164,165]. Winner cells proliferate occupying the entire space left [166] (Fig. INTRO 13). The competitive interactions start when some cells carry a mutation that confers them a proliferative disadvantage [146,166] or a shortage of growth factor (such as Dpp), [165]. Cells that confront each other release soluble factors [167] and express some specific molecules defining the loser or winner status [168,169]. Cells can be eliminated by cell-cell intercalation [170] when embedded by winner cells, a phenomenon known as engulfment [171], or by extrusion from the tissue and phagocytosis by professional haemocytes [172,173]. CC can also be triggered by local tissue crowding, without a specific molecular signature [174]. In 2004, Oliver and colleagues found that *Bst* (*Belly spot and tail*, a mutation in a ribosomal gene) mutant

cells were eliminated by *wt* cells during development of chimeric blastocysts [175], summarising in mice the phenomenon observed in the fly.

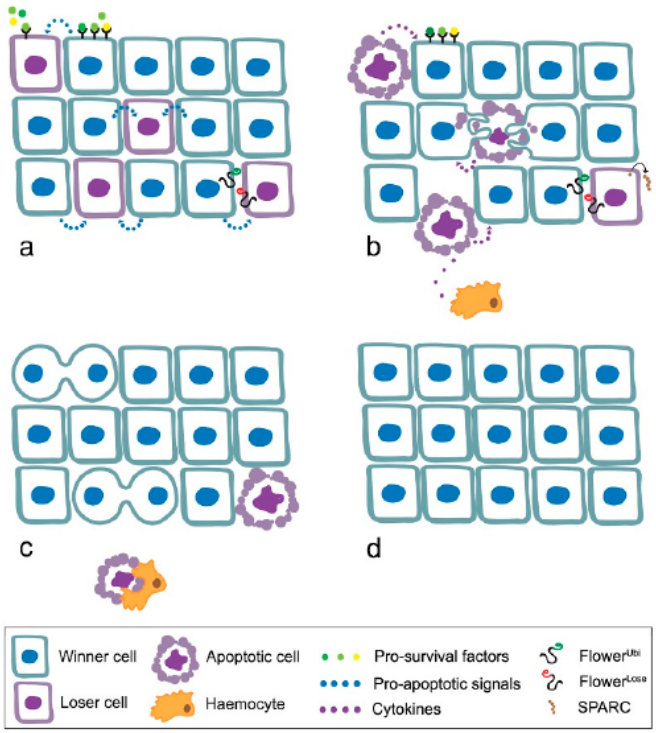

Figure INTRO 13 | Graphic representation of the cell competition mechanism [138].

MYC Involvement in Cell Competition

As mentioned above, MYC plays a central role in the induction of CC. In 2004, two studies displayed the competitive characteristics of cells with high MYC levels. In the *Drosophila* wing disc, MYC-overexpressing cells trigger apoptosis of surrounding *wild-type* cells and proliferate colonising the space previously occupied by loser cells. This mechanism was defined super-competition [98,166]. Soluble factors not yet identified seem to be sufficient to induce MYC-mediated cell competition (MMCC): in co-culture experiments, cells with different MYC levels secrete signals that induce a competitive behaviour without a mechanical contact [167]. In an *in silico* analysis, nine miRNA targeting JNK signalling components have been identified, and it has been suggested that the exchange of signals between the competitive cells take place through extracellular vesicles [176]. In *Drosophila* germinal stem cells (GSCs), MMCC has a physiological role driving cell differentiation and, in this situation, loser GSCs do not undergo apoptotic death but are excluded from the ovary germline niche [177]. p53 is also essential to CC; it

has indeed been shown that MYC-overexpressing cells require a p53 *wt* function to successfully compete: in fact, p53 LOF compromises their metabolism and thus reduces their capacity to trigger CC [178]. Competitive cells have been shown to exhibit a specific signature that governs their fate in the mechanism. Flower (Fwe), a trans-membrane protein, has been identified in 2010 and it seems to commit cells to a loser or winner status depending on the isoform that cell expresses: the Fwe^{Ubi} isoform is constitutively expressed by epithelial cells, and it is down-regulated in loser cells, which rather express the Fwe^{Lose} isoforms. Fwe^{Lose} knockdown in prospective loser cells rescues their loser status [168]. Another CC fingerprint is SPARC (Secreted protein, acidic, cysteine-rich), a cell matrix glycoprotein up-regulated in loser cells at the beginning of CC. It seems to transiently inhibit the Caspase cascade activation [169]. The most recent gene involved in CC is *ahuizotl (azot)*, which seems to integrate Fwe^{Lose} and SPARC information in loser cells [179].

In 2013, a physiological role for MMCC has been found in the mouse epiblast, that has been found to be normally composed of cells expressing different MYC levels. As in *Drosophila* tissues, competitive phenomena between cells with higher (winners) and lower (losers) MYC levels are triggered, and loser cells undergo apoptotic death [180]. CC also shapes heart development in mammals: in this organ, MMCC induces proliferation of high MYC-expressing cardiomyocytes, which substitute the surrounding neighbours that do not show a sufficient proliferation rate [181,182].

The involvement of MMCC in cancer will be discussed in the following chapters.

THESIS AIMS

Cancers are complex communities, where intricate relationships among the different cells that compose the tumour mass guide the fate of the entire society. MYC plays a central role in tumour progression, being involved in many, if not all, biological processes, and is thus found at the centre of a multitude of signalling pathways.

With the aim to study MYC involvement in these intricate relationships, I carried out a genetic dissection of some central cell behaviours associated with the onset and progression of tumours.

The thesis is composed of three parts, as follows:

Part 1. Onset:
MYC-Expressing Epithelial Fields Are Prone to Multifocal Tumourigenesis

Part 2. Growth and vessel formation:
Growth and tracheogenesis are separable traits in *Drosophila* cancers

Part 3. Overt malignancy:
Highly Competitive Cancers Undergo Growth Decline Upon Apoptosis Inhibition

PART I - MYC-EXPRESSING EPITHELIAL FIELDS ARE PRONE TO MULTIFOCAL TUMOURIGENESIS

The concept of "cancerisation field" derives from the observation of regions adjacent to the tumour area showing inappreciable histological alterations. These apparently normal pre-cancerous areas were discovered to be more susceptible to the development of malignancies compared to normal tissues [183].

In both *Drosophila* and mammals, a mechanism known as MYC-mediated cell competition (MMCC) evokes the aforementioned phenomenon, hence the hypothesis of its involvement in the development of pre-cancerous fields [184,185].

Here I used the *Drosophila* imaginal wing disc to mimic field formation by over-expressing MYC in the P compartment and examining specific markers usually found in mammalian precancerous areas. I first showed that MYC up-regulation is sufficient as to induce specific cellular responses, characteristic of mammalian pre-cancerous fields. Successively, I induced different second mutations in the MYC-overexpressing epithelial tissue, demonstrating its propensity to the development of multifocal lesions, a typical tumour phenotype observed in human pre-cancerous fields.

Summing up, I have identified MYC as a molecule possibly involved in the formation of a pre-cancerous field, thus establishing a genetic model in which to investigate the molecular basis of this intricate early cancer trait.

INTRODUCTION

1.1 FIELD CANCERISATION

The molecular mechanisms responsible for the initiation of tumourigenesis are largely unknown. It is now quite clear that cancer origin is clonal: each cancerous cell is an adapted form of a previous cell, in which a series of pre-neoplastic or "initiating" mutations happen, which make the cell more and more susceptible to further mutations.

Despite the genetic alterations, cell clones with pre-neoplastic mutations can appear histologically and morphologically normal [186]. In 1953 for the first time, Slaughter and colleagues introduced the concept of "field cancerisation". Studying oral carcinomas, they observed that the probability to develop recurrences or second primary tumours were higher in areas adjacent to a primary tumour, even after surgical resection. A pre-neoplastic field does not show malignant features but is defined by the presence of cancer-associated genetic or epigenetic alterations, and it does not necessarily display morphologically alterations (Fig. PART-I 1) [183,187].

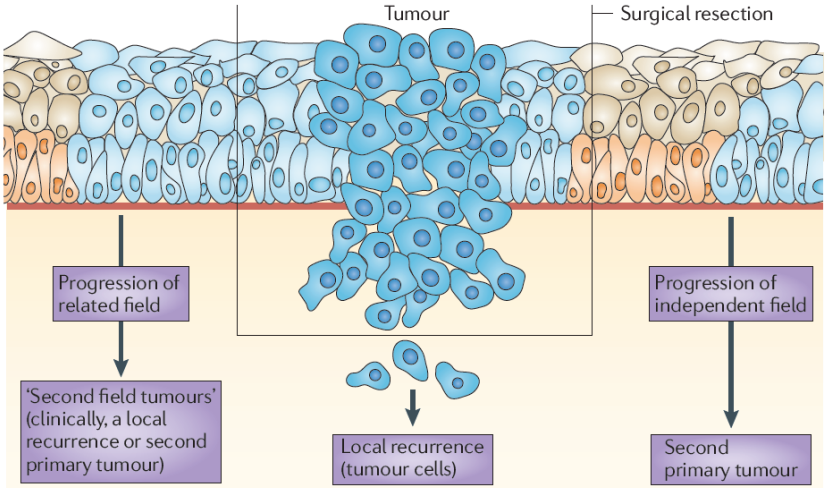

Figure PART-I 1 | Graphical description of field cancerisation [187]

In the carcinogenesis model proposed by Slaughter, the onset of genetic alterations in a healthy cell led to the formation of a clonal area or *patch* of homogeneously mutated cells resulting in a pre-cancerous field, susceptible to the onset of further mutations. Subsequent studies have found that this phenomenon was not only associated with human tumours of the oral mucosa, but with epithelial cancers in general, and with some brain tumours [186,188].

Therefore, a field cancerisation is defined as a tissue territory in which, despite its apparently unaltered morphology and histology, genetic alterations make cells prone to successive mutations, resulting in *multifocal tumours*, typical of pre-cancerous fields [183].

1.2 Theories on Field Formation

Two principal hypotheses regarding pre-cancerous field formation have been formulated:

- Polyclonal Origin: specific factors, such as exposure to carcinogens, and also, during organogenesis, some random mutations, can lead to the appearance of genetic alterations into cells of the same tissue, forming multiple patches which can successively originate a pre-cancerous area [189];
- Monoclonal Origin: a single altered cell might colonise a part of territory by clonal expansion and, eventually, cell migration in different areas distant from the field of origin may originate secondary lesions [189].

Although the monoclonal origin is unlikely in discontinuous tissues, such as the glands, both theories are plausible [186]. In the last few years, a hypothesis suggesting CC as a possible initiator of a pre-cancerous field has been formulated. Some genes, among which *MYC*, can transform cells into super-competitors, which are able to over-proliferate colonising the tissue and eliminating the surrounding cells. This expanded cell population has a higher probability to acquire secondary mutations, to subvert tissue homeostasis and to evolve into a tumour (Fig. PART-I 2) [184,185].

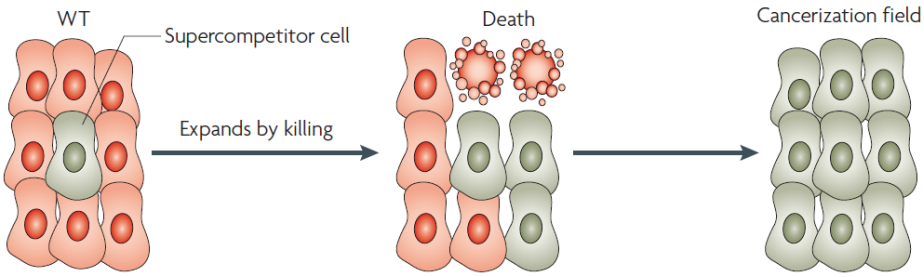

Figure PART-I 2 | MYC over-expressing cells kill the surrounding *wt* cells and expand, colonising the entire territory [185].

1.3 CELL COMPETITION AND CANCER

As previously mentioned, CC has an important role also in the tumourigenic process. It permits mutant cell recognition and its elimination by surrounding *wt* cells [190]. The assumption that CC operates as a tumour suppressor mechanism originates from studies on a *Drosophila* TSGs group: while analysing the oncogenic behaviour of genes involved in cell polarity, such as *lgl, scrib* and *dlg*, and also members of the endocytic pathway, such as *Rab5,* it has emerged that those mutant cells were eliminated when found in a *wt* background [103,107,191,192]. Moreover, at the interface between the mutant and *wt* cells, apoptosis was observed, supporting the hypothesis that cell elimination was carried out through a competitive phenomenon [165,166]. However, the simultaneous expression of oncogenes provided those cells with super-competitive characteristics, unveiling the oncogenic side of CC. In fact, mutant cells over-expressing MYC and bearing *lgl* LOF sent death signals to adjacent *wt* cells and proliferated at their expense [96]. When a constitutively active form of PI3K was expressed in *lgl* mutant cells, these cells did not behave as super-competitors, but they just grew autonomously, showing that PI3K activation is not able to trigger CC [96].

A *Drosophila* study by de la Cova and colleagues has revealed that PI3K is an important growth promoter when overexpressed but, unlike MYC, it does not trigger CC. MYC and PI3K increase protein synthesis in two different ways: MYC increases transcription of several components of the protein synthesis machinery, while PI3K increases the activity of the existing components. Their results prove that different proliferative rates are not sufficient to trigger CC between confronting populations [98,178].

1.4 RAB5: ENDOCYTOSIS AND TUMOUR SUPPRESSION CONTROL

The endocytic trafficking is involved in many processes, among which morphogenetic gradient formation and activation or inhibition of proliferative signalling [193,194]. Endocytosis entails the internalisation of plasma membrane portions in order to form carrier vesicles. Multiple ways of internalisation exist, and these processes consist of blending vesicles (early endosomes) through specific membrane proteins, the syntaxins, involved in the formation of SNARE complexes that mediate the vesicle contact with the

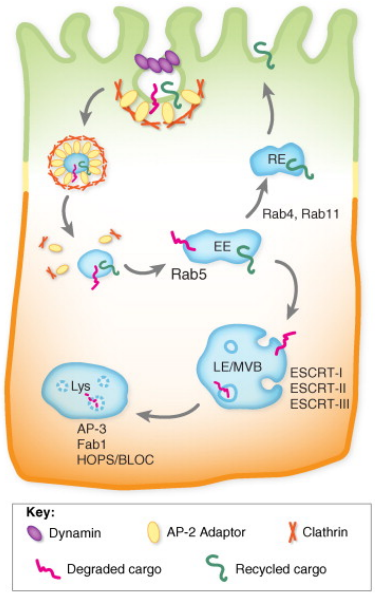

Figure PART-I 3 | The canonical signalling of the intracellular vesicle trafficking [193].

plasma membrane. The entire process is regulated by a small protein with GTPase activity, Rab5. The early endosomes act as station both for recycling of the cargo receptors and for their transport to the lysosomes for degradation [195]. The human genome contains about 60 *Rab* genes and as many proteins, 26 of which are conserved in *Drosophila.* They are located on the cytosolic side of the cell membrane and, following binding with GTP, activate a series of effector proteins involved in vesicle formation, in actin/tubulin-dependent vesicular transport and in vesicle fusion to the membrane (Fig. PART-I 3) [196].

In *Drosophila,* excluding the mutants for *lgl, scrib* and *dlg* that, thanks to the maternal contribution of the respective proteins, succeed in completing larval development [77,197,198], mutant organisms for other TSGs, including *Rab5*, die at the L1 larval instar, without any evident phenotype. The behaviour of these TSGs has been studied through the genetic mosaic technique, which allowed the induction of *Rab5* mutant cells in non-essential organs, such as the imaginal eye or wing disc. It was then possible to observe a mutant phenotype [194]. In *Drosophila* imaginal discs, *Rab5* mutant clones provoked complete loss of tissue architecture, and neoplastic growth (Fig. PART-I 4) [194,199]. When surrounded by *wt* cells, *Rab5* mutant cells, as for *lgl* mutants, were eliminated by CC-mediated apoptosis. When the *Rab5* mutant clones were composed of a group of at least 400 cells, they developed into a highly proliferative tumour instead. The outermost cells continued to be eliminated, while the innermost cells proliferated bypassing CC. In this case, the apoptosis triggered by CC acted as a tumour promoter through the induction of high levels of JNK and, subsequently, of the Dpp/Wg pathway, resulting in cell proliferation. This may also indicate that a greater number of

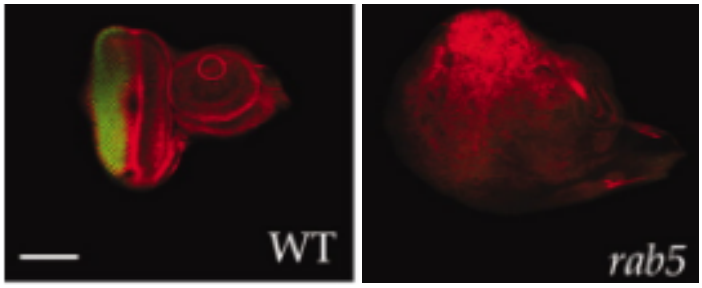

Figure PART-I 4 | Neoplastic phenotype resulting from *Rab5* mutation. On the right, a *Drosophila Rab5* mutant imaginal eye disc compared to the corresponding *wt* (on the left) [194].

cells together create a sort of mechanical barrier as, at the centre of the mass, the homotypic bulk is not exposed to out-competition and keeps on growing, thus eluding tumour suppressor mechanisms [192].

1.5 MARKERS OF FIELD CANCERISATION

Mohan and Jagannathan have grouped the principal markers found associated with the areas adjacent to a primary tumour, morphologically normal but genetically altered. These markers are copious and acquire a relevant role in the clinics, as they provide important indications on the early diagnosis of possible recurrences. Among the many markers, we find high levels of ectopic cytokeratin and cyclinD1, an increase of the proliferation rate, chromosome anomalies, mitochondrial genome modifications, genetic instability, oxidative stress and apoptosis (Fig. PART-I 5) [189].

Genomic markers	Genetic studies chromosomal anomalies/ aberrations	
	Loss of heterozygosity	Califano *et al.*[46]
	DNA sequence analysis	Silveira *et al.*[1]
	Gene profiling	Haaland *et al.*[47]
	Mitochondrial genome changes	Dakubo *et al.*[48]
	Nuclear aberrations	
	Micronuclei	Bloching *et al.*[49]
Indices for genomic instability	Aneuploidy	Ai *et al.*[50]
	Microsatellite markers	Partridge *et al.*[51]
	DNA adducts	Wiencke *et al.*[52]
Squamous differentiation antigens	Cytokeratins - 7, 8, 13, 16, and 19	Copper *et al.*[53]
		Ogden *et al.*[54]
		Bonger *et al.*[55]
		Bosch *et al.*[56]
	Secretory products – ABH antigen	Bonger *et al.*[55]
	Telomerase	Heaphy *et al.*[57]
Proliferation indices	Nuclear antigens	Shin *et al.*[58]
	PCNA	Vanoijen *et al.*[24]
	Ki-67	Kamel *et al.*[59]
	Thymidine labelling index	Lopez Blanc *et al.*[43]
	AgNOR	
Nuclear retinoid receptors	Retinoic acid receptors	Smith *et al.*[60]
	Retinoid X receptors	Fischer *et al*[61]
Oxidative stress	Glutathione S transferase	Bongers *et al.*[62]
	Superoxide dismutase	Ahmed *et al.*[63]
	Heat shock proteins	Kaur *et al.*[64]
Apoptosis	Bcl2, Bax	Birchall *et al.*[65]
	Chromatin condensation factor	Cherkezyan *et al.*[66]
	Caspase	Bascones-Martinez *et al.*[67]

Figure PART-I 5 | Main phenotypic markers found in human pre-cancerous fields [189].

1.6 MYC AND ITS POSSIBLE ROLE IN FIELD CANCERISATION

As previously described, MYC is involved in many physiological but also pathological cellular processes. It is the most expressed gene in human neoplasias and it is well-documented that its hyper-expression triggers oxidative stress and genomic instability [200]. Moreover, MYC is the most potent inducer of CC and MYC over-expressing cells acquire

super-competitive behaviours [166,184]. MYC high levels have also been observed in the prostatic intraepithelial neoplasia (PIN), a pre-cancerous lesion that can be of high or low grade, where MYC presence drives neoplastic transformation. Also in humans, MYC hyper-expression in the nuclei of prostatic luminal cells has been displayed. In this study, Gurel and colleagues show that these luminal cells, which do not complete differentiation, constitute the progenitor cells of a prostatic tumour [201]. In a subsequent study, the MYC over-expressing luminal epithelium of transgenic mice prostate showed a faint pathology, defined as a histologically normal epithelium or low-grade PIN lesion. The apparently normal epithelium of these elder mice evokes the field cancerisation concept. MYC over-expression in these cells could facilitate the acquisition of secondary mutations and the development of tumours [29]. Recently, murine models of lung cancer highlighted the presence of MYC hyper-expression in the normal cells of bronchial tissues, with the successive development of invasive tumours. The authors have shown that MYC inhibition decreased tumour development by about 50-60% [202]. All these observations lead to the hypothesis that MYC hyper-expression and stabilisation may be sufficient for a tissue to become susceptible to the onset of additional mutations and the subsequent development of tumours.

It is also known that MYC deregulation promotes genomic instability [203]. MYC hyper-expression has often been associated with chromosome rearrangements and abnormal recombination [204], and with the amplification of many genes involved in cell cycle or in DNA synthesis, which confer a proliferative advantage to cells [205]. Also, DNA sequencing highlighted that several chromosome regions were involved: c-MYC alters the stability of many genes and genomic sites [206,207]. In *Drosophila*, Greer and colleagues have observed that MYC overexpression in the dorsal compartment of the wing disc provokes an increase of double-strand breaks (DSBs) and that the spontaneous mutation rate was twice compared to a control compartment. Therefore, when an increase in MYC levels persists, the mutation frequency in the entire genome is intensified [208].

About a decade ago, MYC involvement in oxidative stress induction has been found in human and rat fibroblasts. It has been shown that MYC transcriptional activation triggered an increase of different factors involved in the metabolic balance. An alteration in these genes led to ROS production, which caused chromosome and DNA damage not associated with apoptotic death [209]. Among the different MYC target genes, some are

directly involved in the oxidative stress control, such as TFAM (Transcription Factor A, Mitochondrial). TFAM is a mitochondrial gene that encodes a protein essential for a correct mitochondrial biogenesis and its deregulation results in ROS increase [210,211]. Many genes regulated by MYC are involved in ROS level control and c-MYC triggers oxidative stress through several mechanisms [209]. c-MYC mediates p53 activation, which induces the transcription of genes involved in the oxidative metabolism and ROS production; some MYC target genes, such as ODC (Ornithine DeCarboxylase), can directly cause an increase of ROS levels; finally some studies have shown that MYC-overexpressing cells present deletions also in mitochondrial DNA, opening the possibility that MYC-induced oxidative stress may directly depend on an imbalance of cell metabolism that also involves mitochondria functionality [209]. Nevertheless, the molecular mechanisms at the basis of MYC-dependent ROS overproduction still present several unresolved issues.

MYC ectopic expression provokes a sensitisation of cells to apoptosis. At the end of the '80s, it has been displayed that rat fibroblasts presented more apoptotic signs when activated Ras was combined to MYC overexpression [212]. Successively, a correlation between cell death and MYC overexpression in normal B lymphocytes was also observed [213]. These mechanisms involve mainly the TP53 and the pro-survival Bcl-2 pathways, and recent findings associated MYC with cell death rather than with cell cycle progression: MYC can drive cell transformation by inducing changes in cell death (for example increasing Bcl-2 proteins and breaking down TP53 function) [214]. MYC is involved in apoptosis also in *Drosophila*: it is known that MYC overexpression induces autonomous cell death, and this process requires the pro-apoptotic genes *rpr, grim* and *hid*. Moreover, p53 is induced by MYC over-expression but it is not involved in MYC-mediated autonomous cell death. It was shown that lowering MYC levels protects the imaginal wing disc cells from death following DNA damage [157]. CC provokes non-autonomous cell death instead, essential for the winner cells to repopulate the developing tissue [166,215]. Being MMCC a possible strategy adopted by tumour cell to expand [216,217], it is plausible that cell signals released by loser cells are intercepted by tumour cells to promote their own growth [217].

RESULTS AND DISCUSSION

The first observations about the existence of pre-cancerous fields happened while analysing tumours from the oral mucosa, and they were defined as tissue areas carrying histologically normal, but genetically altered, cells. These areas were shown to be more susceptible to the onset of new mutations, leading to the development of multifocal tumours [183,218].

As previously described, MMCC has been hypothesised as a possible mechanism able to prime a pre-cancerous field [184,185]. Moreover, activated forms of K-RAS have been frequently found in human cancerisation fields [188], and it is known that KRAS promotes MYC stabilisation and accumulation *via* the MAPK signalling [219].
The hypothesis that MYC may pioneer field cancerisation is also supported by some evidence in mammals [29,202].

Starting for these assumptions, the idea that a cell may be subject to selective forces and acquire the capacity to transiently express high MYC levels, forming in time a pre-cancerous field, led me to develop a *Drosophila* epithelial model that would allow to mimic the formation of a MYC-overexpressing (hereafter referred to as MYC^{OVER}) field as a possible result of MMCC.

Using the UAS-Gal4 system (see Methods), I induced MYC expression under the control of the *hedgehog* (*hh*) promoter, active in the P compartment of the imaginal wing disc, and observed that the organ did not display evident morphological alterations, except for a slight increase in cell size: nuclei in the P compartment (marked with Ubi-GFP) were more distant than those in the A compartment, where MYC expression is untouched (Fig. RES-I 1). This evidence represented a MYC well-known property and recapitulated what happens in pre-cancerous fields [146,186].

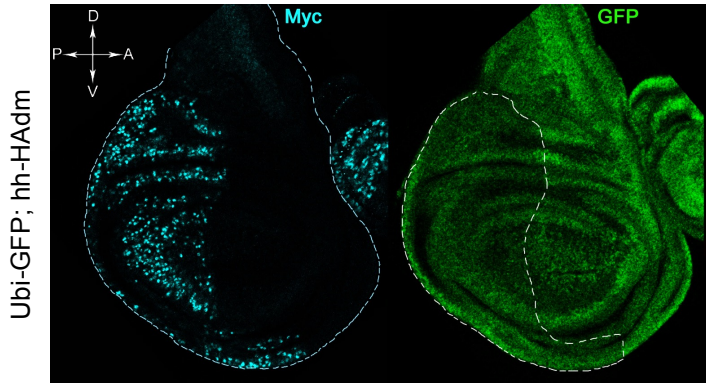

Figure RES-I 1 | On the left, MYC staining displays protein overexpression (cyan) in the P compartment of the wing disc. On the right, the same wing disc marked by Ubi-GFP_{nls}. The boundary between the A and P compartments is outlined by a dotted line.

Successively, with the aim to verify if a MYC^{OVER} tissue area could represent a cancerisation field, I investigated different typical markers found in human pre-cancerous fields (Fig. PART-1 5). I examined genetic instability, oxidative stress, proliferation and apoptosis by using the UAS-Gal4 system.

I then overexpressed MYC under the control of the *engrailed* (*en*) promoter (the determinant of the larval P compartments) and compared my results with those obtained in imaginal wing discs overexpressing a constitutively active form of PI3K ($PI3K^{CAAX}$), a strong growth inducer not involved in cell competition [98], with the aim to demonstrate that mutations conferring growth capabilities are not sufficient to provide cells with pre-cancerous properties.

Before analysing the specific markers, I verified that the expression of $PI3K^{CAAX}$ (marked by GFP) succeeded in activating the PI3K/AKT signalling cascade, and I found this was the case, as demonstrated by AKT activation (Figure RES-I 2).
In humans, pre-cancerous fields are often associated with PI3K GOF mutations [220], and my laboratory previously demonstrated that transient PI3K clonal expression impacted MYC levels [150]; therefore, it was mandatory to verify that our $PI3K^{CAAX}$ construct did not impact on the endogenous MYC levels, as $PI3K^{CAAX}$ overexpression is utilised as a control in my experimental model. As can be seen in Figure RES-I 2, $PI3K^{CAAX}$ overexpression did not increase MYC endogenous levels.

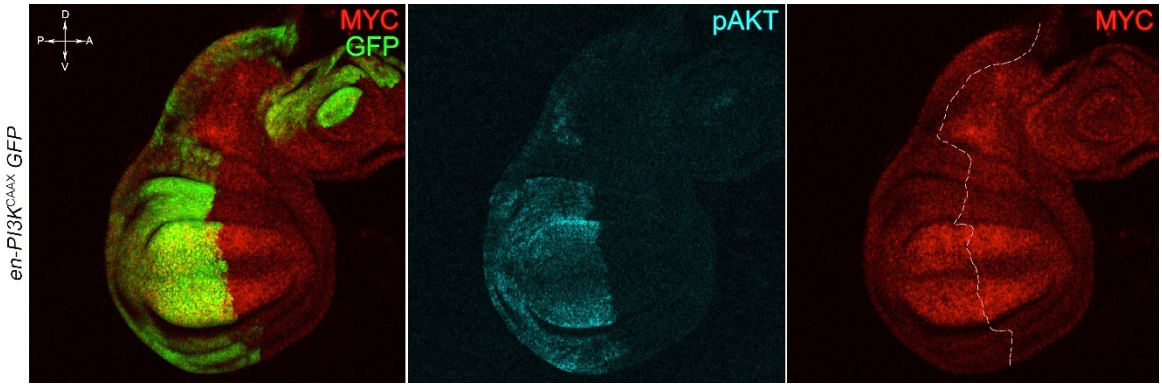

Figure RES-I 2 | PI3K^{CAAX} Expression in the P compartment (GFP^{+}). pAKT staining (cyan) shows active AKT (cyan). MYC staining (red) displays that in the P compartment it is expressed at comparable levels as in the A compartment.

A statistical analysis supported the qualitative data: as can be observed in Figure RES-I 3, PI3K^{CAAX} overexpression in the P compartment (green bar) of the wing disc does not increase MYC protein abundance over the endogenous levels (compare to the A compartment, grey bar).

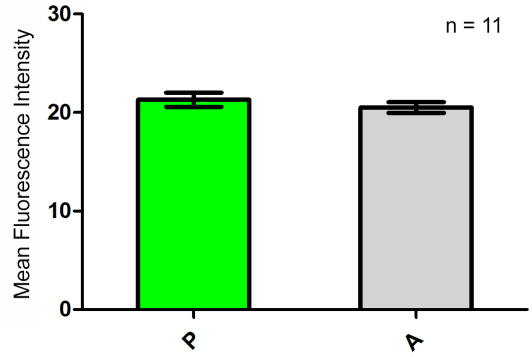

Figure RES-I 3 | Comparison between the MYC protein expression in the *en*-PI3K^{CAAX} wing discs. The green bar represents the P compartment of discs in which PI3K^{CAAX} is overexpressed, compared with the A compartments (grey bar). The comparison does not show significant difference. n is indicated.

To investigate if MYC^{OVER} territories showed an enhancement in genetic instability, I used an antibody against the γ variant of the phosphorylated H2 histone, which detects Double Strand Breaks (DSBs). If not repaired, DSBs damage triggers a number of cell signals, among which DDRs (DNA Damage Response proteins). The H2AX (or H2Av in *Drosophila*) histone phosphorylation is the first chromatin modification that occurs following a DSB, resulting in the assembling of multi-protein complexes which attempt to repair DNA damage [221].

The anti-γH2Av staining (red) in *en-dm*, GFP wing discs evidenced an increase in DSBs in the MYC^{OVER} P compartment (GFP^{+}) compared to the A compartment (Fig. RES-I 4). I performed the analysis both in early and in late L3 wing discs. The graph in Figure RIS-II 4 shows an about twofold increase in DSBs in the P compartments (green bars) of both early and late L3 wing discs with respect to the A compartments. The increase is thus kept constant throughout development.

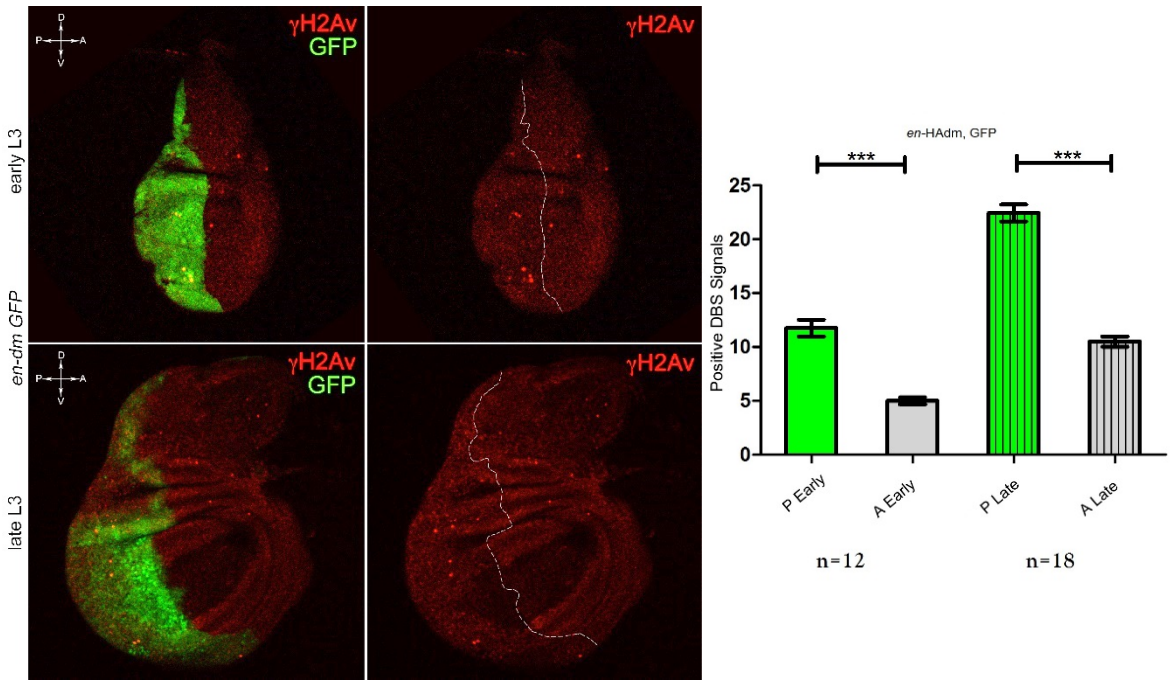

Figure RES-I 4 | On the left, an immunostaining against γH2Av in *en-dm*, GFP imaginal wing discs. The P compartments of the imaginal discs (MYC^{OVER}) are marked in green (GFP^{+}). In the upper panel, an early L3 wing disc is shown, and in the lower panel, the same analysis is observable in the late L3 wing discs. On the right, a graph representing the DBSs counted in the P (green bar) and A (grey bar) compartments. n are indicated. ***=$p \leq 0.001$.

To verify that hyper-expression of a gene involved in cell growth is not sufficient to increase genetic instabiity in a tissue, I expressed PI3K^{CAAX} in the P compartment of the wing discs and I analysed γH2Av expression. Differently to what happened with MYC overexpression, the activation of PI3K^{CAAX} did not result in a significant increase of DSBs (Fig. RES-I 5).

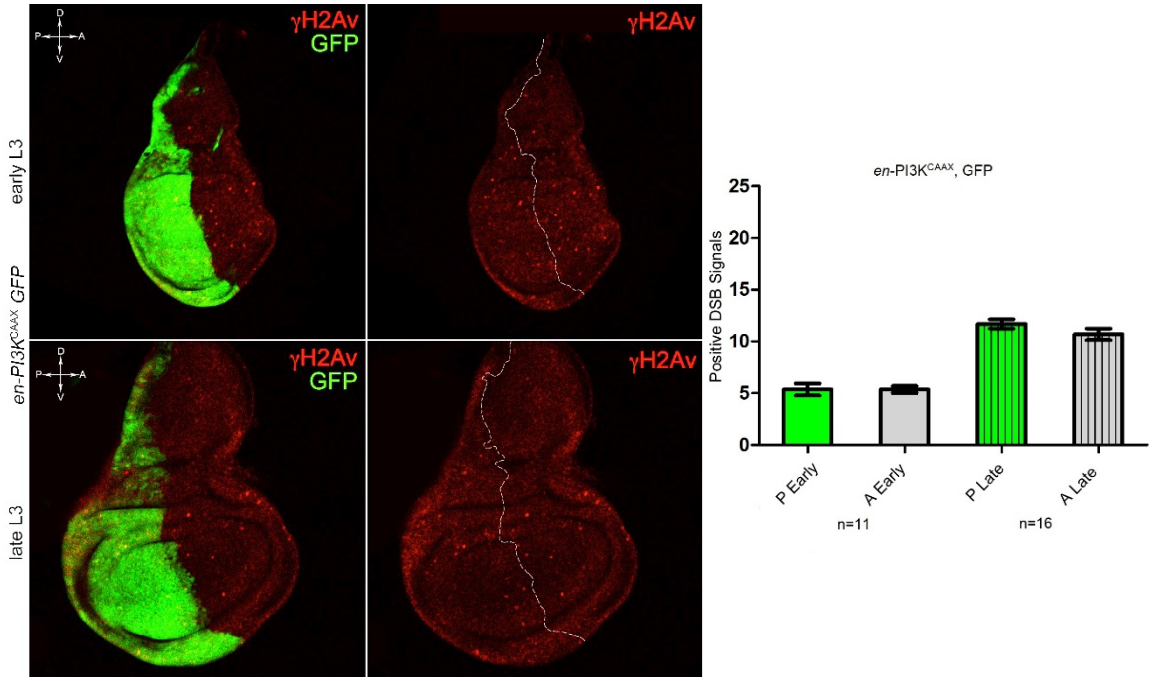

Figure RES-I 5 | On the left, anti-γH2Av staining (red) in *en-PI3K^{CAAX}*, GFP imaginal wing discs. The P compartments are marked in green (GFP^{+}). In the upper panel, an early L3 wing disc is shown and, in the lower panel, the same analysis is displayed in late L3 wing discs. On the right, a graph representing the DBSs counted in the P (green bar) and A (grey bar) compartments. n are indicated.

Figure RES-I 6 shows a comparison of the DSB signals across the different genotypes and compartments. While it is quite clear that MYC and PI3K overexpression in the P compartments shows a different impact on DSB activation, A compartments do not seem to respond consistently, demonstrating that, in this case, transgenic expression did not provoke non-autonomous effects.

Altogether, these data indicate that MYC overexpression is sufficient to trigger genetic instability, and this damage does not seem to be induced by a simple increase in growth, as PI3K^{CAAX} overexpression had no effects on this phenotypic trait.

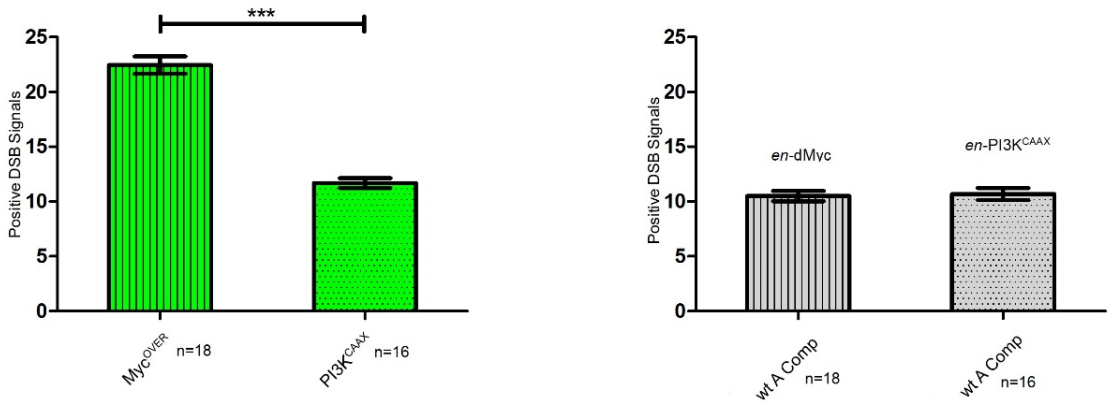

Figure RES-I 6 | On the left, a graph showing the DSBs counted in the MYC^{OVER} and $PI3KC^{AAX}$ P compartments. On the right, a graph showing the DSBs counted in the respective A counterparts. n are indicated. ***=$p \leq 0.001$.

Another typical marker associated with human pre-cancerous fields is an increase of the proliferative index [189]. To detect this, I performed an immunofluorescence (IF) assay against the mitotic marker Phospho Histone H3 (PH3) in imaginal wing discs overexpressing MYC or PI3K in the P compartments.

The H3.3 histone variant is indeed known to play a pivotal role during mitosis both in *Drosophila* and mammals [222,223].

The analysis of PH3 staining highlighted a 23,3% increase in the $PI3K^{CAAX}$ P compartments (see upper panel, Fig. RES-I 7), and a 45,24% increase in MYC^{OVER} P compartments with respect to their A counterparts (see lower panel, Fig. RES-I 7). This result was not unexpected, as PI3K activation plays an important role in cell growth and proliferation [224].

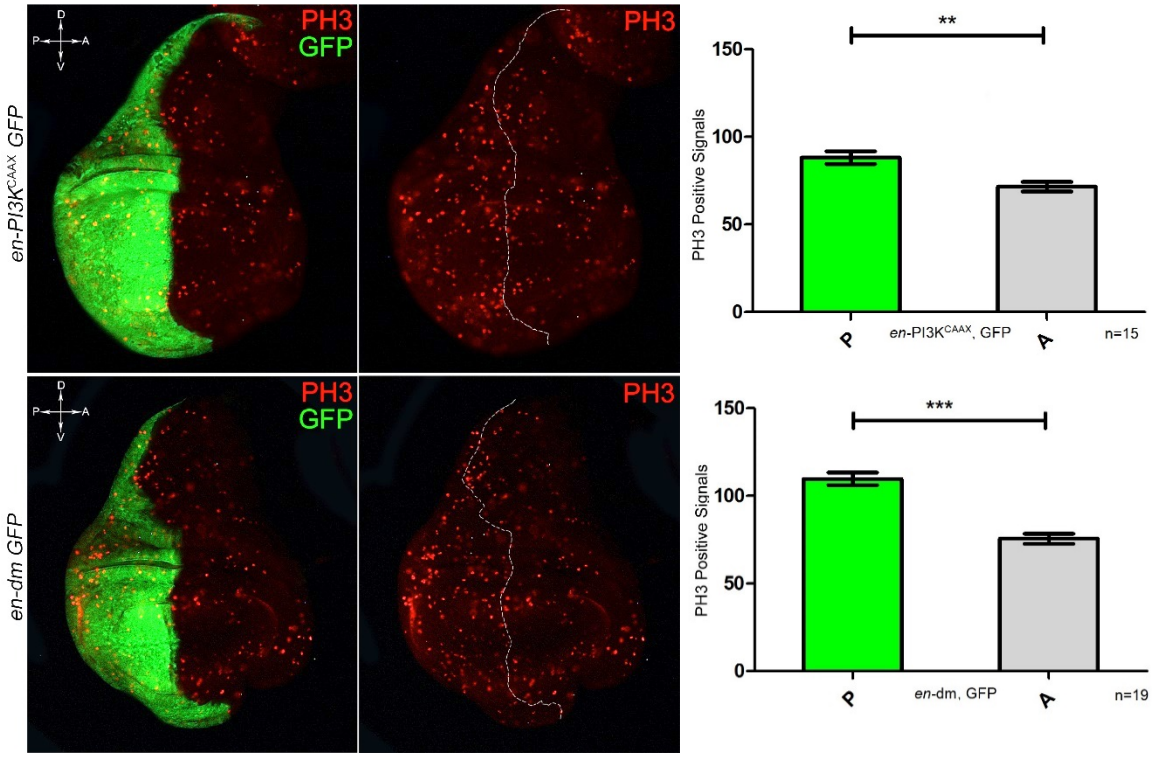

Figure RES-I 7 | On the left, PH3 staining (red) in *en-PI3K*^{CAAX} GFP (upper panel) and *en-dm*, GFP (lower panel) in imaginal wing discs. The P compartments are marked in green (GFP^{+}). On the right, the graphs display the PH3 signal comparisons between the MYC^{OVER} and PI3K^{CAAX} P compartments (green bars) and their respective A counterparts (grey bars). n are indicated. **=$p \leq 0.01$; ***=$p \leq 0.001$.

Of note, MYC overexpression was able to induce a twofold PH3 signal increase respect to PI3K constitutive activation, compared to the respective A compartments (compare Fig. RES-I 7, lower panel with upper panel).

Also in this case, no significant non-autonomous effects were observed, as the A compartments of both MYC^{OVER} and PI3K^{CAAX} -expressing P compartments showed comparable PH3 signals (Fig. RES-I 8, right graph). Figure RES-I 8 shows also a graphical comparison between the P compartments expressing MYC and PI3K.

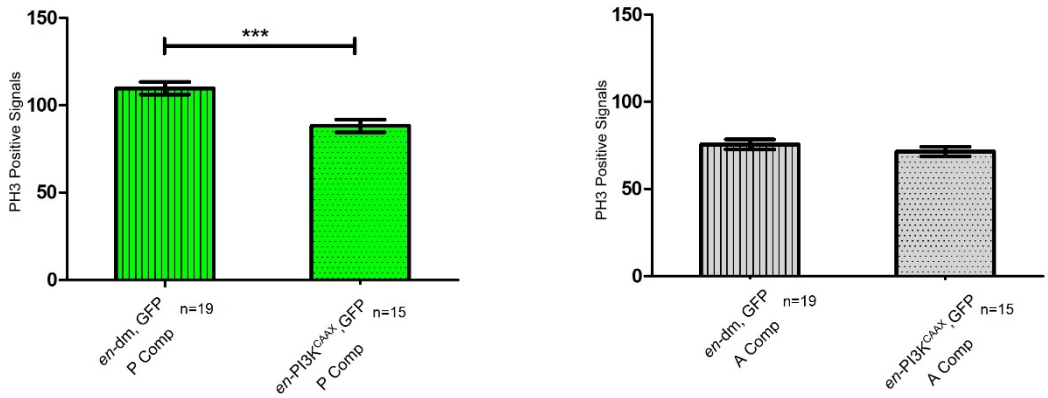

Figure RES-I 8 | On the left, a graph showing the comparison between the PH3 signals counted in the MYC^{OVER} (green striped bar) and $PI3K^{CAAX}$ (green dotted bar) P compartments. On the right, a graph showing the comparison between the PH3 signals counted in the A counterparts of MYC^{OVER} (grey striped bar) and $PI3K^{CAAX}$ (grey dotted bar). n are indicated. ***=$p \leq 0.001$.

I then analysed the oxidative stress through detection of the Reactive Oxygen Species (ROS), another typical marker associated with human field cancerisation [189], in MYC^{OVER} and $PI3K^{CAAX}$ territories.

ROS were visualised by the use of DHE (DiHydroEthidium), a compound that permeates cell membranes and reacts with the superoxide anion, resulting in a red fluorescent product intercalating DNA [225].

Figure RES-I 9 shows a potent ROS activation (red) in the MYC^{OVER} P compartment (GFP^{+}), compared to the A compartment. This evidence is supported by a statistical analysis: DHE mean fluorescence intensity is considerably increased (197%) in the MYC^{OVER} P compartment (in the upper panel, green bar) compared to that measured in the A compartment of the same wing discs (Fig. RES-I 9, upper graph). On the contrary, $PI3K^{CAAX}$ P compartment does not show evident signs of ROS activation (Fig. RES-I 9, lower panel).

A comparison of the DHE mean fluorescence intensity between the A compartments of the two genotypes under exam revealed a significant difference between the *en-dm* and the *en*-$PI3K^{CAAX}$ organs (Fig. RES-I 10), suggesting some non-autonomous effects of MYC overexpression in the P compartment on the overall organ stress response.

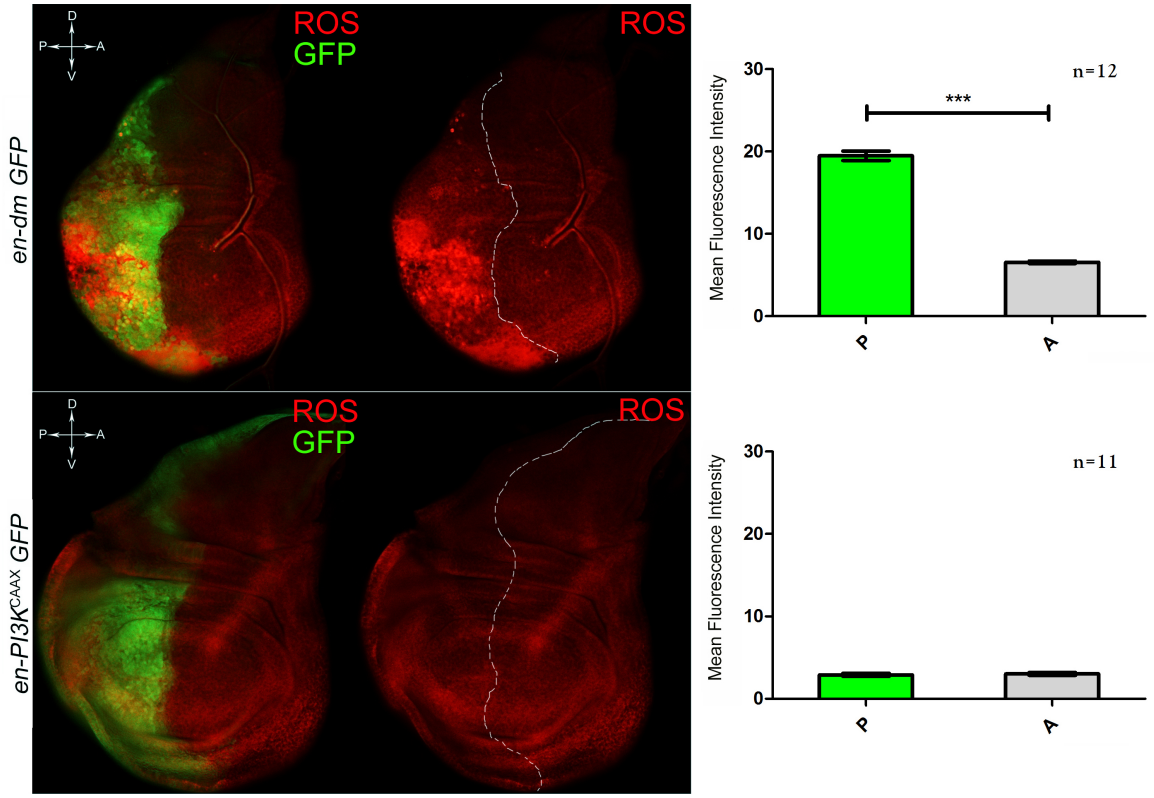

Figure RES-I 9 | On the left, DHE staining (red) in *en-dm*, GFP (upper panel) and *en-PI3K*^{CAAX}, GFP (lower panel) imaginal wing discs. The P compartments are marked in green (GFP^{+}). On the right, the graphs display DHE mean fluorescence intensity in the MYC^{OVER} and PI3K^{CAAX} P compartments (green bars) and in their respective A counterparts (grey bars). n are indicated. ***=p≤ 0.001.

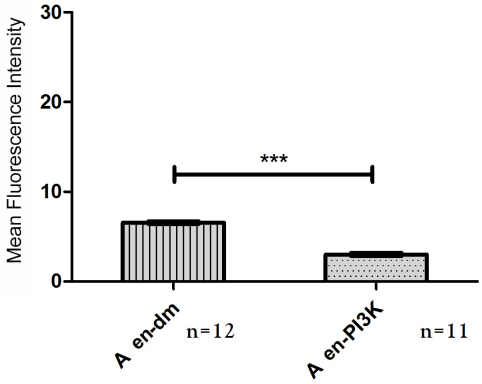

Figure RES-I 10 | The graph shows an increase of DHE mean fluorescence intensity in the A compartment of *en-dm*, GFP wing discs (grey striper bar) compared to the A compartment of *en-PI3K*^{CAAX}, GFP wing discs. n are indicated. ***=*p*≤ 0.001.

The last marker of field cancerisation examined was apoptotic cell death. It is well known that excess MYC provokes cell-autonomous apoptosis, resulting in a block of MYC activity that may be detrimental to cells [214], but the apoptotic process is sometimes beneficial to the tissue (see paragraph 3.1 of Part III). As expected, the P compartment (GFP^+) of the *en-dm* wing discs displayed a strong activation of Caspase 3 (Cas3, red) (Fig. RES-I 11), while $PI3K^{CAAX}$ overexpression in the P compartment did not trigger cell death mechanisms.

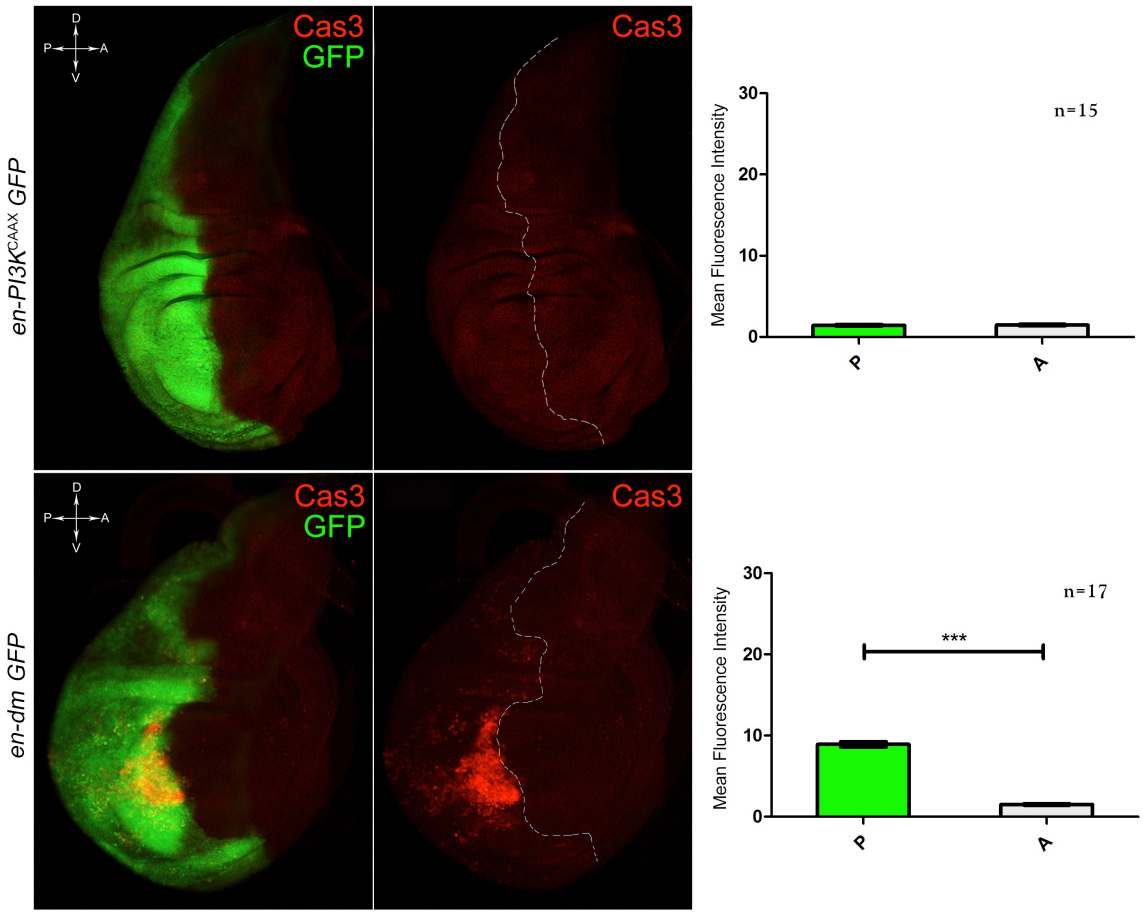

Figure RES-I 11 | On the left, Cas 3 staining (red) in *en-PI3K*^{CAAX}, GFP (upper panel) and *en-dm,* GFP (lower panel) imaginal wing discs. The P compartments are marked in green (GFP^+). On the right, the graphs display Cas3 mean fluorescence intensity in the MYC^{OVER} and $PI3K^{CAAX}$ P compartments (green bars) and in their respective A counterparts (grey bars). n are indicated. ***=$p \leq 0.001$.

Altogether, these findings confirmed that MMCC is an excellent candidate for the formation of a pre-cancerous field, as MYC overexpression is sufficient as to trigger a number of typical markers found in human pre-cancerous fields.

This evidence prompted me to investigate the phenotypic consequences of the induction of TSG mutations in MYC^{OVER} territories *vs wt* territories. To address this question, I built a genetic system that allowed me to express MYC in a restricted area of the wing disc (the P compartment) and to induce secondary mutations of interest later in development in the same organ. I used a combination of the UAS-Gal4 and Flp-FRP systems in order to express MYC in the P compartment of the wing disc from the onset of development under the control of the *hh* promoter, and to induce mutant mitotic clones later in time. The A compartment has been used to assess the clonal phenotype promoted by the same mutations in a territory carrying the endogenous MYC expression.

I first decided to analyse the *lethal giant larvae (lgl)* mutation (widely described in the General Introduction). Lgl protein regulates the apical-basal polarity in the epithelia and it is known that *lgl* mutant clones induced in a *wt* background are unable to grow in the wing pouch region of the wing disc, where MYC levels are very high, and they are eliminated by MMCC [96]. Simultaneous MYC overexpression in *lgl* mutant clones indeed rescues them from death and transforms $lgl^{-/-}$ cells from losers into super-competitors [96]. But what happens when *lgl* mutation is induced in a cell already addicted to MYC, surrounded by other MYC^{OVER} neighbours?

Out of 346 wing discs observed, only 79 showed the presence of *lgl* mutant tissue. 22 discs (28%) displayed "regular" *lgl* mutant clones, that in the A compartment were smaller in size compared to their *wt* twin clones, or were eliminated by CC, as revealed by the permanence of *wt* twin clones [95]. However, in the MYC^{OVER} compartment, the $lgl^{-/-}$ clones were larger than the *wt* twins (data not shown). This suggests that the *lgl* mutant cells have a greater ability than the surrounding neighbours to exploit the excess MYC protein, hence the gain of a competitive advantage over the *wt* tissue. The remaining 57 wing discs with *lgl* mutant tissue (72%) displayed a novel phenotype: the *lgl* mutant tissue was composed of small nests scattered all across the P compartment, which appeared punctated. In Figure RES-I 12 we can observe three examples of this novel phenotype with different severity. MYC staining (red) highlights preferential protein accumulation in the mutant cells, despite it is overexpressed in the whole P compartment. The middle and right panels are a magnification of the region squared in the left panel. The asterisk in Figure RES-I 12A, left image, shows a *wt* twin clone in the wing pouch region of the A compartment, indicating that the *lgl* mutant clone has been eliminated. I

then analysed the presence of apoptosis in the P compartment (MYC^{OVER}) to understand mutant cells' capacity to trigger death in the surrounding cells. As previously mentioned, MYC overexpression itself sensitises cells to apoptosis. Cas3 positivity (cyan) was often associated with high MYC levels in adjacent cells, whether they were *wt* or mutant (Fig. RES-I 12, middle and right panels, arrowheads), indicating that competitive interactions are at work in this tissue.

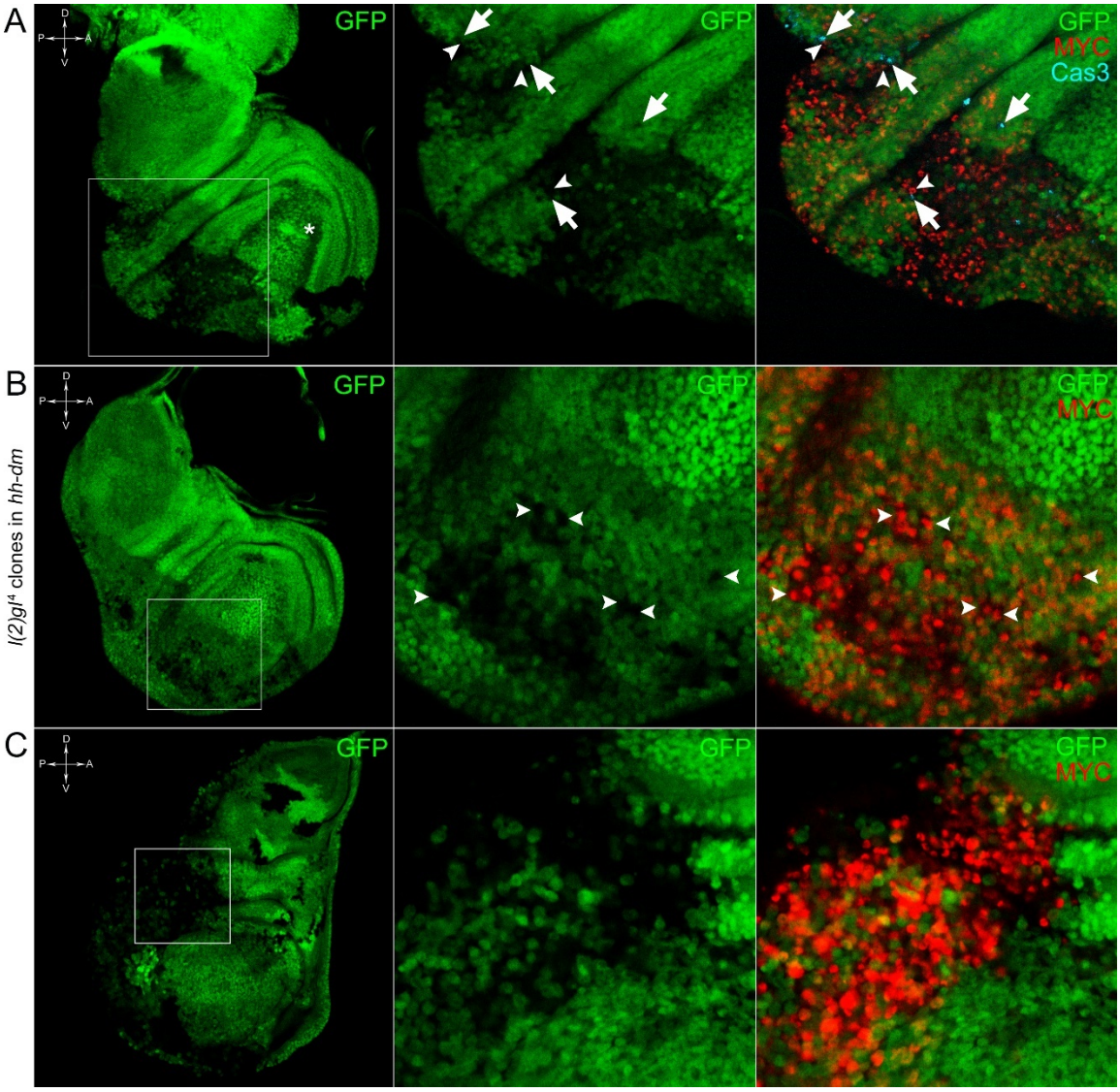

Figure RES-I 12 | *lgl*$^{-/-}$ clones (GFP^{-}) induced in a *w, hs-Flp/+; lgl*^{4}*, FRT40A/Ubi-GFP, FRT40A*; *hh-Gal4/UAS-dm* background (GFP^{+}). *wt* twin clones are GFP^{2+}. Magnifications allow a detailed view of cell-cell dynamics in the P compartment. A: the asterisk indicates a *wt* twin clone (GFP^{2+}) in the A compartment. Arrowheads indicate cells with high MYC levels (red), while arrows point to Cas3-positive cells (cyan).

During the analysis, I observed that 47% of these wing discs exhibited an extreme phenotype (Fig. RES-I 13). The MYC^{OVER} P compartments of these organs were almost completely mutant (GFP$^-$), and the whole disc structure appeared severely compromised. As indicated by the arrowheads, in these organs high MYC expression (red) was observed in the mutant areas (GFP$^-$). This deep organ alteration suggests an invasive, malignant behaviour of these cells that was possibly promoted by clone confluence during growth.

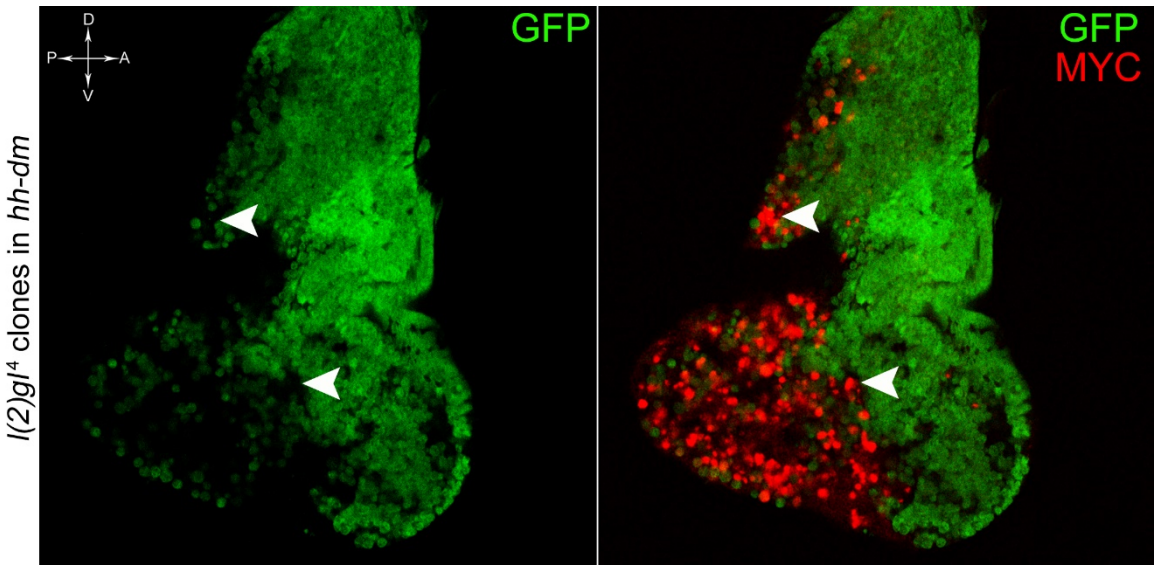

Figure RES-I 13 | *lgl*$^{-/-}$ clones (GFP$^-$) induced in a *w, hs-Flp/+; lgl*^{4}*, FRT40A/Ubi-GFP, FRT40A*; *hh-Gal4/UAS-dm* background (GFP$^+$). *wt* twin clones are GFP^{2+}. The GFP$^-$ clonal area spreads throughout the entire P compartment. The arrowheads indicate some *lgl* mutant cells with high MYC levels (red).

The most interesting aspect of this model is that it faithfully reproduced the distinctive characteristic of human pre-cancerous fields: multifocality [218]. The multifocal phenotype had never been associated with *lgl* mutation in *Drosophila,* Therefore, it represents a novel trait acquired by *lgl* mutant cells in a MYC^{OVER} field.

To verify that a MYC^{OVER} field represented a *bona fide* pre-cancerous area, and that multifocality did not result from specific interactions between *lgl* and MYC, I induced *Rab5* mutation in the MYC^{OVER} field. Like *lgl*, entire organs mutated for *Rab5* show neoplastic growth, and *Rab5* mutant cells induced in a *wt* background suffer from cell competition and are eliminated (see the dedicated section in the Introduction of this part) [192,194,199,226]. Using the same clonal system as above, I induced *Rab5* mutant clones in animals whose P compartments overexpressed MYC. In Figure RES-I 14, the multifocal lesions are evident in the MYC^{OVER} P compartment (MYC staining, red). *Rab5* mutant

cells (GFP$^-$) are scattered all across the MYC^{OVER} field. In this case, 100% of the wing discs bearing mutant clones showed multifocal phenotype, while in the A compartment *Rab5* clones were eliminated. I analysed the presence of apoptosis (Cas3 staining, cyan) in the P compartment (MYC^{OVER}) and, as it happened with *lgl* mutation, cell death was observed both in *wt* and in mutant cells with equal/higher MYC expression compared to the P compartment background (in Fig. RES-I 14A, right image, dying cells are indicated by the arrows and neighbouring cells with higher MYC levels are indicated by the arrowheads). Even in this case, a preferential accumulation of the MYC protein in mutant areas is observable (MYC staining in red, cells are indicated by the arrowheads).

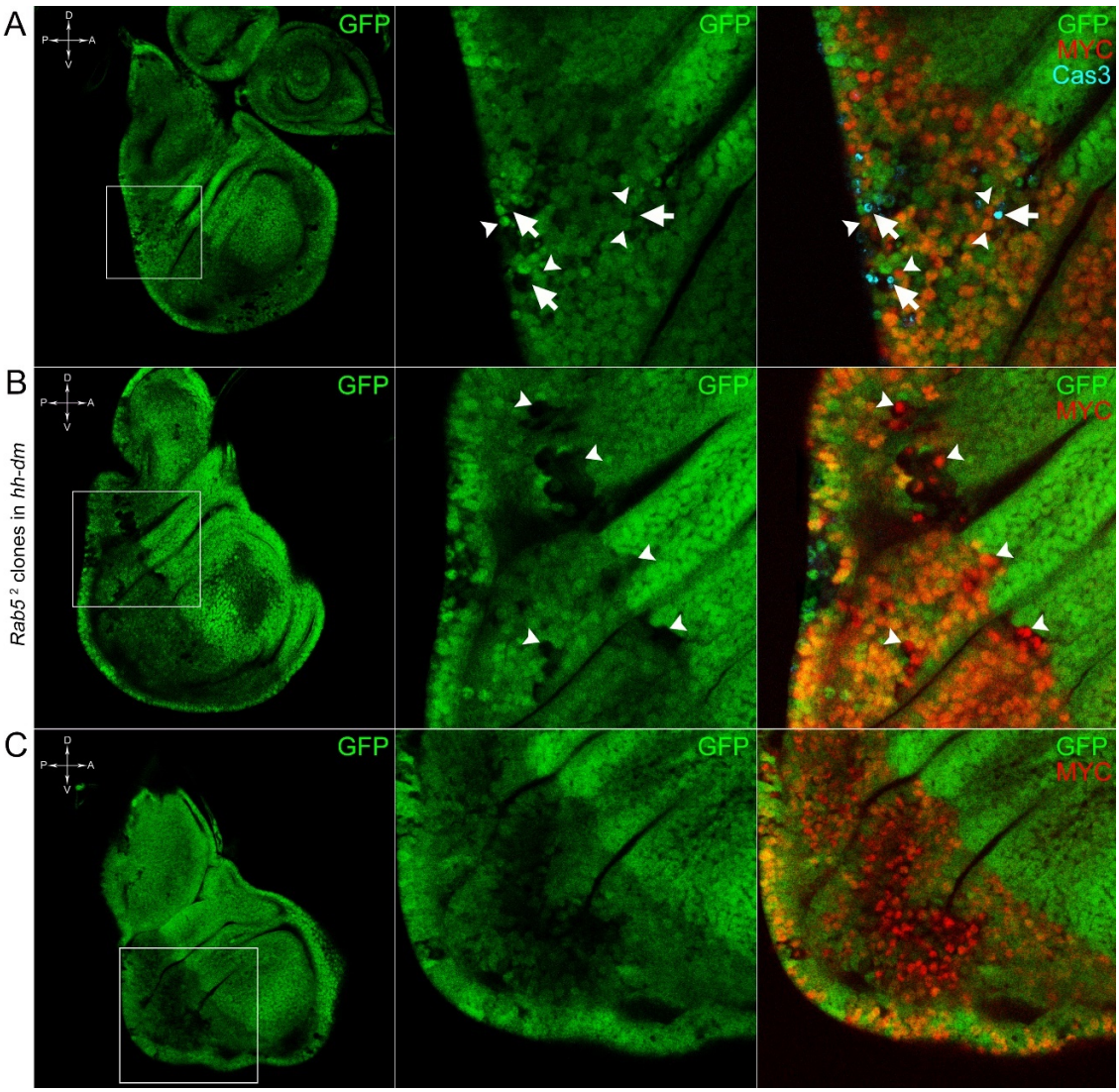

Figure RES-I 14 | *Rab5* mutant clones (GFP$^-$) induced in a *w, hs-Flp/+; Rab5^2, FRT40A/Ubi-GFP, FRT40A; hh-Gal4/UAS-dm* background (GFP$^+$). *wt* twin clones are GFP^{2+}. Magnifications allow a detailed view of cell-cell dynamics in the P compartment. Arrowheads indicate cells with high MYC levels (red), while the arrows show Cas3-positive cells (cyan).

29% of the multifocal wing discs showed a severe phenotype: the organs appeared deeply altered, and I performed aPKC staining to observe possible impacts of multifocal growth on apical-basal cell polarity. As can be observed in Figure RES-I 15, the magnification of the squared region in A shows an altered aPKC localisation (cyan, cells are indicated by the arrows) in *Rab5* mutant cells (GFP^-). In panel B, the impairment of aPKC expression (cyan) is evident across the entire MYC^{OVER} P compartment. This characteristic is consistent with Rab5 function: the endocytic trafficking is indeed essential in the maintenance of cell polarity, and mutations in genes involved in endocytosis provoke the expansion of cell's apical domain in *Drosophila* [199].

Altogether, this evidence indicated that MYC overexpression in a territory of the wing discs is able to promote multifocal malignant lesions following mutation of different TSGs.

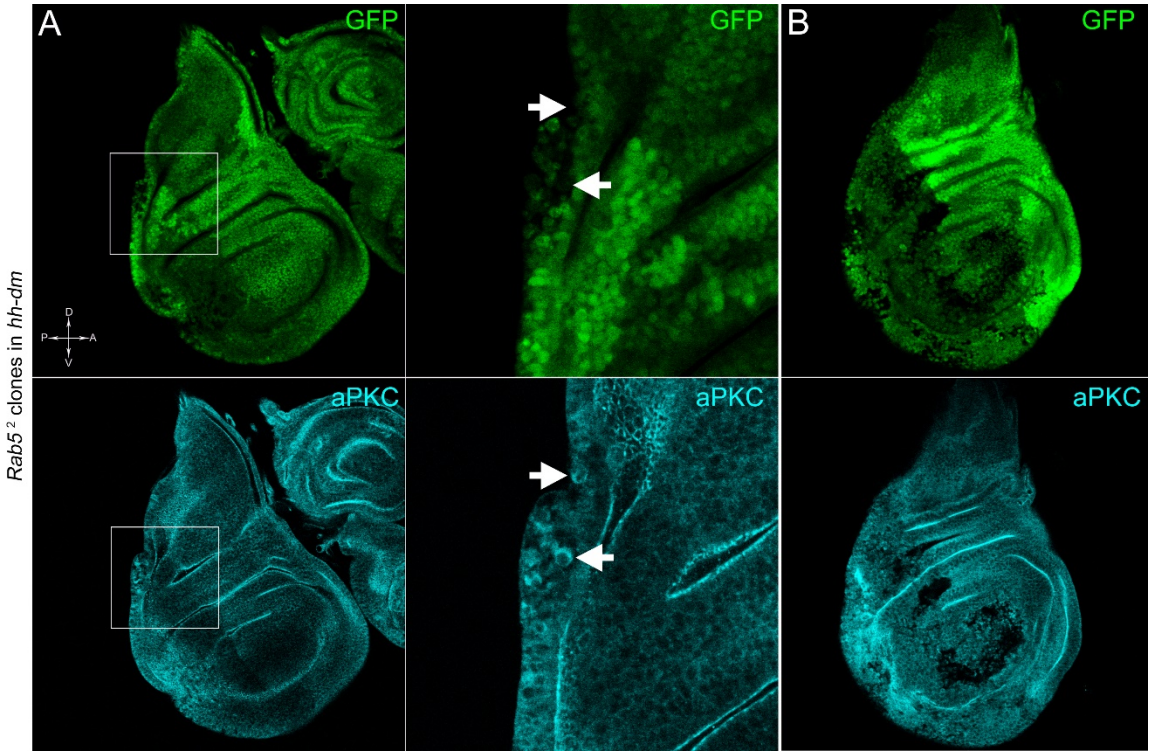

Figure RES-I 15 | *Rab5* mutant clones (GFP^-) induced in a *w, hs-Flp/+; Rab5*^{2}*, FRT40A/Ubi-GFP, FRT40A*; *hh-Gal4/UAS-dm* background (GFP^+). *wt* twin clones are GFP^{2+}. Magnifications allow a detailed view of the P compartment. A: in the magnification, the arrows show cortical expression of aPKC (cyan) in mutant cells (GFP^-). B: aPKC staining (cyan) reveals an impairment in cell polarity throughout the P compartment of the wing disc.

To assess if multifocality may be considered a trait arising from specific properties conferred by MYC to the mutant cells, I repeated the same experiments as above in a PI3K^{CAAX} territory.

Using the same system as above, I overexpressed PI3K^{CAAX} in the P compartment of the larvae and first analysed *lgl* mutant behaviour. In Figure RES-I 16 we can observe two *lgl* mutant clones (GFP^{-}, indicated by the arrows) in the PI3K^{CAAX} P compartment (marked in red by En staining). They are located outside the wing pouch where, instead, we observe the presence of *wt* twin clones (GFP^{2+}) that indicate that mutant clones were eliminated by CC in this region. Therefore, despite the over-expression of PI3K^{CAAX}, *lgl*$^{-/-}$ clones continue to die in this area of the wing discs where MYC is physiologically expressed. A statistical analysis of the clonal areas in the P and A compartments showed that *lgl*$^{-/-}$ mutant clones increased in size in the PI3K^{CAAX} P compartment compared to the mutant clones in the A counterpart (Figure RES-I 16, graph). This evidence confirmed PI3K involvement in cell growth [224].

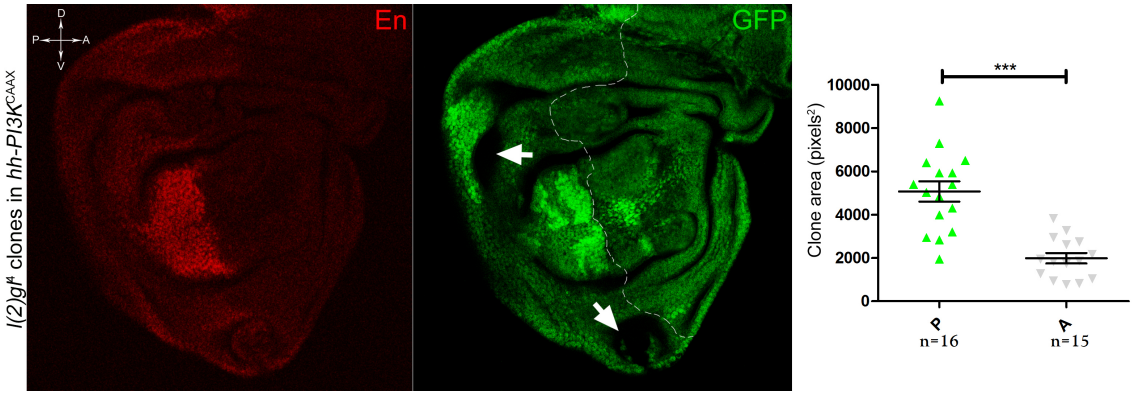

Figure RES-I 16 | *lgl*$^{-/-}$ clones (GFP^{-}) induced in a *w, hs-Flp/+; lgl*^{4}*, FRT40A/Ubi-GFP, FRT40A; hh-Gal4/UAS-PI3K*^{CAAX} background (GFP^{+}). *wt* twin clones are GFP^{2+}. In the left panel, the P compartment is marked by En staining (red). The dotted line indicates the A/P boundary. In the graph, *lgl*$^{-/-}$ clonal areas are shown in P (green) and A (grey) compartments. n are indicated. ***=$p \leq 0.001$.

The most important observation was the total absence of multifocal growth in this system.

I then analysed the behaviour of the *Rab5*^{2} mutation in a PI3K^{CAAX} background. In Figure RES-I 17 the graph (right) indicates that the mutant clones do not show significant growth difference in the P and A compartments. PI3K^{CAAX} overexpression in the P compartment is not sufficient to confer a competitive advantage to *Rab5* mutant cells (GFP^{-}); mutant

clones in the P compartment indeed appear of similar size as those originated in the A compartment (arrows). Finally, no multifocal growth was observed in all the samples analysed.

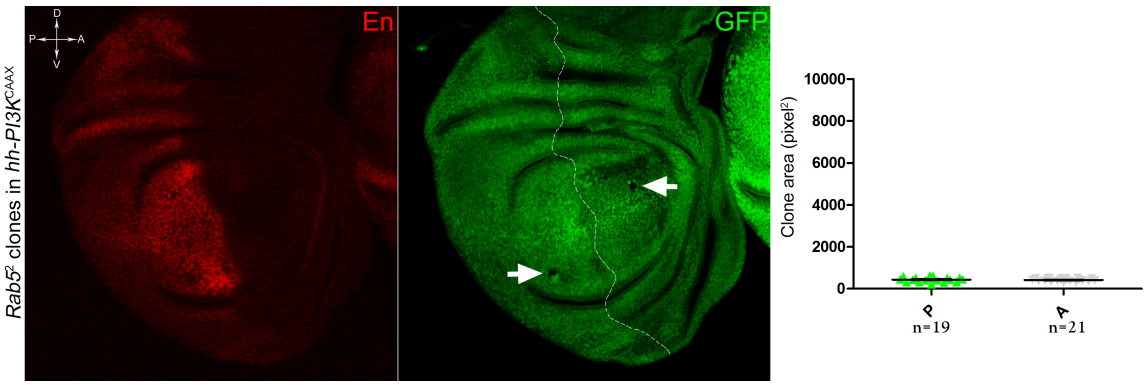

Figure RES-I 17 | *Rab5 mutant* clones (GFP^-) induced in a *w, hs-Flp*/+; *$Rab5^2$, FRT40A/Ubi-GFP, FRT40A*; *hh-Gal4/UAS-$PI3K^{CAAX}$* background (GFP^+). *wt* twin clones are GFP^{2+}. In the left panel, the P compartment is marked by En staining (red). The dotted line indicates the A/P boundary. In the graph, *$Rab5^{-/-}$* clonal areas are shown in P (green) and A (grey) compartments. n are indicated.

These latter findings indicate that MYC may specifically confer *lgl* and *Rab5* mutant cells the capability to grow in a disseminated manner all across the modified territory. This seems to be a specific characteristic of MYC, as the growth inducer PI3K, although increasing *lgl* growth abilities outside of the wing pouch region, did not induce any modifications in mutant cells' behaviour. MYC thus seems to emerge as a good candidate to pioneer pre-cancerous fields by cell competition-mediated tissue colonisation.

METHODS

GENETIC SYSTEMS

UAS-Gal4 [227]

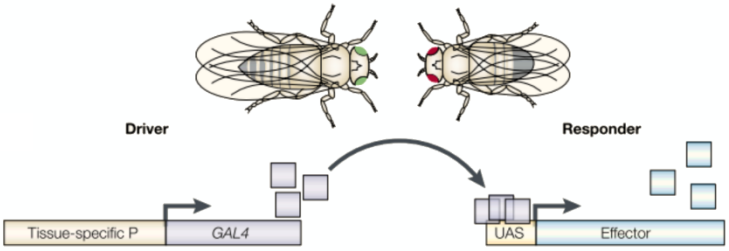

The UAS-Gal4 binary system has represented a true revolution in *Drosophila* gene analysis. This simple tool consists of two genetic elements from *S. cerevisiae*, the Gal4 trans-activator protein and its target Upstream Activating Sequence (UAS). They are specific to each other, and when Gal4 is placed under the control of the desired promoter, the UAS-downstream sequence is transcribed in the desired pattern.

Flp-FRT [228]

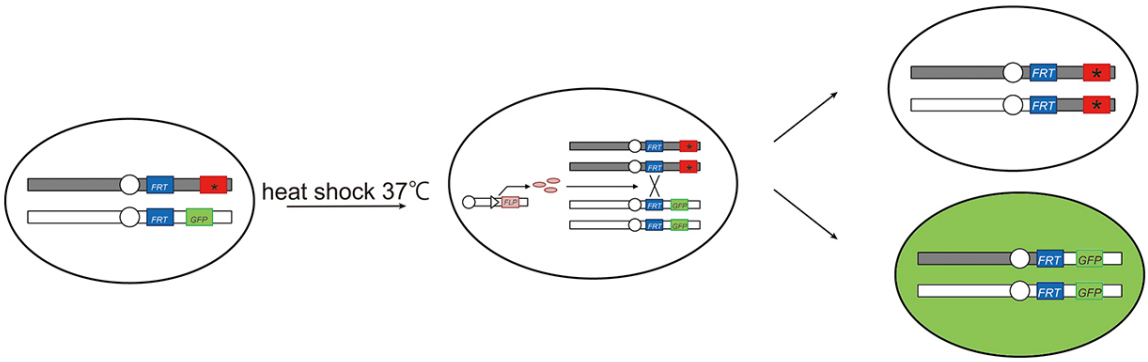

This simple system accounts for mitotic recombination to obtain a pair of genetically different twin cells through arm exchange in somatic tissues. FRT pericentromeric cassettes are recognised, bound and cut by an inducible Flippase and, at mitosis, a cell heterozygous for a recessive mutation and a cell marker (as an example, GFP) will generate a cell homozygous for the mutation (GFP^-) and a cell homozygous for the cell

marker (GFP^{2+}). The background will be GFP^{1+}. This allows phenotypic analysis at a cellular level of recessive lethal genes.

PROTOCOLS, REAGENTS AND STATISTICAL ANALYSIS

Fly manipulation

For Flp-FRT clones, larvae were heat-shocked at 48±4 hours AEL for 10 minutes in a water bath at 37°C and allowed to grow for additional 72 hours at 25°C before being dissected in PBS1X (Phosphate Buffer Saline, pH 7.5) and fixed for 20 minutes in formaldehyde (Sigma) 3.7% in PBS.

Immunofluorescence

Frozen or fresh larvae were permeabilised in PBS-Triton 0,3% for 1-hour RT, blocked for 10 minutes in PBS-Triton 0,3%, 2% BSA (Bovine Serum Albumin, Sigma) and incubated overnight at 4°C in PBS-Triton 0,3%, 2% BSA with primary antibodies. Tissues were then incubated with secondary antibodies for 2-3 hours at room temperature. After opportune washes, imaginal wing discs were isolated from the carcasses and mounted on microscopy slides using the anti-quenching mounting medium FluoromountG (Beckman Coulter). The following antibodies and dilutions were used: mouse α-MYC (1:5 P. Bellosta), rabbit α-active Caspase 3 (1:100, Cell Signalling Technologies), rabbit α-aPKCζ (1:200, sc-216 - Santa Cruz Biotechnology), rabbit α-pAKT (1:100, Cell Signaling), rabbit α-PH3 (1:100, Upstate Technology), mouse α-γH2Av (1:50, DSHB), mouse α-En (1:50, DSHB). Alexa Fluor 555 goat α-mouse and α-rabbit (1:500, Invitrogen) and DyLight 649-conjugated goat α-mouse and α-rabbit (1:800, Jackson ImmunoResearch Laboratories) were used as secondary antibodies. Nuclei were counterstained with DAPI (4',6-diamidine-2'-phenylindole dihydrochloride, Sigma). Samples were analysed with Leica TSC SP2 laser confocal microscope and entire images were processed with Adobe Photoshop software or ImageJ free software from NIH. All the images shown represent a single confocal stack unless otherwise specified. Magnification is 400X unless otherwise specified.

DHE staining for ROS detection

Larvae were dissected in PBS1X and imaginal wing discs were incubated in PBS1X - DHE (Dihydroethidium, Invitrogen Molecular Probes) at a final concentration of 30μM in

gentle shaking, before being fixed for 10 minutes in formaldehyde (Sigma) 3.7% in PBS and imaged immediately.

Statistical analysis

For the analysis of markers associated with field cancerisation, the number of wing discs analysed was 11÷21 from different larvae for each sample. Each experiment was performed at least in triplicate to strengthen statistics. For the experiment as to Figure RES-I 12, the total number of discs analysed was 346, and for the experiment as to Figure RES-I 14, the total number of discs analysed was 158. Mean Fluorescence Intensity and clone area (in $pixel^2$) were measured using ImageJ free software (NIH) on images captured with a Nikon 90i wide field fluorescence microscope at a magnification of 200x. *p*-values are as follows: $p \leq 0.01$=**, $p \leq 0.001$=***. Mean, Standard Deviation and the t-Student test *p*-value were calculated with GraphPad Prism software, San Diego, California, USA.

PART II - GROWTH AND TRACHEOGENESIS ARE SEPARABLE TRAITS IN *DROSOPHILA* CANCERS

Drosophila cancers represent an excellent model to study the molecular basis of carcinogenesis, as a number of genetic tools have been developed by the fly community [229]. As previously described, many human phenotypic cancer traits are functionally conserved in *Drosophila*, and tumour growth and migration are particularly relevant, as they allow development of the primary mass and spreading of tumour cells in different districts of the organism.

My laboratory previously identified MYC as a Hippo downstream target in *Drosophila* [154], and also showed that its overexpression in cells carrying mutations in cell polarity genes was sufficient to confer them a proliferative potential and tumour features [96]. Successively, in *Drosophila* imaginal wing discs we have also found a novel cancer hallmark: tumour-associated tracheogenesis, which is functionally and molecularly analogous to human tumour neo-angiogenesis [136].

Here I have extended our previous work showing that tumour growth and tracheogenesis are separable traits in *Drosophila* epithelia. The Hippo, JNK and Ras/MAPK pathways are essential in cancer progression, and the activity of the two molecules I found involved in growth and tracheogenesis, MYC and FOS respectively, are at the intersection of these signalling cascades.

2.1 MAIN SIGNALLING PATHWAYS INVOLVED IN GROWTH AND MIGRATION IN COOPERATIVE CANCER MODELS

The genetic system I have used in this part of the thesis to model epithelial cancer progression accounts on the oncogenic cooperation between *lgl* LOF and the constitutively active form of Ras (Ras^{V12}). Loss of cell polarity is a well-known alteration that provokes Hippo (Hpo) signalling pathway deregulation [93]; this, in conjunction with Ras signalling activation, triggers uncontrolled growth and proliferation in the mutant cells. Moreover, the Hpo cascade inactivation provokes Yki nuclear translocation, which allows transcription of genes involved in cell proliferation, among which MYC. These mutated cells develop into malignant tumours, in which we observed signs of angiogenesis-like mechanisms [136]. It was also observed that an activation of the JNK signalling cascade confers both migratory and invasion characteristics to tumour cells through MMP1 induction and, in *Drosophila* cancer models, recent studies have found a correlation between the Hpo and JNK pathways in cancer growth and migration [230]. Here I am going to describe these three fundamental networks.

2.1.1 The Hippo Pathway and Its role in Growth Control

Described for the first time in *Drosophila*, the Hpo pathway represents the main regulatory signalling cascade in organ growth and proliferation. It is conserved from *Drosophila* to humans and it is largely involved in cancer development. The Hpo cascade transduces signals from the plasma membrane to the nucleus through its downstream transcription co-activator Yorkie (Yki), which promotes cell proliferation [231]. The Hpo signalling is composed of a central kinase core consisting of four components: two central protein kinases, Hpo and Warts (Wts), that activate the signalling cascade, and two co-factors, Salvador (Sav) and Mob As a Tumour Suppressor (Mats). A functional Hpo signalling leads to Wts phosphorylation, activating its kinase activity [232,233]. The Wts/Mats complex phosphorylates Yki, and sequesters it into the cytoplasm, inhibiting its nuclear functions [234-236].

The Hpo cascade is modulated by a number of upstream signallings, including cell polarity [237]. Hpo regulation by Lgl-aPKC proteins has been shown to be tissue-specific: in

imaginal eye discs, *lgl* knockdown or aPKC activation are not sufficient to hamper cell polarity or to activate the JNK cascade in mutated cell clones but, despite this, there is a mislocalisation of RASSF (Ras-Associated Factors) and Hpo, resulting in Yki activation (Fig. PART-II 1, upper panel). How Lgl-aPKC deregulation influences Hpo in this organ is still an unresolved question [93], and being both Lgl and Hpo also involved in the endocytic trafficking, a hypothesis is that Lgl-aPKC regulate Hpo at the apical membrane where it is activated [238]. In the imaginal wing disc, deregulation of *lgl* or aPKC genes affects cell polarity, and the JNK signalling is required to promote Yki activation [239]: pJNK binds to and phosphorylates Ajuba (Jub), an upstream regulator of the Hpo cascade, which in turn binds to and inhibits Wts (Fig. PART-II 1, lower panel) [240].

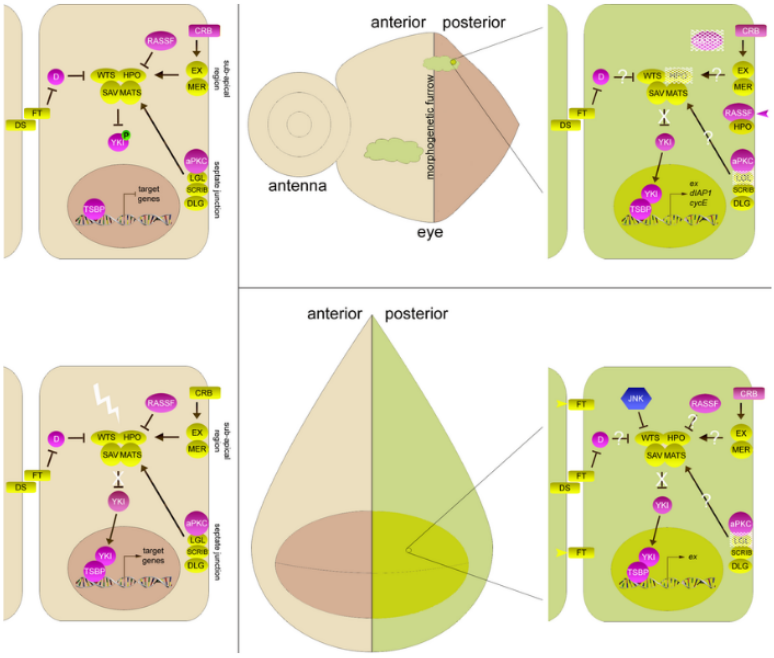

Figure PART-II 1 | Schematic representation of Hippo deregulation in imaginal epithelia: in the upper panel, a schematics of the imaginal eye disc, and, in the lower panel, a schematics of an imaginal wing disc. On the left, the tissue-specific physiological signalling pathways are represented. On the right, the mechanisms that lead to Hpo deregulation in the two epithelial organs following alterations in polarity [241].

The main components of the *Drosophila* Hpo signalling are conserved in mammals, and include Mst1/2 (Hpo homologues) [242], Sav1 (Sav homologue) [243], Lats1/2 and Mob1 A/B (respectively Wts and Mats homologues) [244-248] and finally YAP and TAZ, the Yki homologues [249,250]. Similarly to what happens in *Drosophila*, Mats1/2 and Lats1/2 are regulated by Sav1 and Mob1A/B, and phosphorylate YAP and TAZ (Fig. PART-II 2), [234,251].

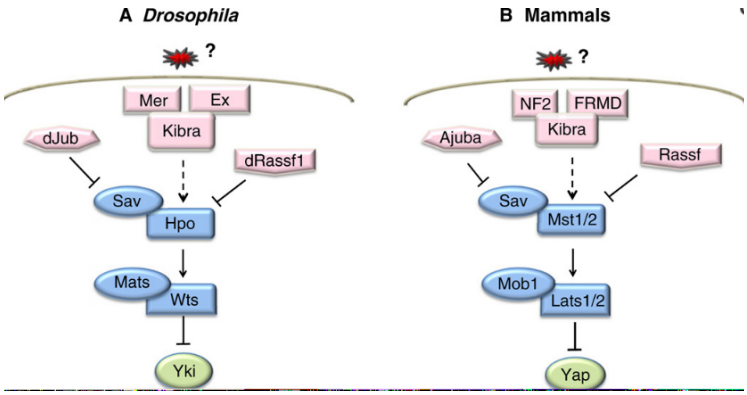

Figure PART-II 2 | The Hippo pathway components in *Drosophila* (on the left) and mammals (on the right) [252].

In *Drosophila*, Yki knockdown reduces the excessive growth caused by mutants of the Hpo core proteins [253], and this property is conserved also in mammals [254]. Therefore, Yki is the final effector of the Hpo cascade and regulates gene transcription. Being a transcriptional co-activator, it binds different tissue-specific partners in the nucleus: in *Drosophila* imaginal wing disc, the Yki main partner is Scalloped (Sd) and, in mammalian cells, the transcriptional factors TEAD 1-4, the orthologues of Sd, are key partners of YAP [255-258]. More recently, other Yki co-transcriptional partners have been found: Homothorax (Hth) and SMAD proteins [259,260].

Alterations in one of the core proteins of the Hpo signalling provoke a release of Yki, which moves to the nucleus and, binding different tissue-specific transcription co-factors, induces the expression of its target genes, such as *CycE*, *dIAP1*, *MYC* and the miRNA *bantam*, resulting in cell proliferation, tissue growth and resistance to apoptotic signals [154,256,261,262]. Hpo pathway deregulation contributes to the excessive growth that characterises the oncogenic cooperation between Ras and polarity genes [106,107]. In *Drosophila* imaginal eye discs, *scrib*$^{-/-}$, Ras^{V12} tumour cells show expression of Yki targets, and its knockdown reduces significantly tumour growth; despite this, mutant clones still display invasive abilities [106]: other pathways are thus possibly involved in this trait.

2.1.2 The Ras/MAPK Signalling Cascade

Ras family proteins belong to the small G protein class. Membrane receptors (such as EGFR) receive extracellular signals and activate Guanine nucleotide Exchange factors (GEFs), which subsequently induce transient Ras expression. Ras promotes activation of several downstream signalling cascades and, in physiological conditions, these signals are inhibited when GTP is hydrolysed to GDP through the GTPase-Activating Proteins (GAPs)[1] [109,263]. Ras signalling pathways are involved in many cellular processes such as growth, proliferation, survival, migration and differentiation, and its mutations are found in about 30% of human tumours. The most represented Ras mutation is its constitutively active form, Ras^{V12} (a Glycine-Valine exchange in position 12 takes place, resulting in a permanent bond with GTP). Mammalian genomes present three forms of Ras that encode H-RAS, K-RAS and N-RAS. Even the *Drosophila* genome contains three Ras genes, but only Ras1 has functional homology with mammalian Ras [109,263,264]. The main downstream effectors of Ras, both in *Drosophila* and mammals, are the Raf/MAPK and PI3K signalling pathways (Fig. PART-II 3) [265].

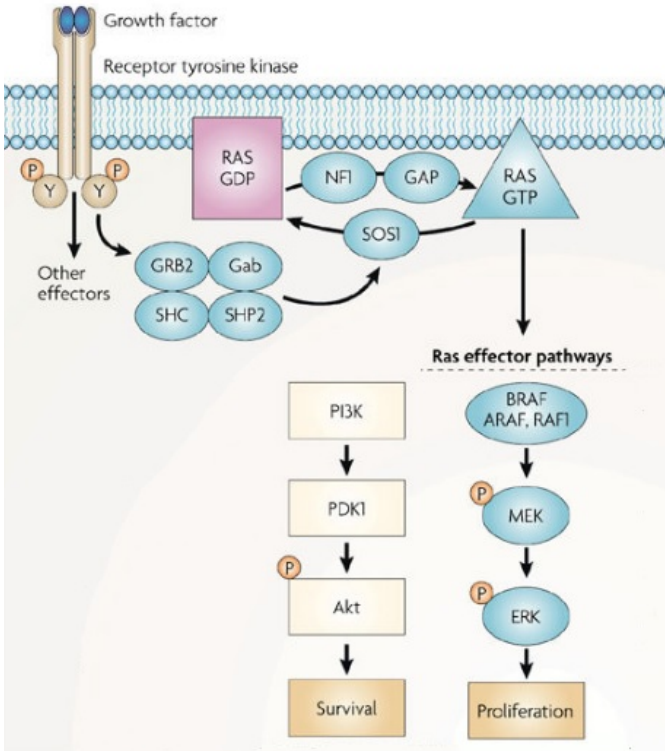

Figure PART-II 3 | Ras regulation and its main downstream signalling pathways (Adapted from Schubbert, Shannon and Bollag, 2007).

Among the Ras downstream signalling cascades, the Raf/MAPK pathway is the most studied. Raf proteins (serine-threonine kinase family) activate the MEK-MAPK cascade. Activated MAPK can phosphorylate the nuclear factors JUN and FOS, whose activation leads to transcription of genes involved in cell cycle control, survival, etc. Raf/MAPK

[1] The GTPase-Accelerating Proteins or GTPase-activating proteins are regulatory proteins which bind to activated G proteins and stimulate their GTPase activity, resulting in signalling arrest.

activation can transform cells into malignant derivatives and Raf activating mutations are frequently found in human tumours [266].

The Ras active form (Ras-GTP) can directly bind the catalytic subunit of PI3K, which moves to the membrane and phosphorylates PIP_2 to PIP_3. PIP_3 is able to activate AKT (a Protein Kinase B), whose activity promotes growth and survival of cells. AKT is found activated in many tumours [266,267].

Activation of the Ras signalling is considered a hallmark of cancer both in fruit flies and mammals. In fact, it promotes proliferation and migration of cancer cells, but also differentiation. For example, in *Drosophila* wing discs Ras triggers cell proliferation and also determines cell fate [104,268]. Very recently, studies in *Drosophila* have shown that the Hpo pathway is essential in determining the output of Ras activity. Hpo deregulation switches Ras pro-differentiation functions into proliferation signals. In the physiology, Hpo controls two Ras target genes maintaining a correct equilibrium between proliferation and differentiation: the Yki-Sd complex directly transcribes Pointed (Pnt) and Capicua (Cic): Pnt allows cells to perceive Ras signalling inputs, while Cic inhibits Pnt function sending cells towards differentiation. Therefore, in healthy cells, the Hpo pathway acts as a tumour suppressor signalling by inhibiting mutated Ras, while Hpo alterations promote hyper-proliferation and tumour development [269]. In cancer, Ras permits cells to increase their proliferative capacity through the transcriptional regulation of growth factors and their receptors, activation of nuclear proteins such as c-MYC and CycD, and inhibition of cell cycle negative regulators [263]. In *Drosophila,* Ras^{V12} ectopic expression is sufficient to induce cell proliferation and hyperplastic growth [270] by increasing MYC and CycE levels [104]. Both Raf/MAPK and PI3K signalling pathways contribute to the inhibition of pro-apoptotic molecules and to the increase of pro-survival factors [263]: an activated Ras signalling is able to block Hid activity [117,271]. Moreover, in mammals, Ras promotes angiogenesis by producing inflammatory cytokines, which trigger the immune response, whose cells release pro-angiogenic factors [263]. Also in *Drosophila*, Ras activation by the FGF/EGFR signalling (VEGF/VEGFR mammalian orthologues) is essential to tracheal cell migration [272] and, as previously described, the *Drosophila* tracheal system is comparable to the mammalian circulatory system.

2.1.3 The JNK Pathway and its Contribution to Cancer

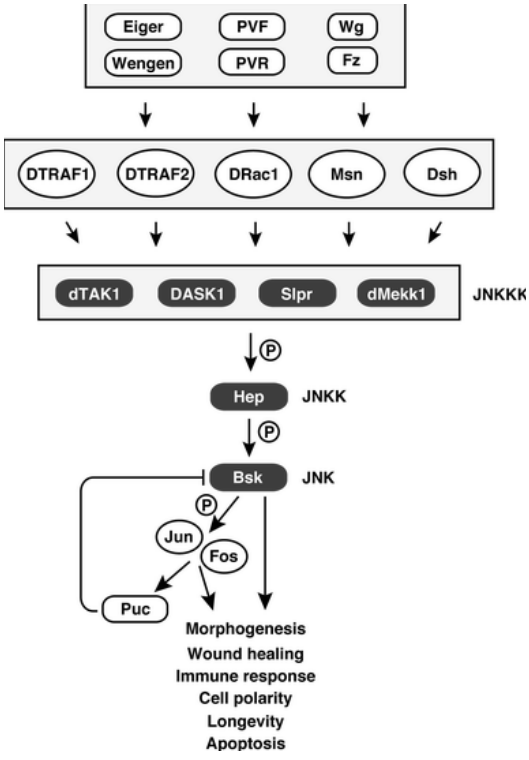

Figure PART-II 4 | The canonical *Drosophila* JNK pathway [352].

The Jun NH_2-terminal Kinase (JNK) signalling pathway is an intracellular kinase cascade involved in fundamental biological processes, among which proliferation, migration, differentiation, morphogenesis and cell death [273]. In *Drosophila*, many conserved members of this signalling pathway have been characterised [274]. It is activated by stress, and its final effector is the AP-1 transcriptional complex composed of Jra (Jun-Related Antigen or dJun) and Fra (or Fos-Related Antigen), encoded by the *kayak* (*kay*) gene [275]. In the fruit flies, only one JNK exists: Basket (Bsk), whose activity is regulated by Hemipterous (Hep is a JNKK, the mammalian MKK7 homologue) phosphorylation [276-278]. Therefore, the JNK signalling core is characterised by Hep→Bsk→Jun/Kay signal transduction [274]. Hep phosphorylation is carried out by upstream JNKKKs (Tak1 and 12, Mekk1, Ask1, Slpr) [279,280]. The JNKKKs can be activated by different stimuli: the Ras superfamily GTPases, members of the JNKKK kinase superfamily such as Misshapen (Msn), or factors binding the Tumour Necrosis Factor (TNF) receptor (Fig. PART-II 4) [279,281-283]. The JNK signalling is inhibited by the phosphatase Puckered (Puc), which is transcribed by the AP-1 complex itself (Fig. PART-II 4) [284].

In *Drosophila,* the pro-apoptotic role of activated JNK is carried out through regulation of *reaper, hid* and *grim*, three pro-apoptotic genes [285] whose activity causes inactivation of the DIAP1 pro-survival protein [286]: in imaginal discs, Rpr-dependent cell death is partially rescued by *bsk* knockdown, indicating a JNK signalling involvement in cell death. DIAP1 usually leads to dTRAF1 (a *Drosophila* JNKKKK) degradation, and being DIAP1 inhibited by Rpr, the apoptotic JNK cascade (dTRAF1→dASK1→Hep→Bsk) is available to transduce the signal [287]. JNK-mediated apoptosis can be also activated by p53, resulting in *rpr* upregulation and, although JNK can trigger apoptosis through *hid* and *rpr* [288,289], JNK-dependent cell death cannot be arrested by caspase signalling

inhibition [290]: this evidence suggests the presence of caspase-independent apoptotic mechanisms downstream of the JNK pathway [291-293].

In *Drosophila* epithelial cancers, JNK cascade activation plays a role both in tumour suppression and promotion [103,133,294]. *lgl, scrib* and *dlg* mutant clones are eliminated by JNK-dependent apoptosis, resulting in tumour containment [103,111,294]. On the contrary, in tumours where apoptosis is blocked by an active Ras signalling [48], JNK cascade activation acts as a tumour promoter by transcribing genes involved in growth and invasion [111,119,295-297]. Activation of JNK signalling in tumour cells increases cell motility through a Fra-dependent release of MMP1: MMP1 inhibition indeed abolished tumour invasion and Fra down-regulation decreased MMP1 levels [111,119]. Cooperation between mutations in polarity genes and activated Ras^{V12} up-regulates MYC levels [96,153], and recent *Drosophila* studies have found that MYC is directly involved in the suppression of tumour invasion: Ma and colleagues have shown that the MYC/MAX complex directly transcribes *puc*, which blocks the JNK cascade, while MYC inhibition promotes JNK activation and tumour cell migration [298]. They also investigated MYC expression in human cancers to associate MYC levels with tumour aggressiveness and, by analysing the Oncomine database, they found that c-MYC levels were lower in metastatic than in non-metastatic tumours [298].

2.2 Cooperative Oncogenesis in *Drosophila* Imaginal Wing Discs as a Model to Study Growth and Tracheogenesis

As previously described, *Drosophila* epithelial tumours have helped explain many fundamental aspects of tumour biology. In *Drosophila*, genetic techniques of clonal induction allow mimicking the onset and progression of human cancer. Mutations in cell polarity genes and in the Ras/Raf/MAPK signalling pathway are found in a high percentage of human cancers, and in *Drosophila* these altered cells are able to survive and proliferate in a *wt* background, ultimately resulting in malignant masses [101-103,263]. In *lgl,* Ras^{V12} cells, the Hpo, Ras/MAPK and JNK pathways are all involved in a number of malignant traits (See 2.1 paragraph). As an example, in *lgl*, Ras^{V12} cells, loss of cell polarity triggers JNK pathway activation, which promotes growth and invasion, the latter through MMP1 expression and consistent degradation of the basement membrane

[111,119,299]. Active Ras signalling inhibits JNK pro-apoptotic activities by stimulating, on the other hand, its pro-invasive properties [300].

It is thus conceivable that a number of cells in the cancer mass up-regulate MYC and contribute to tumour expansion through JNK inhibition [298]. In these cells, the JNK pathway is active and they may implement several strategies to migrate, co-opt vessels and grab oxygen: several phenotypes have indeed been observed which closely resemble those found in angiogenic mammalian tumours [136,137].

RESULTS AND DISCUSSION

PRELIMINARY RESULTS

As described in the dedicated Introduction, our and other laboratories have developed several models of epithelial cancers based on the oncogenic cooperation between LOF mutations in polarity tumour suppressor genes and activated/overexpressed oncogenes [96,101,103,107]. A number of phenotypic traits have been characterised in these models that closely resemble those encountered in human cancers, such as overgrowth [103], basement membrane degradation [96,101], invasiveness [101,102], tracheal co-option and branching [136,137] and capability to trans-differentiate into distinct cell species [136,301]. Many efforts have also been dedicated to the isolation of pathways and molecules supporting these different traits, and key questions are still open about the molecular basis of two opposite cell behaviours: the ability of cancer cells to grow *in situ* and the ability to migrate away from the developing mass. Is one ability the result of cell's incompetence to accomplish the other? And what molecules are found at this crossroad?

Our laboratory previously characterised some basic cancer hallmarks in a clonal model of epithelial neoplasia [136]. Briefly, this model was obtained by combining the LOF of the polarity gene "*lethal giant larvae*" (*lgl*), extensively described in the general Introduction, with an activated form of the *Ras* oncogene, Ras^{V12}. As with other cooperative models, the fundamental traits of the tumour masses were obvious, but during my Master Degree Thesis I contributed to characterise for the first time a number of tracheal modifications supporting tumour growth, such as tracheal branching, tracheal co-option and tracheal mimicry, with tumour cells trans-differentiating in tracheal cells and forming chimeric vessels [136]. Our data defined tracheogenesis as a new hallmark of *Drosophila* cancers, comparable to mammalian tumour-associated angiogenesis, and were successively confirmed by another study [137].

Here I include two figure panels illustrating the essential molecular and structural markers found in *lgl*; Ras^{V12} clonal tumours, necessary to gain a full understanding of the results of this Chapter.

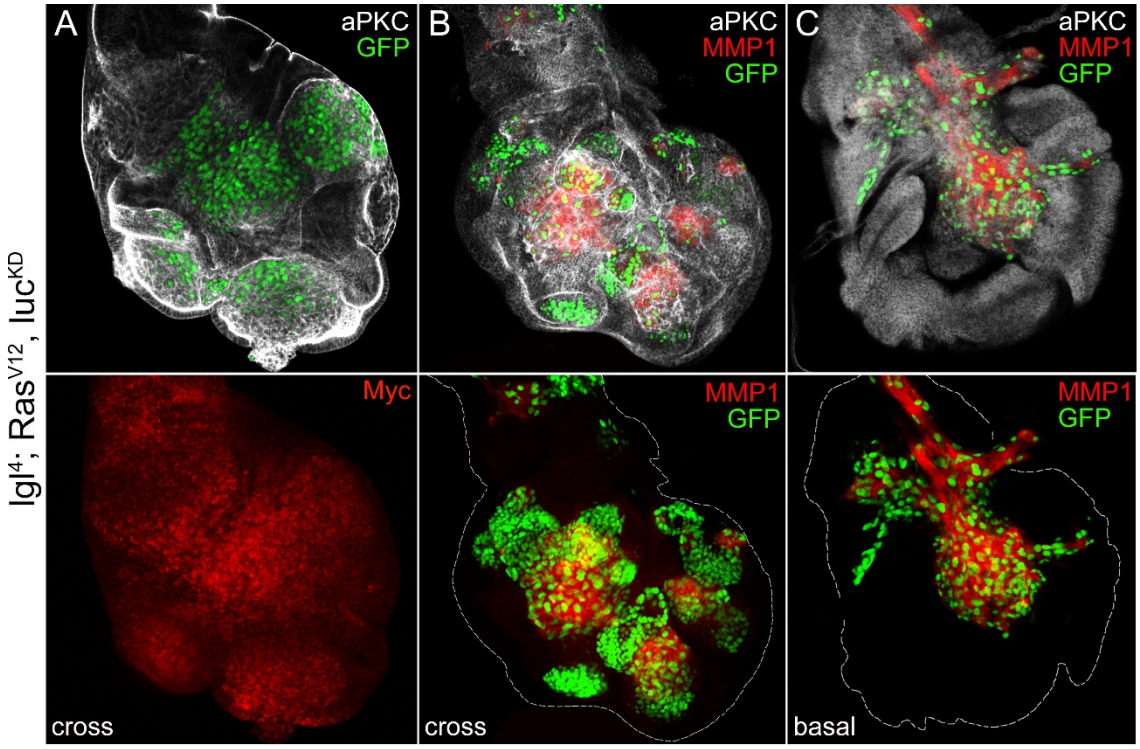

Figure PREL-II 1 | Immunofluorescence staining of wing discs from *yw, hs-Flp, tub-Gal4, UAS-GFP/w; l(2)gl*^{4}*, FRT40A/tub-Gal80, FRT40A; UAS-Ras*^{V12}*, luc*^{KD}*/+* late L3 larvae. Mutant clones are GFP^{+}. A: aPKC (white) is a polarity marker, while MYC oncoprotein (red) marks clone cell nuclei. B: several cancer cells secrete MMP1. C: the basal side of the clone-containing organs shows abnormal tracheal networks mainly composed of cancer cells. Disc profiles are outlined where necessary.

Figure PREL-II 1 displays some basic features of the larval epithelial organs carrying *lgl*; *Ras*^{V12} clonal tumours induced by the MARCM system (see Methods section). The *luc*^{KD} construct has been introduced as an irrelevant dsRNAi to make the collected data comparable with those obtained in the successive experiments. Throughout the chapter, the *lgl*; *Ras*^{V12}, *luc*^{KD} genotype will be referred to as *lgl*; *Ras*^{V12}. GFP-positive mutant cells up-regulate the oncoprotein MYC (Fig. PREL-II 1A, bottom), secrete the metalloprotease MMP1 (Fig. PREL-II 1B) and compose tube-like structures connecting with the endogenous vessels at the basal side of the organ (Fig. PREL-II 1C, adapted from Grifoni *et al.*, 2015). *lgl*; *Ras*^{V12} mutant cells are thus able to grow in a wild-type background, as activated Ras confers *lgl* mutant cell the capability to escape apoptotic death induced by the wild-type neighbours and to form *in situ* masses which alter tissue and organ shape [96,107].

The following panel shows that these mutant cells up-regulate the effector molecules of the main pathways known to be involved in cancer growth modulation.

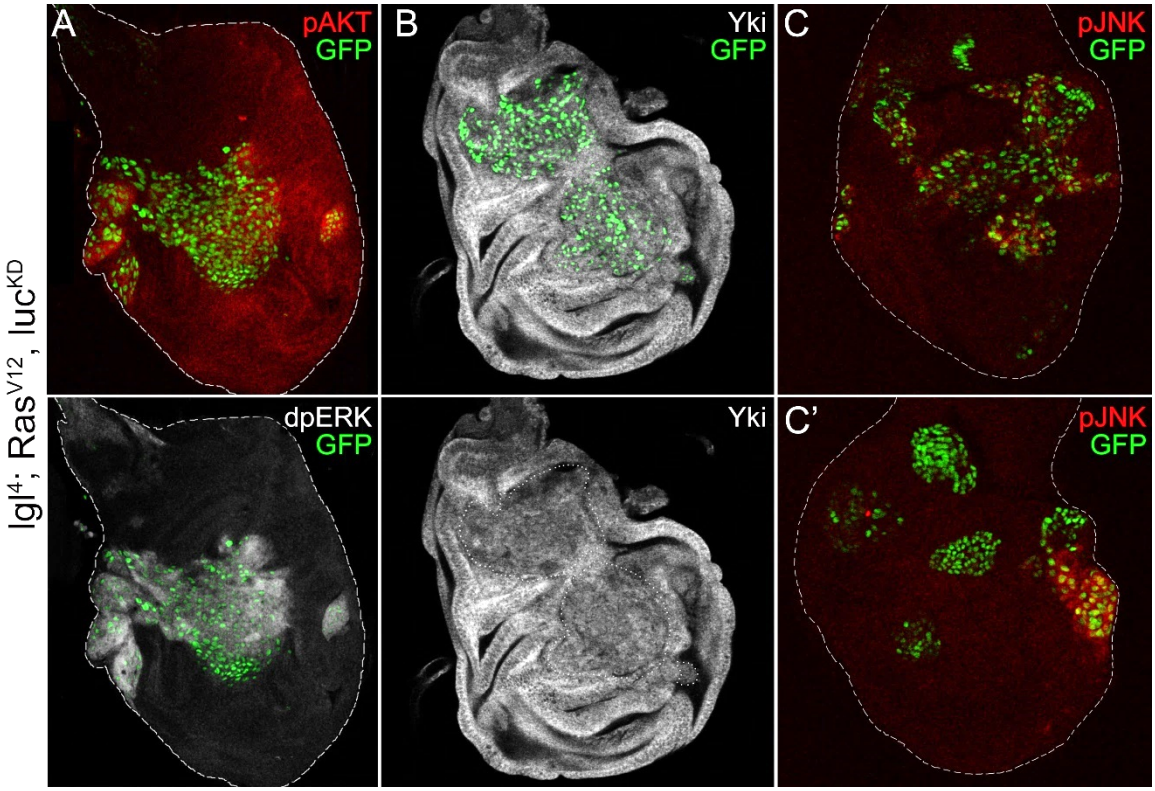

Figure PREL-II 2 | Immunofluorescence staining of wing discs from *yw, hs-Flp, tub-Gal4, UAS-GFP/w; l(2)gl*^{4}*, FRT40A/tub-Gal80, FRT40A; UAS-Ras*^{V12}*, luc*^{KD}/+ late L3 larvae. Mutant clones are GFP^{+}. A: pAKT (upper, red) is a PI3K-effector molecule activated by Ras, while dpERK (bottom, white) is the final MAPK. B: cancer cells show reduced nuclear exclusion of Yki (white), the effector molecule of the Hpo pathway. Clone profile is outlined in B, lower panel. C, C': some mutant cells/clones display from mild to high pJNK levels (red). Disc profiles are outlined where necessary.

As can be appreciated in Figure PREL-II 2A, upper panel, some mutant cells up-regulate pAKT, the main effector of PI3K, that is in turn regulated by activated Ras [104]. Despite this, findings obtained in my lab demonstrate that the essential traits of *lgl*; *Ras*^{V12} mutant cells are conserved following PI3K knockdown; as a confirmation, tumour phenotypes are fully recapitulated in organs carrying *lgl*; *Raf* ^{Act} mutant cells, which do not show pAKT activation [302]. As expected, *lgl*; *Ras*^{V12} mutant cells show a potent up-regulation of the final MAPK dpERK (Fig. PREL-II 2A, lower panel, white), and the Hpo pathway downstream co-activator Yki shows partial nuclear localisation in the mutant cells (Fig. PREL-II 2B, white), as already observed in other studies [107,301]. Finally, some groups of *lgl*; *Ras*^{V12} cells up-regulate the final effector of the c-Jun N-terminal signalling cascade, pJNK (Fig. PREL-II 2C-C', red), and this may sustain Yki activation downstream of mutated Ras through inhibition of the core kinase Warts (Wts), as it has been recently observed by Enomoto and colleagues [303].

RESULTS AND DISCUSSION

In this Chapter, I will describe my work aimed at understanding the cell-autonomous molecular basis of a cancer cell's tendency to contribute to the primary mass or to form secondary structures such as tracheal-like vessels. As introduced in the preliminary results, a number of pathways involved in mammalian cancer growth are found dysregulated in *lgl*; Ras^{V12} mutant cells. In the attempt to genetically dissect the pro-growth and pro-tracheogenic behaviours of the *lgl*; Ras^{V12} cells, I knocked the different pathway effectors down and evaluated the rescue or the worsening of each trait.

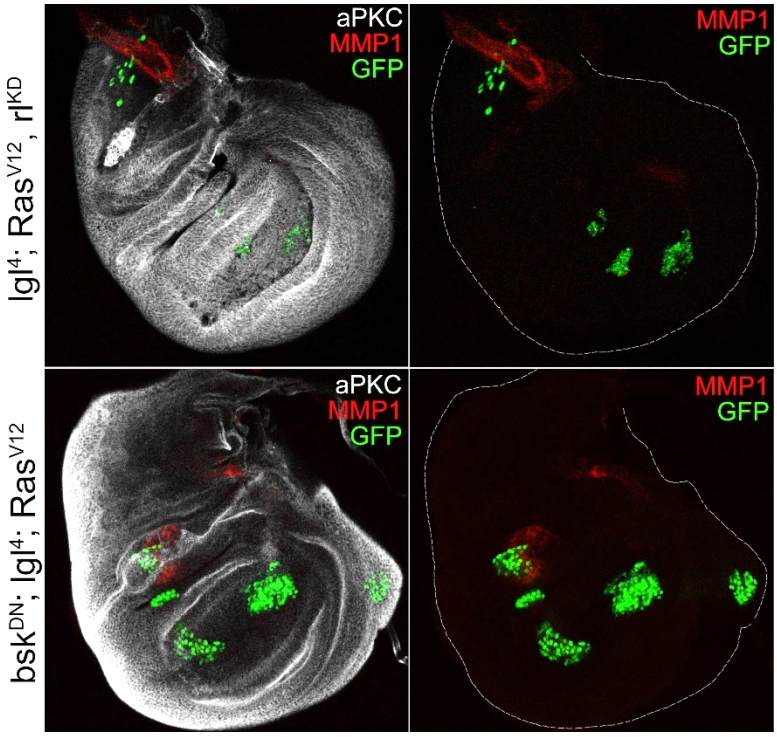

Figure RES-II 1 | Upper panel: immunofluorescence staining of wing discs from *yw, hs-Flp, tub-Gal4, UAS-GFP/w; l(2)gl^4, FRT40A/tub-Gal80, FRT40A; UAS-rl^{KD}/UAS-Ras^{V12}* late L3 larvae. Mutant clones are GFP$^+$. aPKC is marked in white, and no GFP$^+$ cells secrete MMP1 (red). Lower panel: immunofluorescence staining of wing discs from *yw, hs-Flp, tub-Gal4, UAS-GFP/w, UAS-bsk^{DN}; l(2)gl^4, FRT40A/tub-Gal80, FRT40A; UAS-Ras^{V12}/+* late L3 larvae. Mutant clones are GFP$^+$. aPKC is marked in white, and some GFP$^+$ cells in the proximal disc secrete MMP1 (red). Disc profiles are outlined where necessary.

As can be seen in Figure RES-II 1, upper panel, *lgl*; Ras^{V12} mutant cells knocked down for *rolled* (*rl*), the gene encoding the core component of the Ras/MAPK pathway Mitogen-Activated Protein Kinase (MAPK), also called Extracellular signals-Regulated Kinase (ERK) [304], are no more able to form large masses, nor do they form tube-like structures connecting with resident vessels. Consistently, the protease MMP1 delineates

an endogenous tracheal vessel in the *notum* region [305], but no staining is detectable in the epithelium (upper-right figure). A statistical analysis of the clonal areas revealed that the average clone dimensions of the *lgl*; Ras^{V12}, rl^{KD} cells is 10-fold smaller than the *lgl*; Ras^{V12} counterparts (see Fig. RES-II 7). Moreover, no significant differences are seen compared to the *wt* controls. In light of this evidence, I concluded that the MAPK pathway effector transduces both growth and tracheogenic signals in *lgl*; Ras^{V12} transformed cells.

I then investigated the contribution of the JNK pathway to the *lgl*; Ras^{V12} tumour phenotype, by inhibiting the final effector pJNK, that in *Drosophila* is encoded by the *basket* (*bsk*) gene [306]. The JNK signalling pathway has indeed been shown to be involved in tumour growth in different cancer contexts in *Drosophila* [103,111,119,136,294,296,298,303,307,308]. Figure RES-II 1, lower panel, shows a larval wing disc displaying bsk^{DN}; *lgl*; Ras^{V12} clones (GFP^{+}). As can be appreciated, the mutant clones are severely restricted with respect to the *lgl*; Ras^{V12} clones (see Fig. PREL-II 1 for a comparison), showing an average 3-fold reduction in size. With regard to the tracheogenic phenotype, although I observed some epithelial cells expressing MMP1, no tube-like neo-structures were found at the basal side of the discs analysed.

In this case, the growth rescue was less impressive than that seen following MAPK inhibition (see Fig. RES-II 7), but bsk^{DN}; *lgl*; Ras^{V12} clones showed the same roundness coefficient as that of the MAPK-inhibited ones (0.34), lower than that shown by *wt* clones (0.42), indicating poor capacity to form three-dimensional structures (see Table RES-II 1 at the end of the Chapter). Roundness is indeed a parameter of non-*wt* shape and characterises both hyperplastic and neoplastic growth.

In conclusion, either MAPK or JNK inhibition rescued the ability of *lgl*; Ras^{V12} mutant cells to form large and confluent clones and to participate in tracheogenic rearrangements during cancer evolution.

The Hpo pathway, as described in the dedicated Introduction, is an evolutionarily conserved protein network whose components are able to intercept extracellular and intracellular signals and transduce them into plastic cell behaviours [309]. The Hpo pathway may thus be considered as a key modulator in cancer, with different actors modifying

different behaviours in different tissues [310]. As a consequence of Yki knockdown in *lgl*; Ras^{V12} clones, I observed an about 3-fold reduction of the average clone dimensions, similar to that observed following JNK inhibition (see Fig. RES-II 7). As can be seen in Figure RES-II 2, upper panel, some *lgl*; Ras^{V12}, yki^{KD} clones secrete MMP1 (red) and some lose MYC protein expression (red, lower panel, outlined). This was not surprising, as my laboratory previously demonstrated that MYC is a transcriptional target of Yki [154] and c-MYC and YAP show mutual regulation either in the fly [153] or in humans [311]. Table RES-II 1 summarises the fundamental behaviours of these mutant cells, and while growth resulted significantly reduced across the whole disc, MYC expression and cell polarity showed position-dependent phenotypes.

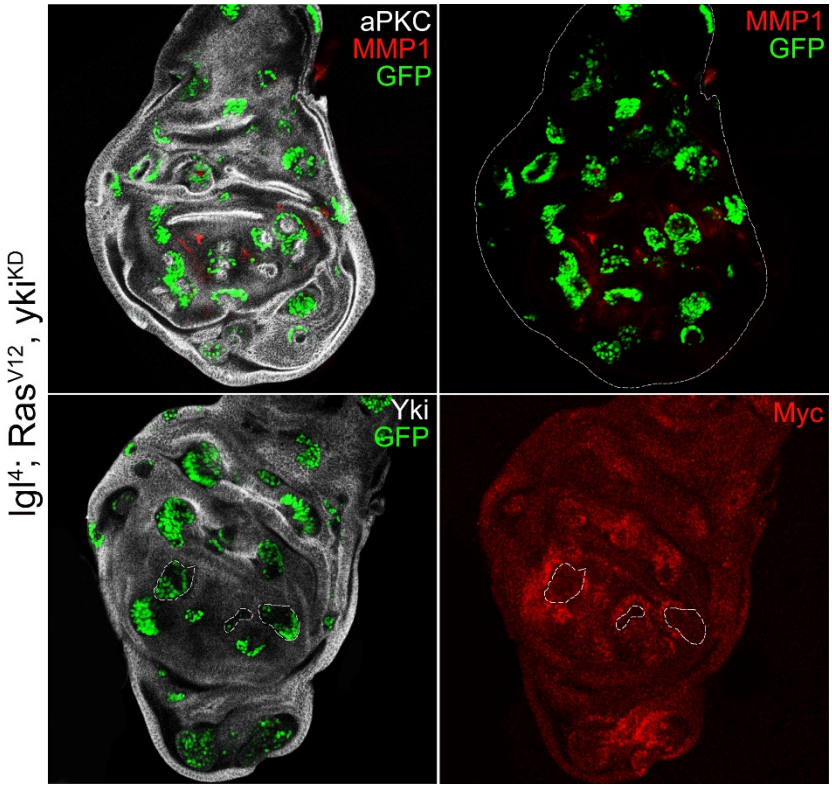

Figure RES-II 2 | Immunofluorescence staining of wing discs from *yw, hs-Flp, tub-Gal4, UAS-GFP/w; l(2)gl^{4}, FRT40A/tub-Gal80, FRT40A; UAS-yki^{KD}/UAS-Ras^{V12}* late L3 larvae. Mutant clones are GFP^{+}. Upper panel: aPKC is marked in white, and some mutant clones secrete MMP1 (red). Lower panel: Yki is marked in white, and some clones showing low MYC levels are outlined in the lower-right panel. The panel shows apical-cross sections of the wing disc. Disc profiles are outlined where necessary.

Concerning the tracheogenic phenotype, a surprising cell behaviour was observed at the basal side of these disc: MMP1 staining revealed that *lgl*; Ras^{V12}, yki^{KD} cells are able to migrate across the disc depth and form tube-like structures capable to connect with pre-

existing tracheal vessels (outlined in red in Fig. RES-II 3). This happened predominantly in the wing pouch region, where some of the mutant clones shown in Figure RESII-2, upper panel, displayed MMP1 secretion. In Figure RES-II 3, lower panel, a mutant clone grown wrapped around a tracheal branch is also shown (arrowhead), a typical case of vessel co-option as those found in *lgl*; *Ras*^{V12} samples [136].

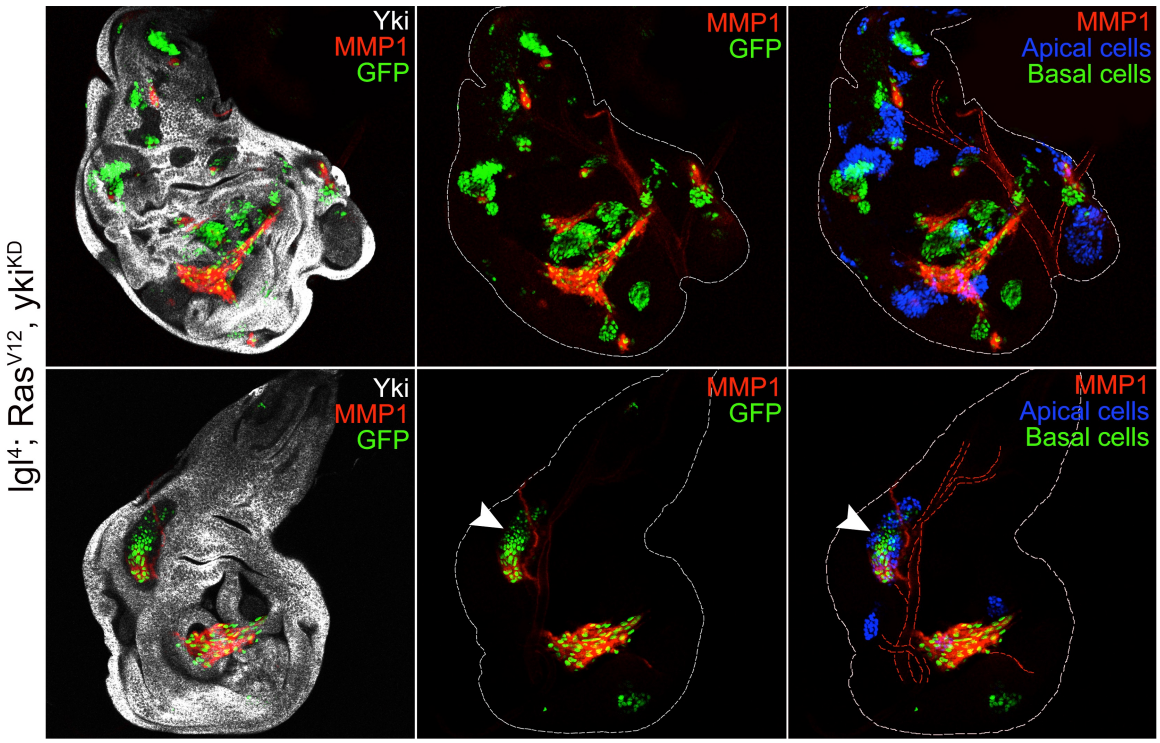

Figure RES-II 3 | Immunofluorescence staining of wing discs from *yw, hs-Flp, tub-Gal4, UAS-GFP/w; l(2)gl*^{4}*, FRT40A/tub-Gal80, FRT40A; UAS-yki*^{KD}*/UAS-Ras*^{V12} late L3 larvae. Mutant clones are GFP^{+}. Yki is marked in white, and mutant cells form tube-like structures while secreting MMP1 (red). The arrowhead indicates a clone wrapped around a tracheal vessel. In the right panel, the apical clones are false-coloured in blue. The panel shows basal sections of the wing disc. Disc profiles are outlined where necessary.

Hpo pathway inhibition was thus extremely informative about the possibility to find different cascades involved in growth and tracheogenesis in our cancer model. Yki knockdown was indeed sufficient to restrict the growth of *lgl*; *Ras*^{V12} cells, but it did not hamper cell migration and propensity to form vessels during tumour evolution.

The Hpo pathway is known to regulate/be regulated by the Ras/MAPK and JNK cascades in many ways: as an example, the Ajuba LIM protein (Jub) is known to be activated by phosphorylation both by dpERK and pJNK in *Drosophila* and mammals, and activated Jub binds the Warts/LATS core kinase and recruits it to junctions, thus promoting Yki/YAP activity [240,312,313].

My laboratory previously investigated the impact of Jub knockdown on the behaviour of *lgl*; Ras^{V12} clones, but no significant differences in growth and/or tracheogenesis were found [302], suggesting that other mechanisms are at work in the modulation of these specific traits in our cancer model.

It has recently been shown that Ras signalling activates a series of transcription factors whose output is modulated by the Hpo downstream effector Yki [269,314]. One of these factors is the oncoprotein MYC, which results up-regulated in most *lgl*; Ras^{V12} cells (Fig. PREL-II 1, lower panel). Activated Ras is indeed known to increase MYC protein levels in the wing disc [104], and mammalian c-MYC is phosphorylated and stabilised by activated ERK [315]. Moreover, c-MYC activity is regulated by pJNK at the post-transcriptional level [316], and *Drosophila* MYC is known to inhibit JNK signalling by activating transcription of the downstream pathway inhibitor *puckered* (*puc*) [298]. Finally, MYC is a transcriptional target of Yki [153,154] and yki^{KD} in *lgl*; Ras^{V12} cells down-regulates MYC in the wing pouch region, where these same clones express MMP1 and show the capability to originate tube-like templates and connect with endogenous vessels (Fig. RES-II 3).

I thus investigated the impact of *dm* (*diminutive*, *dm*, is the *locus* encoding the MYC protein [142]) knockdown on *lgl*; Ras^{V12} cell behaviour.

Figure RES-II 4 illustrates the growth phenotype of *lgl*; Ras^{V12}, dm^{KD} mutant clones and, as can be seen, growth was severely restricted throughout the wing disc and completely abolished in the wing pouch region. In particular, apical, sub-apical and cross sections of the discs are shown, where the most part of stably growing clones are usually found. This incredible growth deficit was in line with the essential functions of MYC in cell proliferation and cell growth [146,317-319], but mass collapse is also known to occur in mammalian cancers following MYC inhibition [320,321]. This is the reason why MYC family proteins are considered promising targets in cancer therapy [322,323].

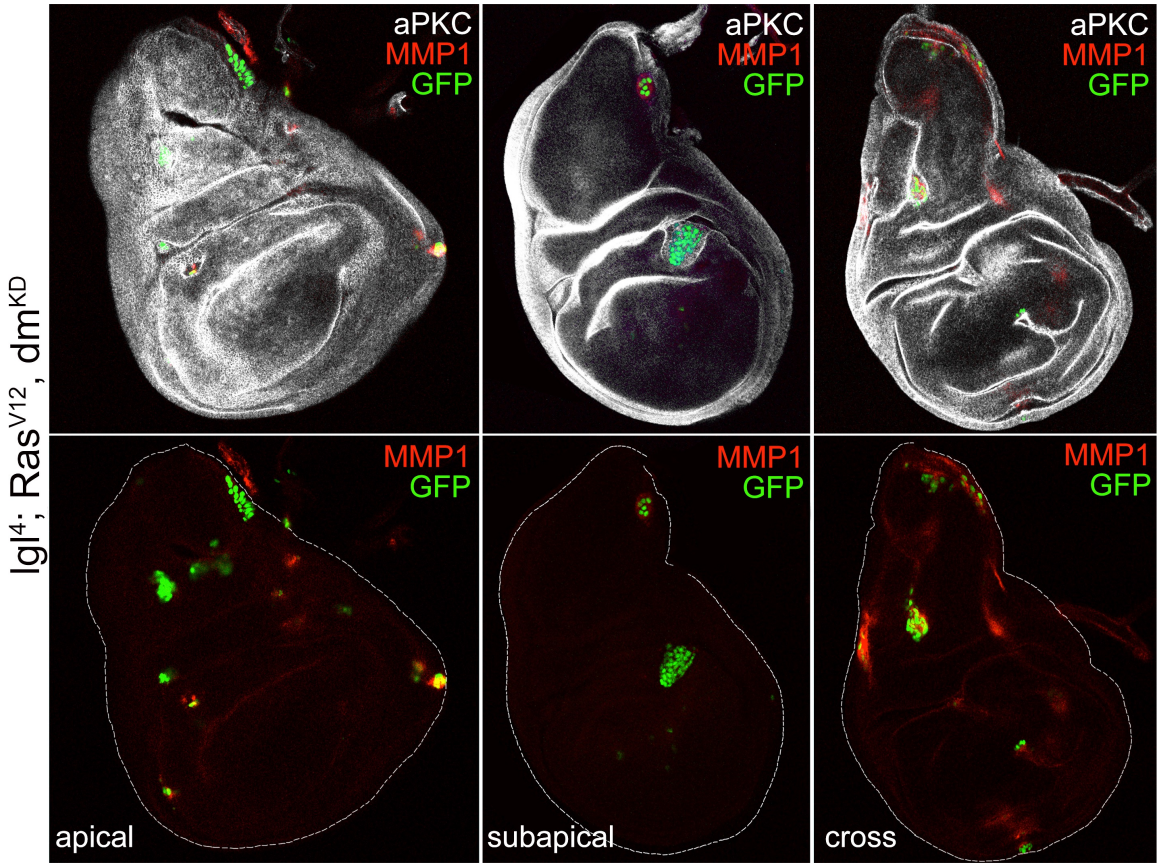

Figure RES-II 4 | Immunofluorescence staining of wing discs from *yw, hs-Flp, tub-Gal4, UAS-GFP/w; l(2)gl*^{4}*, FRT40A/tub-Gal80, FRT40A; UAS-Ras*^{V12}*, UAS-dm*^{KD}/+ late L3 larvae. Mutant clones are GFP^{+}. aPKC is marked in white, and some mutant cells secrete MMP1 (red). The panel shows apical-to-cross sections of the wing disc. Disc profiles are outlined where necessary.

Such as it happened with *yki*^{KD}, the severe growth deficit of *lgl*; *Ras*^{V12}, *dm*^{KD} mutant clones across the disc depth was associated with an amazing migration of the mutant cells towards the basal side of the disc, where they originated tubular structures interconnecting a number of mutant clones (Fig. RES-II 5, arrowheads) and/or connecting with existing tracheal vessels (Fig. RES-II 5, arrows). It is worth underlining the complete penetrance of this phenotype, obtained using two different RNAi constructs (see Methods).

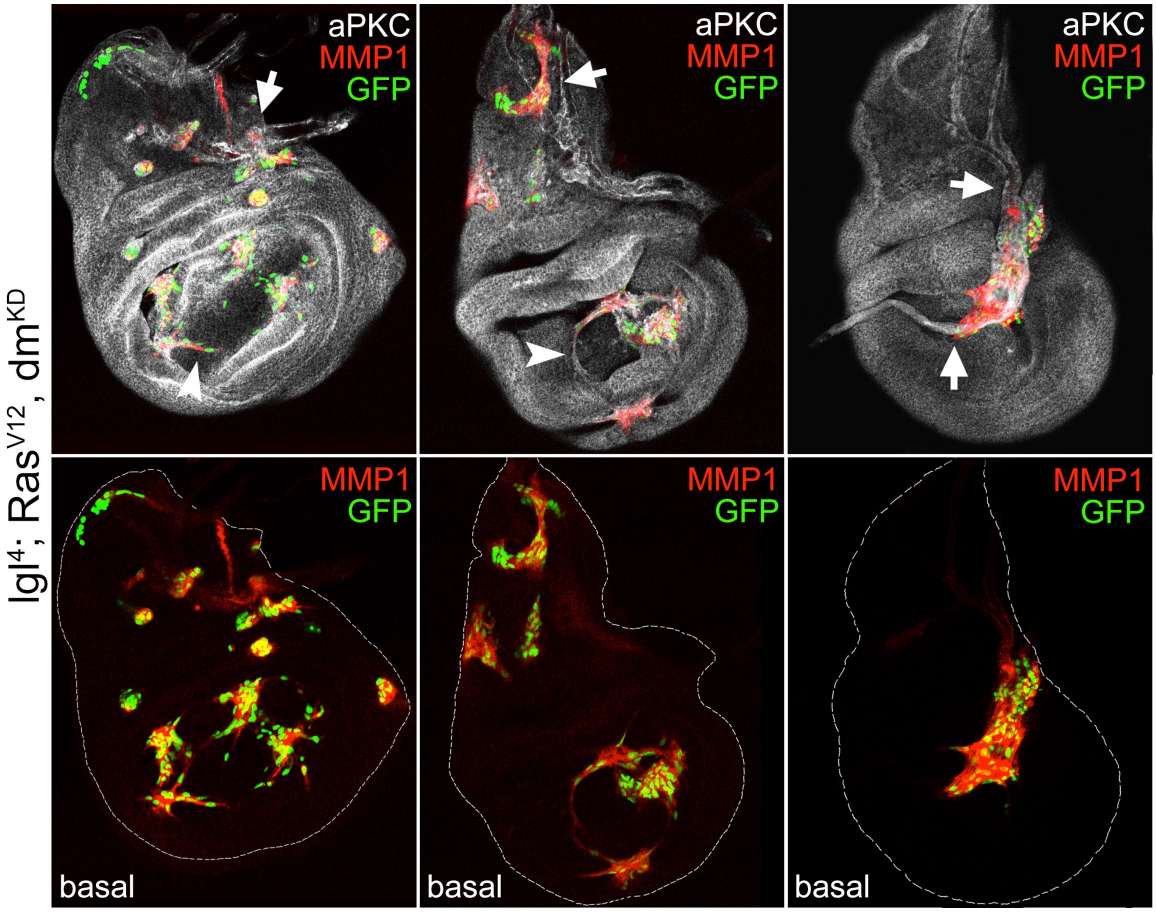

Figure RES-II 5 | Immunofluorescence staining of wing discs from *yw, hs-Flp, tub-Gal4, UAS-GFP/w; l(2)gl*^{4}*, FRT40A/tub-Gal80, FRT40A; UAS-Ras*^{V12}*, UAS-dm*^{KD}*/+* late L3 larvae. Mutant clones are GFP^{+}. aPKC is marked in white, and mutant cells form tube-like structures while secreting MMP1 (red). Arrowheads indicate mutant cells organised in a tubular shape. Arrows indicate mutant cells connecting with resident vessels. The panel shows basal sections of the wing disc. Disc profiles are outlined where necessary.

These findings were convincing evidence that MYC is necessary for the *in situ* growth of *lgl*; *Ras*^{V12} cells; its deprivation induces a hyper-migratory behaviour of these cells, possibly mediated by JNK activation, such as it has recently been shown in other systems [298]. This aspect has to be seriously taken into account while considering MYC as an attractive target for anti-cancer therapy.

As ERK and JNK knockdown were both able to rescue either growth or tracheogenesis, although at different levels (see Table RES-II 1 and Fig. RES-II 7), some common targets were supposed to be responsible for the migratory phenotype.

I concentrated my attention on Fos-Related Antigen (FRA, encoded by the *kayak* - *kay* - gene in *Drosophila*), as it is known to be post-transcriptionally regulated by both ERK and JNK by phosphorylation on distinct residues during fly development [324]. Moreover, FRA and MYC were found among a handful of transcription factors that drive malignant growth of Ras^{V12} $scrib^{-/-}$ tumours [314].

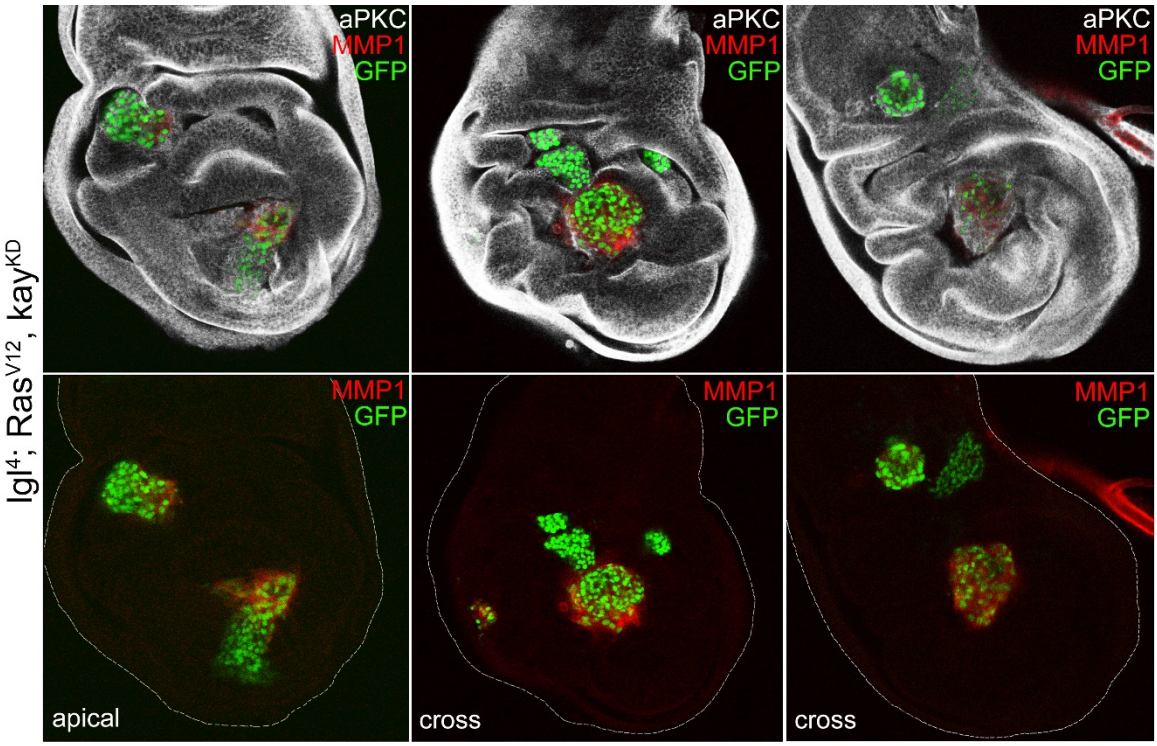

Figure RES-II 6 | Immunofluorescence staining of wing discs from *yw, hs-Flp, tub-Gal4, UAS-GFP/w; l(2)gl*^{4}*, FRT40A/tub-Gal80, FRT40A; UAS-Ras*^{V12}*, UAS-kay*^{KD}*/+* late L3 larvae. Mutant clones are GFP^{+}. aPKC is marked in white, and mutant cells secrete MMP1 (red). The panel shows apical-to-cross sections of the wing disc. Disc profiles are outlined where necessary.

As can be seen in Figure RES-II 6, *kay* ^{KD} does not seem to hamper growth of *lgl*; Ras^{V12} cells. A statistical analysis showed that the average *lgl*; Ras^{V12}, *kay* ^{KD} clone size does not differ significantly from that of the *lgl*; Ras^{V12} samples (Fig. RES-II 7). Other traits associated with overgrowth, such as roundness, loss of apical-basal cell polarity and MYC up-regulation, were also comparable to those of the original *lgl*; Ras^{V12} model (Table RES-II 1). MMP1 secretion was severely reduced compared to the *lgl*; Ras^{V12} samples, but this was expected, as FRA is known to regulate MMP1 transcription downstream of the JNK signalling [119]. Differently to what happened with *lgl*; Ras^{V12} cells, the most part of the *lgl*; Ras^{V12}, *kay* ^{KD} cells were found to compose the primary masses:

no cell scattering and no tube-like structures were indeed found throughout the organ, and very few MMP1-positive cells reached the basal side of the discs.

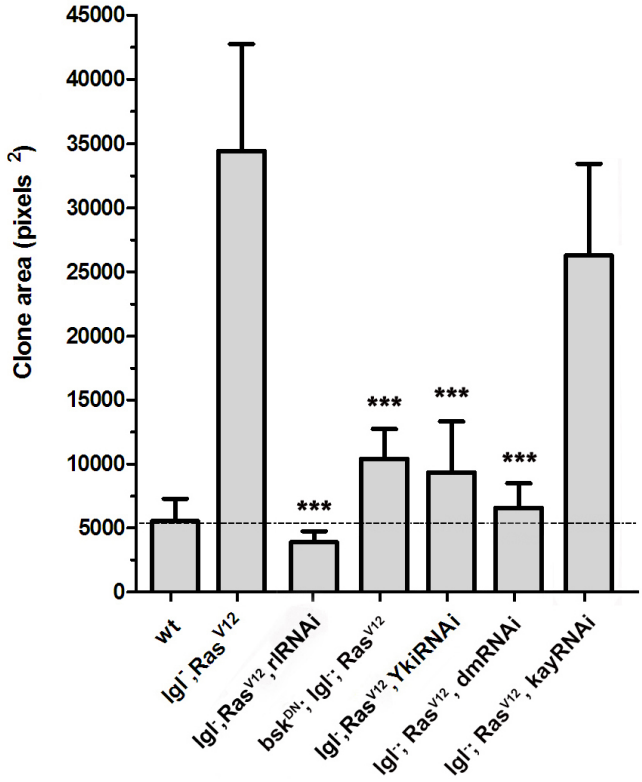

Figure RES-II 7 | A graph shows the average clone area of all the genotypes analysed, sampled all across the imaginal wing disc. The dotted line refers to the area of wild-type clones. Error bars indicate the standard deviation of the mean; n=25-40 each genotype. All the comparisons are statistically significant (***=$p \leq 0{:}001$) respect to the *lgl; Ras^{V12}* samples, except for *lgl; Ras^{V12}, kay^{KD}*.

Table RES-II 1 | A summary of the malignant traits analysed for each genotype. The legend describes the symbols used in the Table.

Clone genotype	Roundness§	A/B polarity loss	Myc expression	Migration/ tracheogenesis
wild-type	0.42	no	~	no
lgl^{-}, Ras^{V12}	0.82	yes	↑(iv)	yes
lgl^{-}, Ras^{V12}, rlRNAi	0.34	no	v	no
bsk^{DN}, lgl^{-}, Ras^{V12}	0.34	no	~	no
lgl^{-}, Ras^{V12}, YkiRNAi	0.47	v	v	yes
lgl^{-}, Ras^{V12}, dmRNAi	0.38	no	-	yes
lgl^{-}, Ras^{V12}, kayRNAi	0.75	yes	↑	no

§ roundness = 1 for perfect circles
↑↓ increased/decreased
~ comparable to surrounding tissue
- not determined
v variable - clone position effect
iv intra-clone variability

n = 25÷40

To quantify the observations concerning the tracheogenic behaviour, I established a Tracheogenic Index (TI), calculated as the ratio between the MMP1-positive clone area found at the disc basal side (where the transverse connective tracheal trunk is found) and the total (apical+basal) clone area. The analysis was performed considering the whole GFP^+ cells present in the wing pouch region. As an example, Figure RES-II 8 represents a wing disc containing *lgl*; Ras^{V12}, dm^{KD} cells. The upper panel shows an apical section of the disc, whose GFP^+ cells represent the "Growth area". The lower panel displays a basal section of the same disc, where the GFP^+ cells represent the "Tracheogenic area". The four images marked with progressive numbers show an apical-to-basal sequence with the GFP^+ area from the previous figure coloured in red. As can be appreciated from the merging yellow areas, cells form a continuum from the apical towards the basal side of the disc, where the most part of the mutant cells resides.

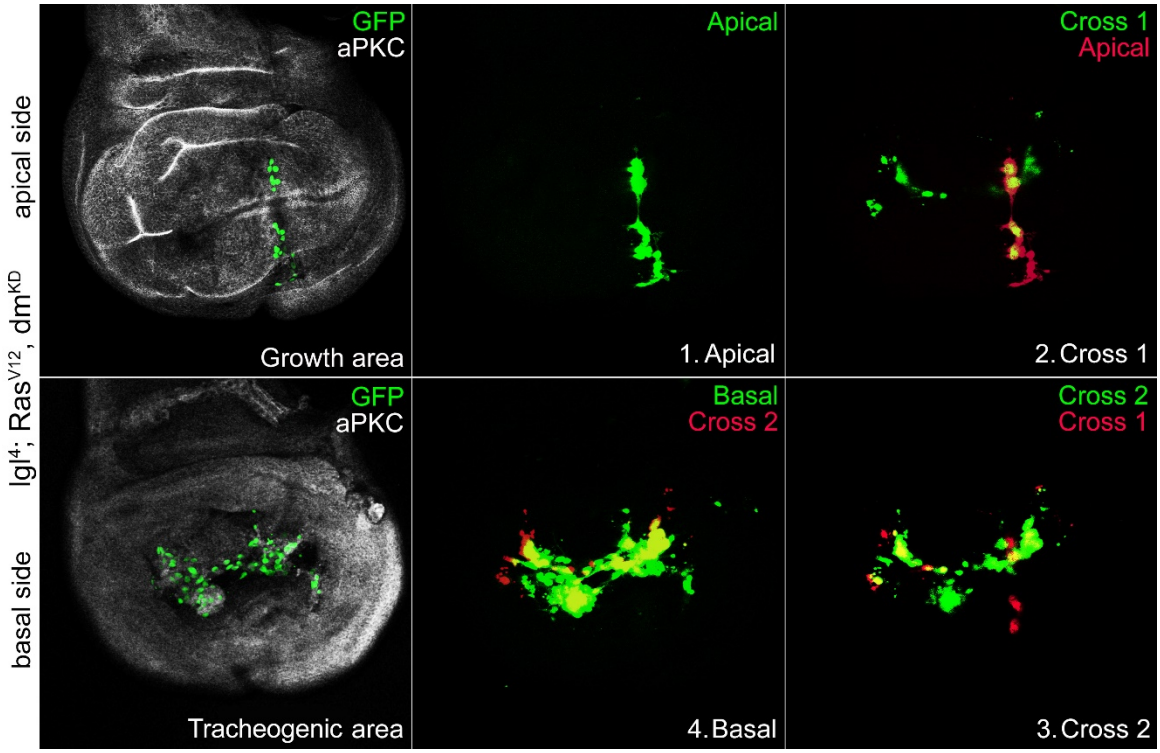

Figure RES-II 8 | Immunofluorescence staining of wing discs from *yw, hs-Flp, tub-Gal4, UAS-GFP/w; l(2)gl*^{4}*, FRT40A/tub-Gal80, FRT40A; UAS-*Ras^{V12}*, UAS-*dm^{KD}*/+* late L3 larvae. Mutant clones are GFP^+. aPKC is marked in white and the red areas represent the GFP^+ cells of the previous panel. The upper panel shows the apical section of the wing disc, while the lower panel shows the basal section of the same disc.

Let us observe what happens with the *lgl*; Ras^{V12}, *kay* ^{KD} cells. In this case, as it is displayed in Figure RES-II 9, the most part of the mutant cells reside at the apical part of the disc; the apical-to-basal sequence indeed shows a progressive reduction of the clonal area.

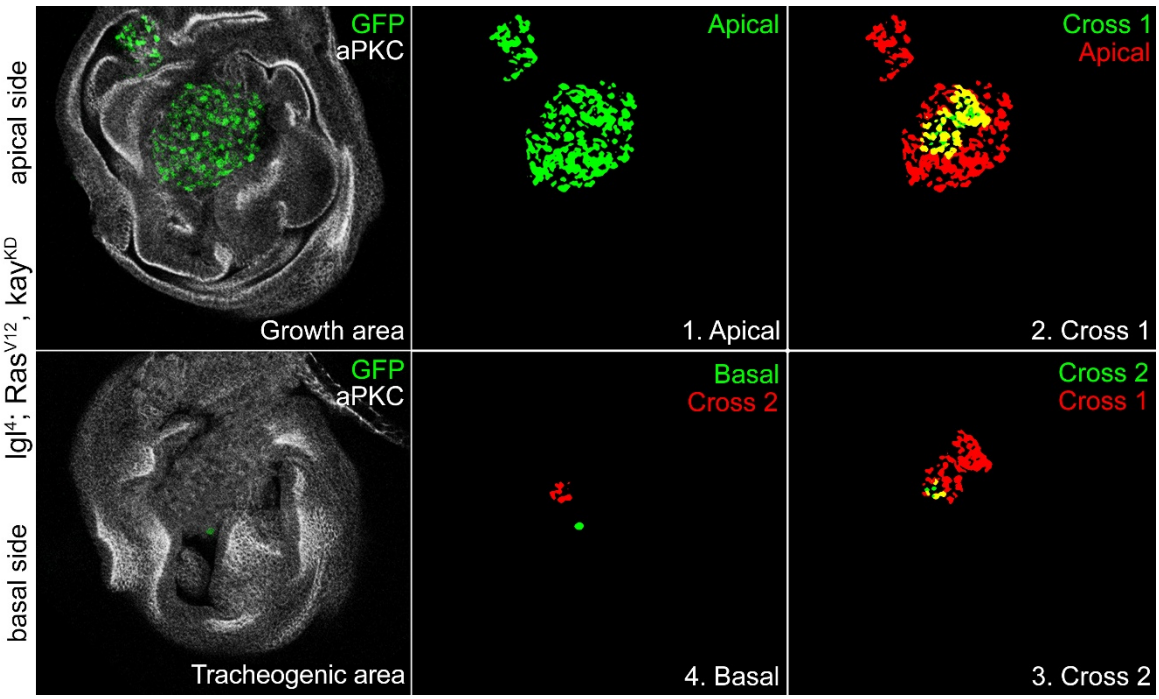

Figure RES-II 9 | Immunofluorescence staining of wing discs from *yw, hs-Flp, tub-Gal4, UAS-GFP/w; l(2)gl*^{4}*, FRT40A/tub-Gal80, FRT40A; UAS-Ras*^{V12}*, UAS-kay*^{KD}*/+* late L3 larvae. Mutant clones are GFP^{+}. aPKC is marked in white and the red areas represent the GFP^{+} cells of the previous panel. The upper panel shows the apical section of the wing disc, while the lower panel shows the basal section of the same disc.

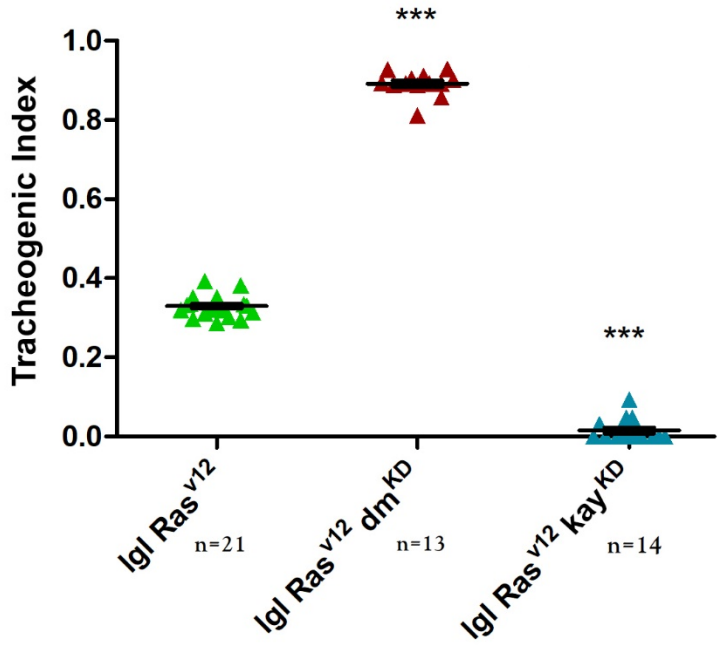

Figure RES-II 10 | Tracheogenic Index of wing discs carrying *lgl; Ras^{V12}, dm ^{KD}* and *lgl; Ras^{V12}, kay ^{KD}* clones, compared to that of *lgl; Ras^{V12}* samples. n is indicated for each sample group. All the comparisons are statistically significant (***=$p \leq 0{:}001$) respect to the *lgl; Ras^{V12}* samples.

The TI calculated for the *lgl*; *Ras*^{V12}, *dm* ^{KD} and the *lgl*; *Ras*^{V12}, *kay* ^{KD} samples are compared to the TI calculated for the *lgl*; *Ras*^{V12} samples in Figure RES-II 10. As can be observed in the graph, while about 35% of the MMP1-positive *lgl*; *Ras*^{V12} cells are found at the basal side of the wing disc, the percentage climbs over 95% for the *lgl*; *Ras*^{V12}, *dm* ^{KD} cells, and drops below 1% in the *lgl*; *Ras*^{V12}, *kay* ^{KD} sample group.

This was an astonishing finding and, beyond the efficiency of the RNAi constructs (see Methods), numbers are sufficiently distant to define the transcription factors MYC and FRA as the main effectors of growth and tracheogenesis downstream of the ERK and JNK pathways in *lgl*; *Ras*^{V12} cancers.

As oncogenic Ras upregulates integrins *via* the ERK/FOS signalling cascade [325], and MYC is known to suppress metastasis by transcriptional repression of the integrin genes [326], a possible mechanistic process explaining the antagonistic activity of MYC and FRA in *lgl*; *Ras*^{V12} mutant cells is the modulation of their integrin-dependent walking capability. This hypothesis is currently under investigation. Figure RES-II 11 recapitulates the findings described in this chapter.

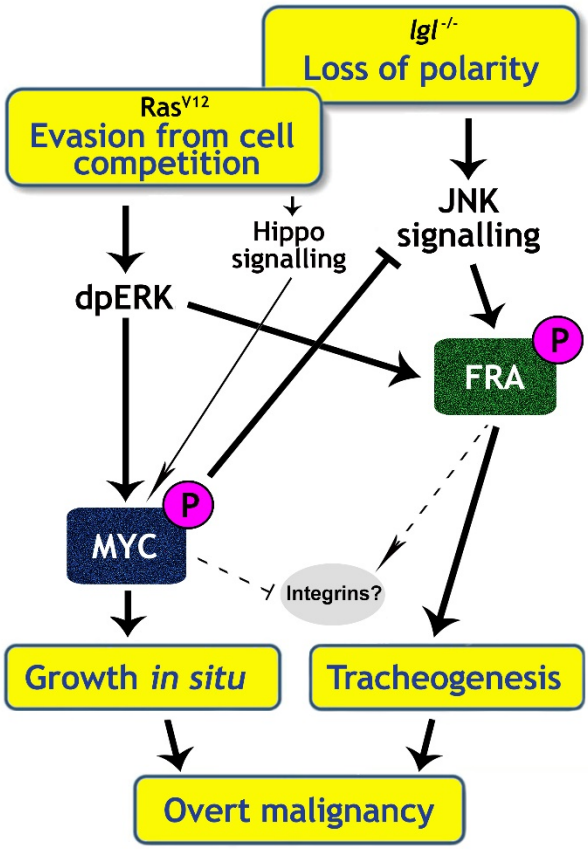

Figure RES-II 11 | A scheme summarising the findings described in the chapter.

During cancer progression, cells provide the growing mass with different abilities which, in time, shape tumour history [327]. Tumour growth and induction/formation of new vessels are both considered essential malignant traits [9]. While mass expansion may hamper organ function, migrating cells may reach distant sites and develop into secondary lesions, typical of deadly cancers [328].

The ERK/JNK pathways downstream effectors MYC and FRA have emerged from my study as potent inducers of growth and tracheogenesis, respectively, in *Drosophila* cancers. To evaluate possible rescue effects at the organismal level, I knocked these genes down in an *lgl* mutant background.

As detailed in the general Introduction, *lgl* LOF mutations provoke malignant growth of the ectodermal derivatives, with individuals undergoing delayed larval development and untimely death caused by formation of huge cancer masses filling the whole larval body [46]. *lgl* knockdown under the control of the tubulin promoter reproduces with full penetrance the same phenotypes as the $lgl^{-/-}$ mutant (Grifoni, FlyBase communication).

As can be seen in Figure RES-II 12, middle panel, *tub-lgl* ^{KD} wing discs grow while fusing with contiguous thoracic discs, and brain tissues are fused with the eye complex and with other discs specifying head and mouth parts. *tub-lgl* ^{KD}, *dm* ^{KD} larvae did not survive beyond L1, while all the *tub-lgl* ^{KD}, *kay* ^{KD} individuals showed nearly complete rescue of both wing disc and brain structure (Fig. RES-II 12, lower panel, please compare the organs with those shown in the upper panel). This finding suggests that inhibition of the migratory and tracheogenic potential of cancer cells is sufficient as to re-establish a series of physiological constraints to cancer progression.

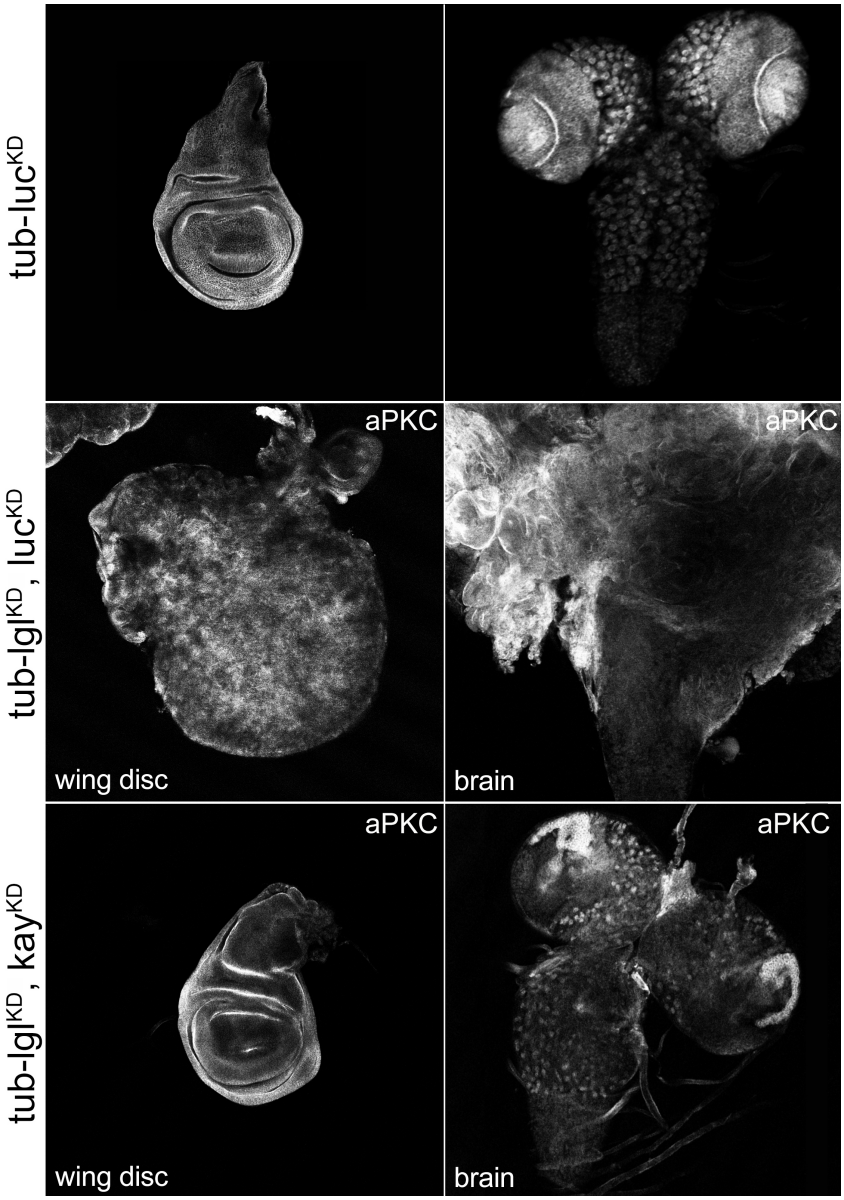

Figure RES-II 12 | Immunofluorescence staining of wing discs from control late L3 (upper panel), *tub-lgl* ^{KD} (middle panel) and *tub-lgl* ^{KD}, *kay* ^{KD} (lower panel) larvae. aPKC (white) marks organ structure. This panel is composed of images taken at 200X magnification.

Despite this surprising organ rescue during the larval life, these animals did not undergo differentiation. A possible explanation is that *kay* ^{KD} did not rescue the ecdysone defects observed in *lgl* mutant animals [329], so halting development at the larval-pupal transition.

Taken together, my results identify a selection mechanism triggered by two related transcription factors, which seem to play opposite roles in shaping cells' fate in cancer evolution.

While I was working on my PhD Thesis, a graduate fellow in my laboratory, now enrolled in the PhD Programme, was developing a brain cancer model based on a neurogenic hypothesis. Through the overexpression of a mutant form of aPKC in the central brain, she was able to inhibit Lgl localisation and induce cancers which kept growing in the adult [63]. Normally, aPKC phosphorylates Lgl restricting it at the basal-lateral membrane of the epithelial cells and at the basal side of the neural stem cells [330]; the mutant form of aPKC used in our study inhibited Lgl function throughout the cell membrane, thus preventing cell differentiation. Despite the highly malignant phenotype of these cancers, my colleague found complete lack of invasion/migration, and asked me to investigate MYC expression in those tissues. As expected, I found a massive MYC up-regulation in the brain regions where the promoter induced Lgl down-regulation, both in larval and adult brains, which also up-regulated Yki (Fig. RES-II 13 A, D and E, arrow and arrowheads). MYC knockdown in this context completely abolished cancer growth (Fig. RES-II 13 C, arrow and arrowheads, compare organ dimensions with B).
This evidence confirmed that MYC role in cancer growth is not tissue-specific, and its high expression in these brain cancers may explain their poor ability to colonise other tissues/organs.

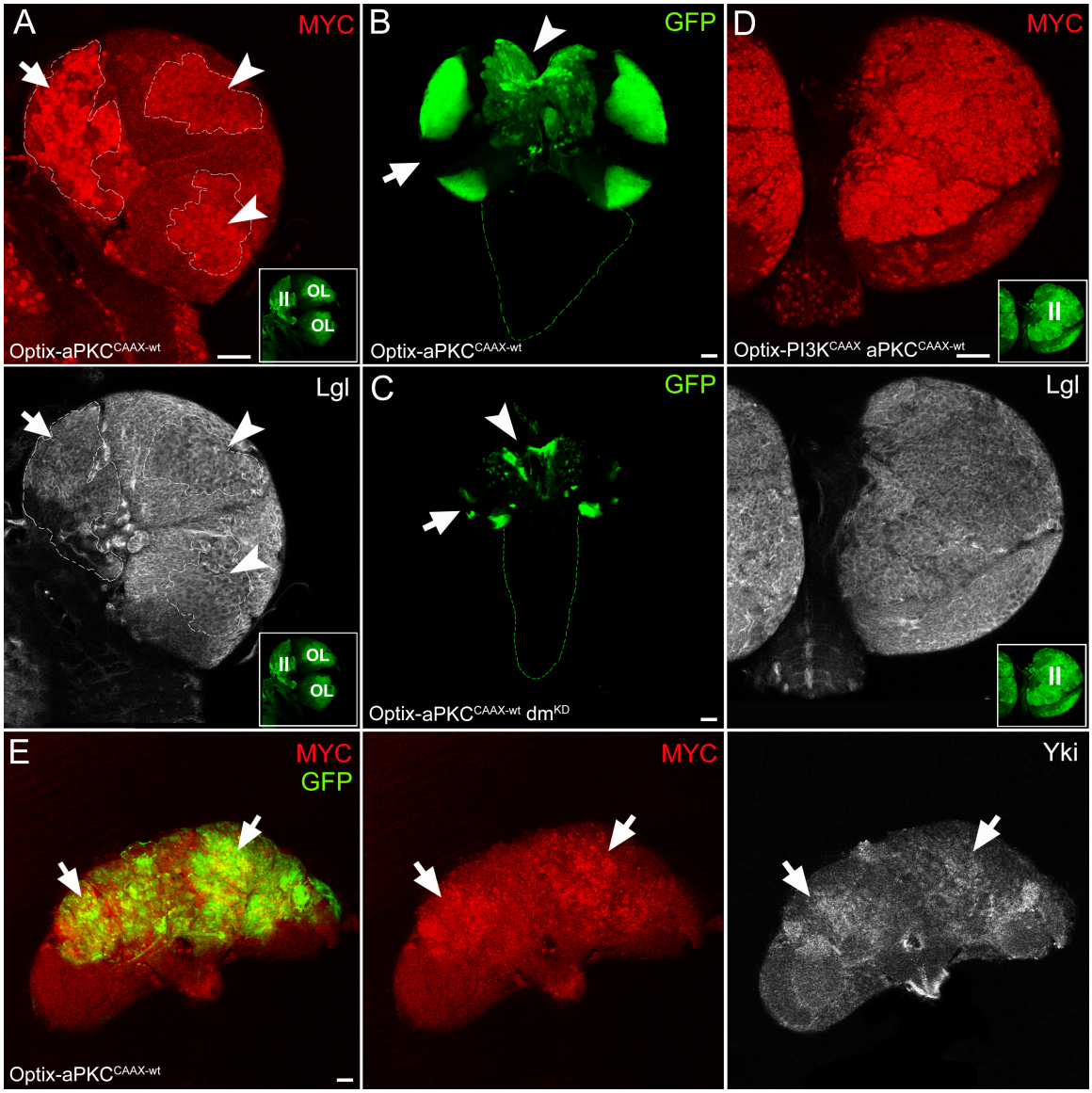

Figure RES-II 13 | (A) MYC (red) and Lgl (white) staining of *Optix-aPKC^{CAAX}* larval brains. Region II in the GFP^{+} inset indicates type II NBs. (B) The arrowhead points to the type II NBs in the DM region. (C) The same regions as in B are indicated in an *Optix-aPKC^{CAAX} dm^{KD}* brain. (D) MYC (red) and Lgl (white) staining of *Optix-PI3K^{CAAX} aPKC^{CAAX}* larval brains. The GFP^{+} inset shows the huge expansion of the type II NBs (region II). (E) *Optix-aPKC^{CAAX}* adult brains from 1-4 days old animals showing MYC and Yki upregulation (arrows). Scale bars are 50µm [63].

METHODS

GENETIC SYSTEMS

MARCM [331]

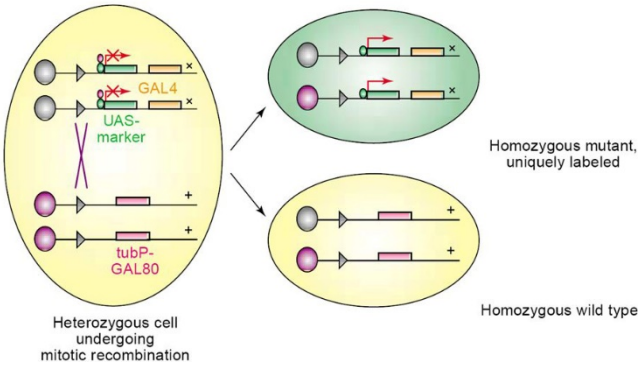

The MARCM system has been developed to induce combined loss-of-function (LOF) and gain-of-function (GOF) mutations in single cells. It takes advantage of the Gal4 repressor Gal80 to specifically inhibit Gal4 function in all but the mutant cells in the organ. The presence of a cell marker under the control of a UAS cassette allows recognising the mutant cells across the tissue of interest.

UAS-Gal4 [227]

See Methods - Part I

PROTOCOLS, REAGENTS AND STATISTICAL ANALYSIS

Fly manipulation

For MARCM clones, larvae were heat-shocked at 48±4 hours AEL for 10 minutes in a water bath at 37°C and allowed to grow for additional 72 hours at 25°C before being dissected in PBS1X (Phosphate Buffer Saline, pH 7.5) and fixed for 20 minutes in formaldehyde (Sigma) 3.7% in PBS.

Immunofluorescence

Frozen or fresh larvae were permeabilised in PBS-Triton 0,3% for 1-hour RT, blocked for 10 minutes in PBS-Triton 0,3%, 2% BSA (Bovine Serum Albumin, Sigma) and incubated

overnight at 4°C in PBS-Triton 0,3%, 2% BSA with primary antibodies. Tissues were then incubated with secondary antibodies for 2-3 hours at room temperature. After opportune washes, imaginal wing discs or brains were isolated from the carcasses and mounted on microscopy slides using the anti-quenching mounting medium FluoromountG (Beckman Coulter). The following antibodies and dilutions were used: mouse α-MYC (1:5 P. Bellosta); rabbit α-aPKCζ (1:200, sc-216 - Santa Cruz Biotechnology); mouse α-phospho-JNK (1:100, G9 - Cell Signaling Technology); mouse α-MMP1 (1:50, 3A6B4 - DSHB); mouse α-dpERK (1:50, MAPK-YT - Sigma); rabbit α-pAKT (1:100, Cell Signaling); rabbit α-Yki (1:100, G. Morata); rabbit α-Lgl (1:400, D. Strand). Alexa Fluor 555 or 568 goat α-mouse and α-rabbit (1:500, Invitrogen); Cy3-conjugated goat α-rabbit (1:200, Jackson ImmunoResearch Laboratories); Cy5-conjugated goat α-mouse and α-rabbit (1:500, Jackson ImmunoResearch Laboratories) and DyLight 649-conjugated goat α-mouse and α-rabbit (1:800, Jackson ImmunoResearch Laboratories) were used as secondary antibodies. Nuclei were counterstained with DAPI (4',6-diamidine-2'-phenylindole dihydrochloride, Sigma). Samples were analysed with Leica TSC SP2 laser confocal microscope and entire images were processed with Adobe Photoshop software or ImageJ free software from NIH. All the images shown represent a single confocal stack unless otherwise specified. Magnification is 400X unless otherwise specified.

Statistical analysis

The number of wing discs analysed was 25÷40 for each sample. Clone shape was measured with ImageJ using the formula 4πA/L2, in which A = clone area and L = clone circumference. By use of this formula, a perfect circle has a value of 1 and more irregular shapes have values <1. All error bars are ± standard error of the mean (SEM), if not differently indicated. *p*-values are as follows: $p \leq 0.01$=**, $p \leq 0.001$=***. Mean, Standard Deviation and the t-Student test *p*-value were calculated with GraphPad Prism software, San Diego, California, USA.

RNA Extraction and Purification, RT-PCR, Sybr Green qPCR

15 L3 larvae were homogenised in a vial with TRI Reagent® (*Sigma-Aldrich*), centrifuged for 5 minutes at 12000g at 4°C, and the supernatant was processed as follows: 300µl of chloroform were added to 1ml of TRI Reagent® (*Sigma-Aldrich*) solution and vortexed

for 10 seconds. The samples were incubated for 10 minutes at room temperature and centrifuged for 12 minutes at 12000g at 4°C. The RNA-containing aqueous phase was transferred to a new tube, where 750µl of isopropyl alcohol were added. Samples were mixed, incubated for 10 minutes at room temperature and centrifuged for 12 minutes at 12000g at 4°C. The pellet was repeatedly washed with 1 ml 75% EtOH and centrifuged at 7500g for 5 minutes at 4°C. The supernatant was removed and the dried pellet was eluted at 55°C for 10 minutes in 50µl of mqH_2O. A DNAse I-treatment followed to avoid genomic contamination.

cDNA synthesis was performed using total DNA free-RNA with oligo(dT) in a 0,2ml tube by using the ThermoScript™ RT-PCR system. The ThermoScript is an engineered avian reverse transcriptase with reduced RNase H activity that shows high thermal stability and produces high amounts of full-length cDNAs. Each mix is prepared as follows: 1µg di RNA + 2X RT Reaction Mix (oligo dT 2,5µM, random hexamers 2,5 ng/µl, $MgCl_2$ 10 mM, dNTPs) + RT enzyme Mix (Retro Transcriptase and RNase OUT) + mqH_2O up to the final volume.

SYBR GreenER qPCR SuperMix (*Invitrogen*) is a ready-to-use cocktail containing all components, except primers and template, for real-time quantitative PCR (qPCR) on ICycler BioRad real time instruments that support normalisation with Fluorescein Reference Dye at a final concentration of 500nM. It combines a chemically-modified "hot-start" version of Taq DNA polymerase. SYBR GreenER qPCR SuperMix is supplied at a 2X concentration and contains hot-start Taq DNA polymerase, SYBR GreenER fluorescent dye, 1 µM Fluorescein Reference Dye, $MgCl_2$, dNTPs and stabilisers. The SuperMix formulation is compatible with melting curve analysis. The amplification is based on 40 cycles x 3 steps: after 3 minutes denaturation at 95°C, each amplification step includes: 30 seconds at 95°, 15 seconds at 56°C, 30 seconds at 72°C. The resulting graph is the relative quantity of the target gene transcript compared to the transcript quantity of the reference gene. For each sample, an amplification curve is shown in a Cartesian graph: the x-axis represents the cycle number and the y-axis represents the Relative Fluorescence unit which is dependent on the amplified cDNA molecules.

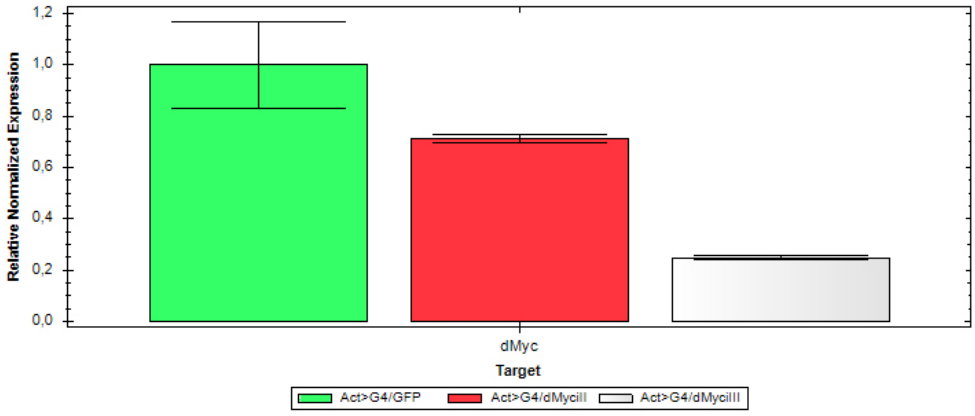

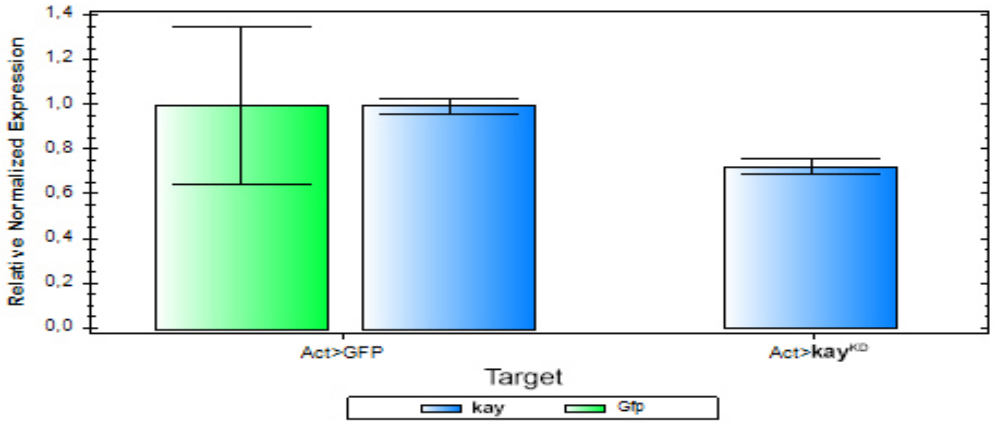

Table 1 | Real-Time PCR primers used and main features. *dm: Drosophila dm* gene, encoding the MYC protein; *kay: Drosophila kayak* gene, encoding the FRA protein; Green Fluorescence Protein construct.

Gene	Primer sequences	Size (bp)	Melting (°C)	**GenBank Accession**
Drosophila melanogaster				
dm	Forward: 5'- TATTAGTCGTCAAACAGTGG-3' Reverse: 5'-GCTGCATACTAAGCTCCTTC-3'	423	55	NM_080323.4
kay	Forward: 5'-GAAGAAGTTGCTGCTCTG-3' Reverse: 5'- ACGTTCTTAGGGTCTTTACT-3'	564	54	NM_167053.2
GFP	Forward: 5'-GGATGCTCTTGGCTCTTC-3' Reverse: 5'-GACAATCTTCTGGTGTCTGG-3'	352	55	

PART III - HIGHLY COMPETITIVE CANCERS UNDERGO GROWTH DECLINE UPON APOPTOSIS INHIBITION

Evasion of apoptosis is one of the hallmarks of cancer, which help cells survive also in stress conditions [9]. Cell death can be induced in a non-autonomous manner, as it happens in cell competition (CC) [98,165,166,332].

In *Drosophila* cancer tissues, loss of cell polarity triggers MYC-Mediated Cell Competition (MMCC) and, in this background, apoptotic death may act by promoting mass expansion, as in the fruit fly a mechanism of compensatory proliferation following cell death has been observed and characterised. Dronc activation (the Caspase 9 mammalian orthologue) stimulates the JNK signalling that, as described in the Introduction to Part II, induces apoptotic death but is also required to promote cancer growth [114,333–335]. In mammals, the apoptotic cell features are described in different models and it has been observed that dying cells promote tumour angiogenesis and feed tumour growth [336].

Here I follow the hypothesis that, in highly competitive cancers, the excess of apoptotic cells may stall the engulfment machinery, so persisting in the tumour tissue contributing to its growth [138] and, with the aim to investigate their role and contribution in cancer progression, I triggered MMCC in a *Drosophila* cancer model and I subsequently inhibited cell death. The preliminary results show that a block of apoptotic cell death results in a smaller tumour mass.

INTRODUCTION

3.1 APOPTOTIC DEATH AND CANCER

Evading apoptosis is a common trait of cancer and its reactivation is an adopted therapy to try blocking tumour growth and progression [9,337]. Apoptosis is a process consisting of autonomous cell death following irreparable cell damage, but recently emerging cancer studies also define cell death as a non-autonomous mechanism [332]. For example, CC (see Introduction and 1.3 paragraph) is a mechanism that triggers non-autonomous apoptosis and dying cells release mitogenic signals which stimulate a compensatory proliferation of the winner cells [166]. Cancer cells try to subvert and exploit cell processes to their own benefit [338], and it is plausible that they take advantage of non-autonomous apoptosis to increase their own fitness: in a *Drosophila* model of intestinal adenoma, MMCC-dependent growth was rescued by apoptosis inhibition [217], thus identifying a pro-tumourigenic role of apoptosis in cancer. Our recent data in human cancers and preliminary data in *Drosophila* models suggest that CC is important not only in the onset but also during tumour progression, and it is precisely during progression that cell death seems to assume a fundamental role, allowing the expansion of tumour sub-clones within the growing mass [110,138]. The close connection between CC and apoptosis emerged also in a recent computational model of tumour growth [339]. In mammals, the role of apoptotic cancer cells has been studied in a murine model of B-cell lymphoma: dying cells expressed MMP and promoted tumour angiogenesis supplying the growing mass with oxygen. Therefore, also in this mammalian cancer model, apoptosis enhances tumour progression [336]. In other studies, the apoptotic index has been associated with malignancy in several kinds of tumours: an increase of the apoptotic rate generally correlates with a poor prognosis [340–342]. Finally, glioma dying cells have been found to promote angiogenesis through Caspase 3-dependent VEGF secretion [343].

3.2 MYC-MEDIATED CELL COMPETITION IN HUMAN CANCERS

The pivotal role of MMCC in cancer has been discussed in paragraph 1.3, and its contribution to the initial expansion of the tumour mass is well known in *Drosophila*. For the first time, my laboratory recently observed signs of MMCC in human cancers. Histological samples of colon, breast and lung human tumours have been analysed and they showed polarity loss and Hpo signalling deregulation. Cancer cells with high MYC

levels were surrounded by Cas3-positive stromal cells: these evidence recap the MMCC mechanism observed in *Drosophila* models. Interestingly, signs of MMCC have also been found in tumour cells surrounded by high-MYC expressing transformed neighbours, highlighting the presence of inter-clonal competition. These data have been supported by *in vitro* models of MMCC [110].

But what is the role of this important mechanism during cancer progression, and what is the contribution of apoptosis?

If the apoptotic cells secrete pro-mitogenic factors and support mass expansion and tumour angiogenesis, is it proper to perseverate in the use of chemotherapeutics that are known to commit cancer cells to apoptotic death?

RESULTS AND DISCUSSION

PRELIMINARY RESULTS

The mechanism of MYC-mediated cell competition (MMCC), extensively described in the general Introduction, has long been speculated to be active in cancer [185,215,344]. Our and other laboratories demonstrated that this is true in different *Drosophila* organs [42,96,105,107,192,217], and findings showing the existence of this phenomenon in human cancers are beginning to appear in the literature [110,345]. Some aspects of the role of cell competition in tumour onset have been clarified in *Drosophila*, and it is widely accepted that cell death is an intrinsic feature of the process, necessary to tumour growth [216,217] as well as to tissue homeostasis in physiological conditions, from flies to mammals (reviewed by Penzo-Méndez and Stanger, 2014).

We recently analysed MMCC in human cancers, and were able to correlate MYC abundance in the tumour parenchyma with the apoptotic cell death at the tumour/stroma interface [110]. In addition, we found islets of dying cancer cells showing low MYC levels in close proximity to malignant neighbours expressing high MYC levels [110]. It is indeed likely that this process, relevant to fitness maintenance, be active in cancer allowing to select and expand cells with the best performance, but functional assays are mandatory to clarify this important issue.

Our laboratory has recently used a *Drosophila* well-characterised model of cancer to define the functional consequences of MMCC in overt malignancies (see Methods for details). In *lgl* $^{-/-}$ animals, the larval epithelial organs show unrestrained growth, complete loss of tissue architecture and ability to fuse with nearby tissues [241]. In this malignant background, we elicited MMCC through induction of GFP^{+} *lgl*$^{-/-}$ *myc*-overexpressing clones, hereafter referred to as *lgl myc*^{OVER}, at day 6 After Egg Laying (AEL), when these organs have already undergone neoplastic transformation [46]. Neutral (GFP^{+} *lgl*$^{-/-}$) clones were induced as a control. After two days from induction, larvae were dissected, and tumours were measured. The tumours were then dissociated into single cells and GFP^{+} and GFP^{-} cells were counted (see Methods for details). Following our hypothesis, we expected an expansion of the fittest cancer cells, i.e. MYC-high expressing cells. With respect to the neutral control, where GFP^{+} cells were about 20%, *lgl myc*^{OVER} samples

indeed contained about 35% GFP$^+$ winner cells (Fig. PREL-III 1A). The overall increase in the final cancer mass with respect to the neutral sample is represented in Figure PREL-III 1B, and the contribution of the GFP$^+$ cells to the post-induction cancer mass can be found in Figure PREL-III 1C. This unprecedented experiment revealed a functional significance for MMCC in remodelling the final cancer mass and composition.

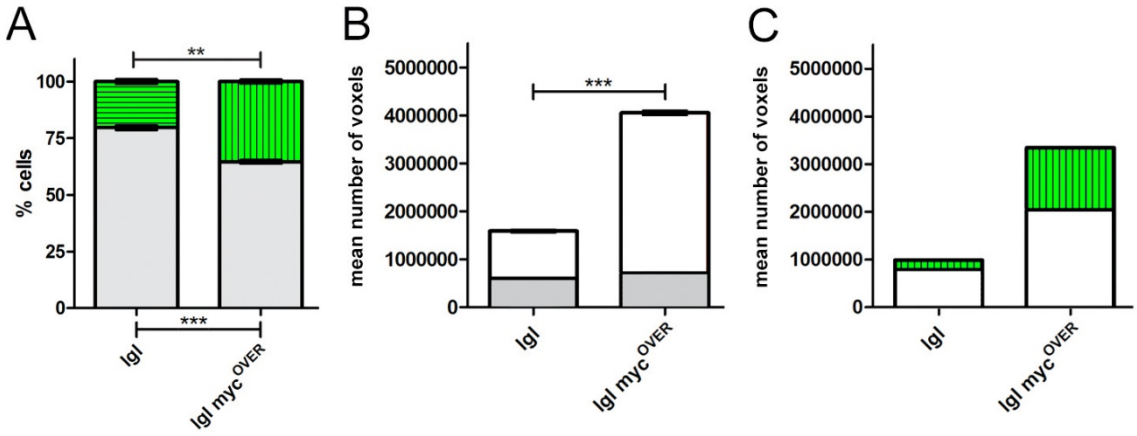

Figure PREL-III 1 | Composition and mass analysis of lgl and lgl myc^{OVER} samples. A: cell count. B: final tumour size. The plain grey regions represent the pre-induction masses. The two genotypes analysed are indicated, and the statistical significance is ***= $p \leq 0.001$ and **= $p \leq 0.01$. From: Simone Di Giacomo, PhD Thesis.

Immunofluorescence (IF) assays for MYC and Caspase 3 (Cas3) on both samples revealed that cell dynamics are very different in highly competitive tumours respect to the neutral tumours. Figure PREL-III 2A represents an organ in which GFP$^+$ *neutral* clones have been induced. Irrespective of the GFP signal, we can observe in cross sections sporadic cell clusters positive to Cas3 signal in which MYC staining is lower compared to the surrounding cells (arrows). Figure PREL-III 2A' shows a closer view of the phenomenon: some cells expressing very low levels of MYC (arrow) are committed to die, as confirmed by Cas3 staining. These data suggest that MMCC shapes cancer evolution through a continuous selection of cells with higher MYC levels, such as it happens in developing organs [98,166,180,347]. In the *lgl myc*^{OVER} samples, widespread Cas3 activation was observed in cells with low MYC levels encircled by or adjacent to GFP$^+$ cells with high MYC expression (Fig. PREL-III 2B). Figure PREL-III 2B' shows a close-up of this phenomenon: large clusters of GFP$^-$ cells (arrows) die when surrounded by high MYC-expressing neighbours.

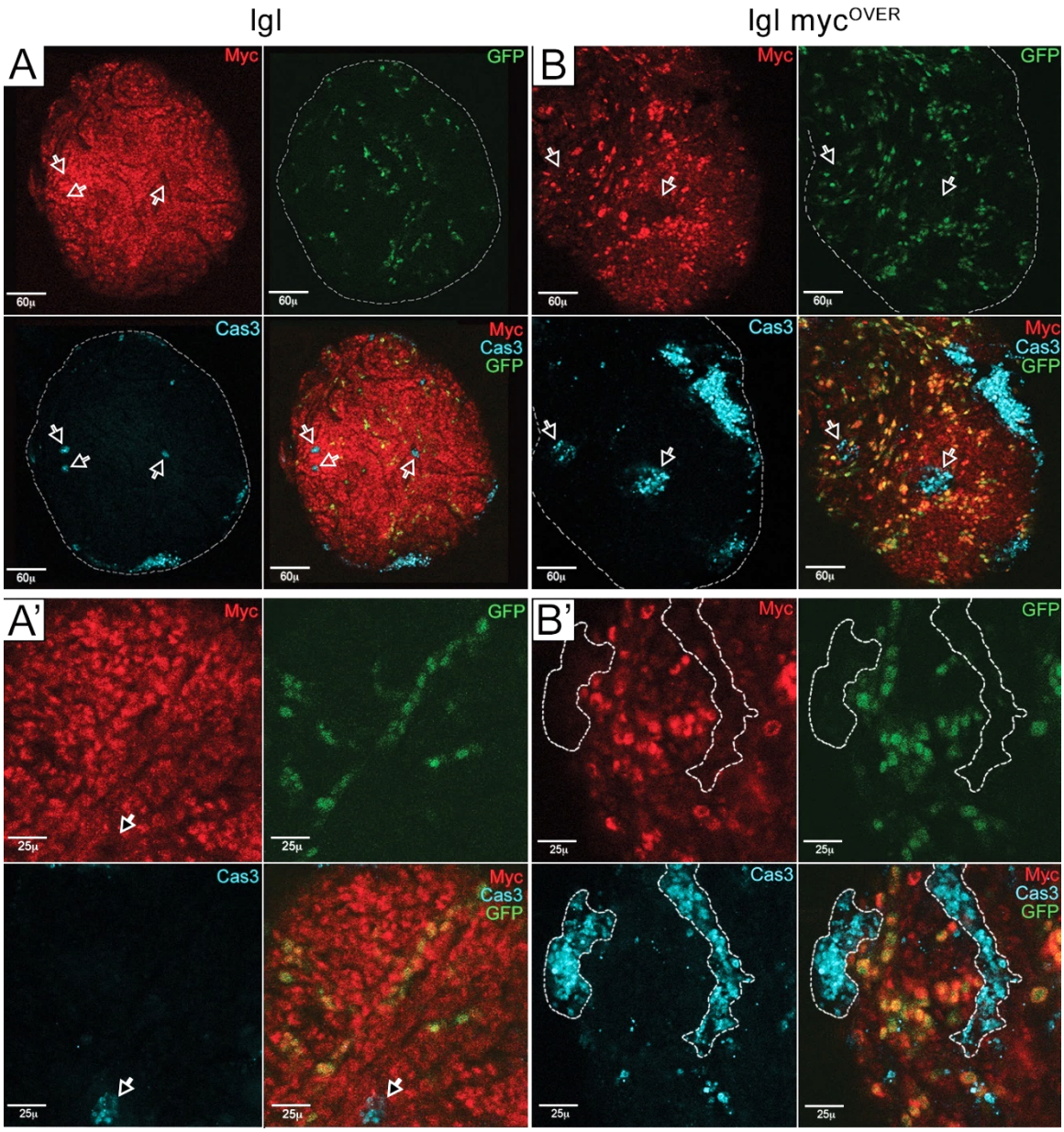

Figure PREL-III 2 | MYC (red) and Cas3 (cyan) staining of *lgl* (A, A') and *lgl myc*^{OVER} (B, B') tumours from *yw, hs-Flp/w; l(2)gl*^{4}*/l(2)gl*^{4}*; act::CD2::Gal4, UAS-GFP/+* and *yw, hs-Flp/w; l(2)gl*^{4}*/l(2)gl*^{4}*; act::CD2::Gal4, UAS-GFP/UAS-dm* larvae, respectively, collected at day 8 AEL in which GFP^{+} clones were induced at day 6 AEL. B: all the images represent disc cross-sections. Scale bars are indicated in each frame. From: S. Di Giacomo, PhD Thesis.

Of note, besides a huge expansion of the winner population, we reported a post-induction increase of the GFP^{-} mass in the *lgl myc*^{OVER} sample (Figure PREL-III 1B, C). As it is known that dying cells emit pro-proliferative factors both in *Drosophila* and mammals [348], in a cancer context cells competent to receive and use these signals may translate them into growth-boosters.

RESULTS AND DISCUSSION

In this Chapter, I will describe my preliminary work dedicated to understanding the impact of apoptotic death on the growth of highly competitive malignancies. By taking advantage of the above-described cancer model, I fed larvae immediately after clone induction with a pan-caspase inhibitor to decrease cell death at the organismal level, and repeated the same measurements as those performed in the experiment illustrated in the preliminary results (see Methods for details).

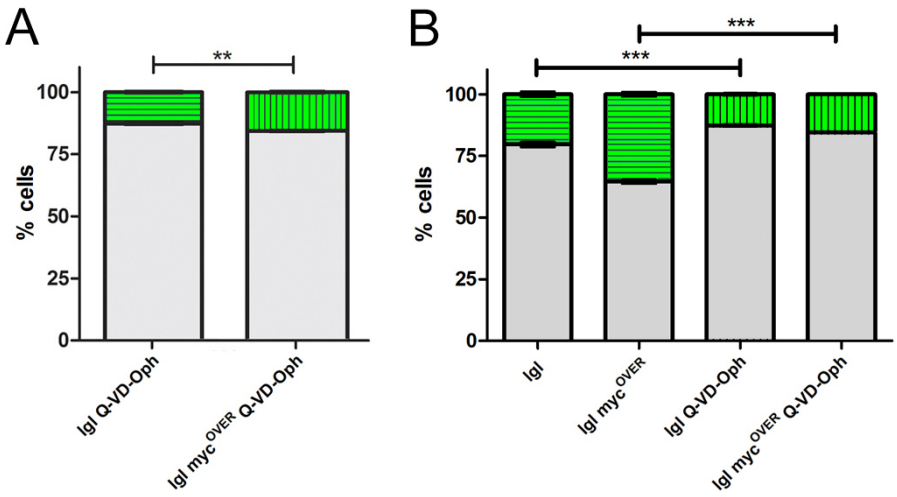

Figure RES-III 1 | Composition analysis of *lgl* and *lgl myc*^{OVER} samples treated with the Pan-Caspase inhibitor Q-VD-Oph. A: cell count. B: cross-comparison of untreated and treated samples. The two genotypes analysed are indicated, and the statistical significance is ***= $p \leq 0.001$ and **= $p \leq 0.01$.

As can be seen in Figure RES-III 1A, the percentage of GFP^{+} cells in the *lgl myc*^{OVER} sample is still significantly different from that counted in the neutral *lgl* samples, but the expansion of the GFP^{+} cells in the *lgl myc*^{OVER} sample is severely restrained respect to what happened in the untreated experiment (Fig. RES-III 1B), confirming that apoptosis inhibition following MMCC induction is sufficient to restrain winners' proliferation.

Concerning the final size of the treated samples, *lgl myc*^{OVER} tumours appeared undersized with respect to the *neutral* ones (Fig. RES-III 2A), but the difference between the untreated and treated *lgl myc*^{OVER} tumours was surprising: treated tumours were less than one-half of the untreated samples (Fig. RES-III 2B, red bars).

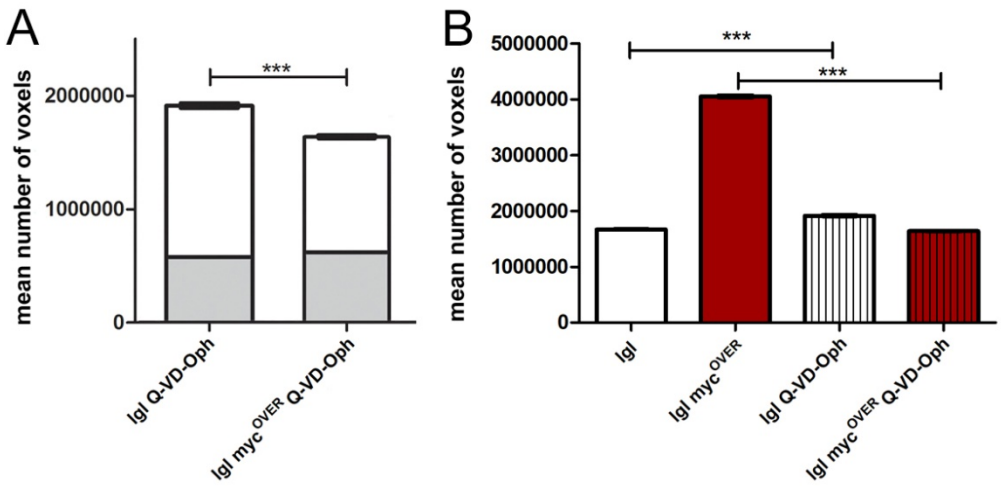

Figure RES-III 2 | Mass analysis of *lgl* and *lgl myc*^{OVER} samples treated with the Pan-Caspase inhibitor Q-VD-Oph. A: final tumour size. The plain grey regions represent the pre-induction masses. B: cross-comparison of untreated and treated samples. The two genotypes analysed are indicated, and the statistical significance is ***= $p \leq 0.001$.

Conversely, the *lgl* neutral samples treated with the pan-caspase inhibitor showed a modest although significant increase in size respect to the untreated siblings (Fig. RES-III 2B, white bars). At the moment, I have no definite explanation for this. Possibly, the few apoptotic cells originating in the neutral samples are successfully removed by professional cells, and this has no impact on the growth of the final mass; apoptosis inhibition in this context may increment tumour volume by accumulating in the system cells which would otherwise have undergone untimely death.

This means that apoptosis is relevant to mass expansion only in highly competitive cancers.

In Figure RES-III 3, you can appreciate at a glance the amazing average difference in size between the *lgl myc*^{OVER} tumours from untreated and treated larvae.

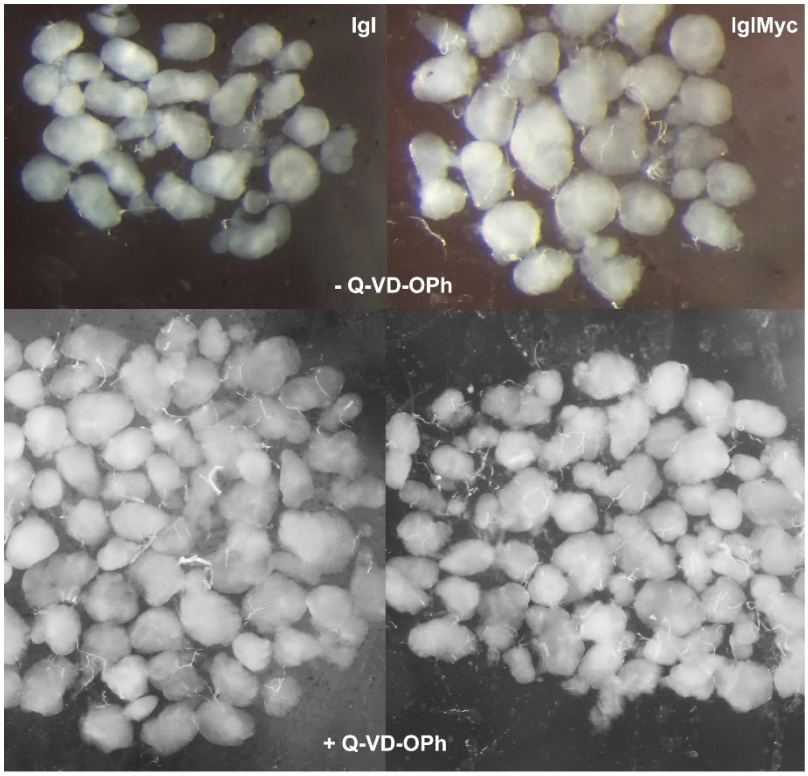

Figure RES-III 3 | Tumours isolated from *lgl* and *lgl myc*^{OVER} untreated (- Q-VD-Oph, upper panel) or treated (+ Q-VD-Oph, lower panel) samples.

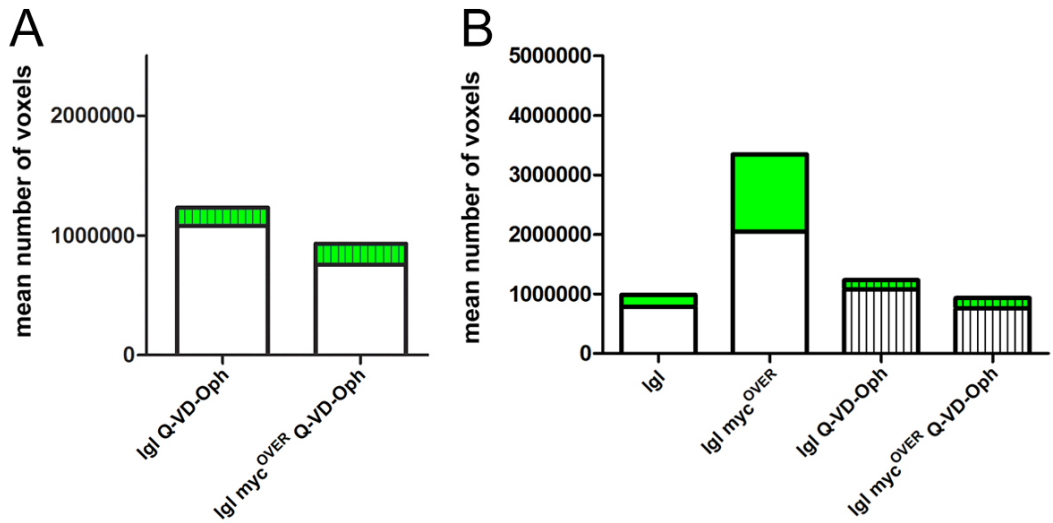

Figure RES-III 4 | Composition analysis of *lgl* and *lgl myc*^{OVER} samples treated with the Pan-Caspase inhibitor Q-VD-Oph. A: post-induction GFP$^+$ vs GFP$^-$ mass comparison. B: cross-comparison of untreated and treated samples. The two genotypes analysed are indicated.

Finally, I calculated the post-induction tumour masses and, as presented in Figure RES-III 4A, while the GFP$^+$ masses are comparable across the two treated samples, cross-

comparison of the untreated and treated *lgl myc*^{OVER} post-induction masses (Fig. RES-III 4B) reveals a huge collapse of both the GFP^{+} and GFP^{-} masses, suggesting that a massive presence of apoptotic cells in the system may stall the engulfment machinery, and the release of pro-growth factors by the dying cells may serve as a propeller to sustain the increase of the whole cancer mass [138].

Figure RES-III 5 displays clone distribution (GFP^{+}) and MYC/Cas3 staining in cross-sections of *lgl* and *lgl myc*^{OVER} samples respectively. As can be seen, MYC expression is not affected by the treatment and, despite the presence of a number of *lgl myc*^{OVER} cells, cell death is nearly absent.

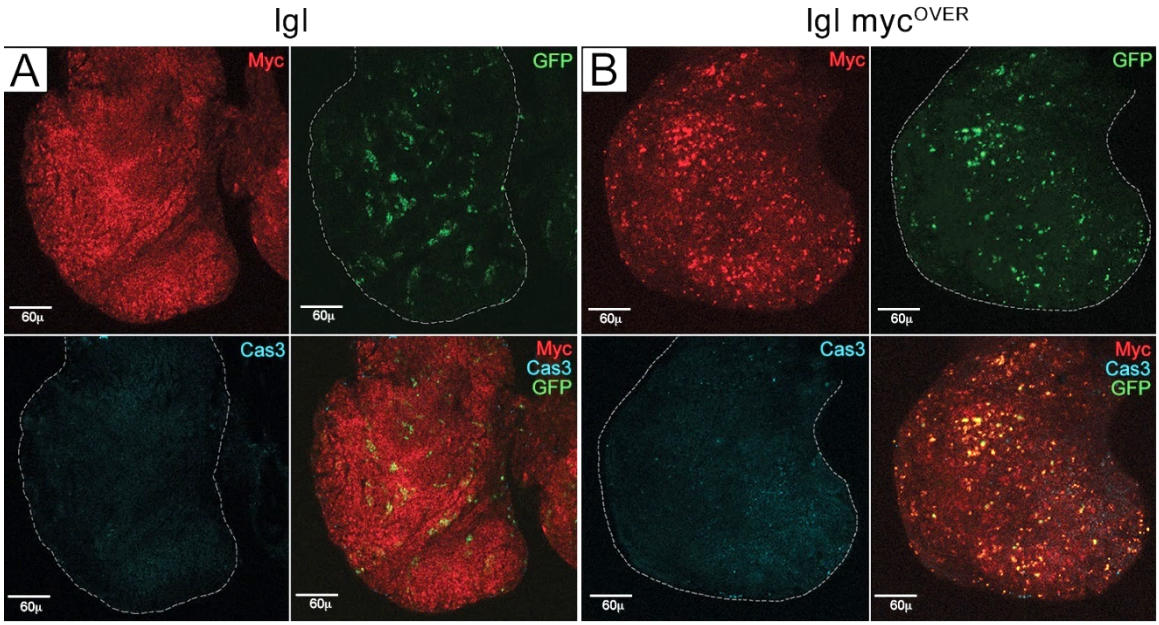

Figure RES-III 5 | MYC (red) and Cas3 (cyan) staining of *lgl* (A) and *lgl myc*^{OVER} (B) tumours *from yw, hs-Flp/w; l(2)gl*^{4}*/l(2)gl*^{4}*; act::CD2::Gal4, UAS-GFP/+* and yw, hs-Flp/w; l(2)gl^{4}/l(2)gl^{4}; act::CD2::Gal4, UAS-GFP/UAS-dm larvae, respectively, collected at day 8 AEL, in which GFP^{+} clones were induced at day 6 AEL, immediately before treatment with Q-VD-Oph. All the images represent disc cross-sections. Scale bars are indicated in each frame.

I then tested the effect of the same compound as above on the clonal cancer system I investigated in PART II. We are thus going to analyse a heterotypic context, with cancer cells sharing the organ with *wt* cells. In this case, apoptotic death is not scattered across the transformed organ, but is mainly confined to the tumour/stroma interface [107], as it is for human cancers [110].

For this experiment, larvae were fed with the pan-caspase inhibitor Q-VD-Oph 24h after clone induction, and imaginal wing discs were isolated 48h after treatment. To obtain comparable measures, I calculated the total GFP^+ area in the wing-pouch and normalised it to the total wing pouch dimensions. As can be seen in Figure RES-III 6, *lgl* Ras^{V12} clones grown in animals fed with the pan-caspase inhibitor show an average size reduction of about 40%, suggesting that, also in heterogeneous backgrounds, a systemic decrease of cell death restrains tumour growth. The wing discs in Figure RES-III 6 represent the average clone phenotype of untreated/treated animals.

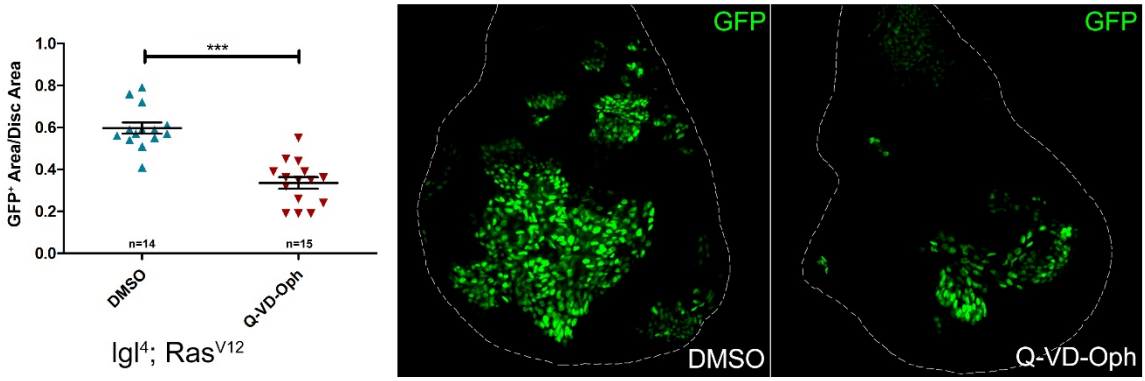

Figure RES-III 6 | Ratio between the *lgl; Ras*^{V12} GFP^+ clonal area and the total area, calculated in the wing pouch region for each experimental sample group. n is indicated in the graph. The comparison is statistically significant *(***=p≤0,001)*. The confocal images are cross-sections of representative wing discs from untreated (DMSO) and treated (Q-VD-Oph) larvae. Disc contour is outlined where necessary.

These preliminary results encourage to plan a genetic dissection of the apoptotic pathways in different cancer models, to determine *in vivo* the impact of apoptosis on cancer growth and aggressiveness.

METHODS

GENETIC SYSTEMS

Flp-Out [349]

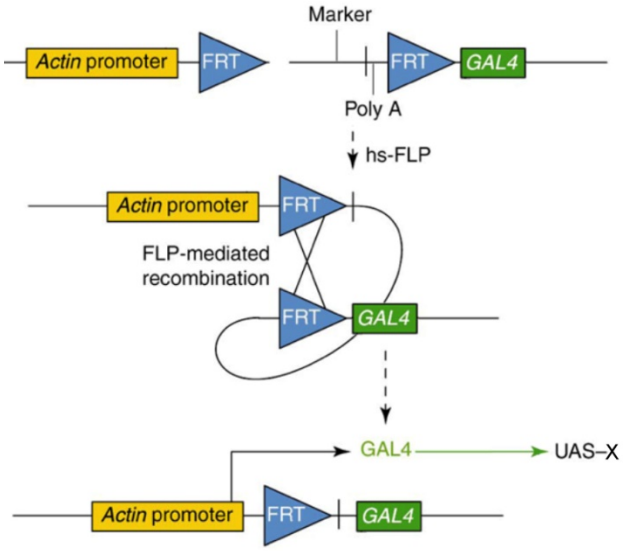

The Flp-Out technique has been developed to induce clonal expression of UAS-constructs by combining the UAS-Gal4 [227] and the Flp-FRT [228] binary systems. Briefly, a stop sequence containing a selection marker, flanked by two FRT cassettes, disrupts contiguity between the gene of interest and its promoter. When Flippase expression is induced, usually through a heat-shock, the stop sequence is removed, and the gene of interest is transcribed.

MARCM [331]

See Part II Methods.

PROTOCOLS, REAGENTS AND STATISTICAL ANALYSIS

Fly manipulation and treatments

At 144±2 hours development at 25°C, female larvae of the right genotypes were selected, transferred in an eppendorf vial plugged with foam and immersed for 2 minutes in a water bath at 37°C. After the heat-shock, larvae were immediately transferred to fresh food and allowed to grow for additional 48 hours at 25°C. Heat-shock duration was set to obtain about 1/5 of GFP^+ cells in the final control mass 48 hours after clone induction. Q-VD-OPh (Sigma-Aldrich) [350] was added to standard food at 500µM final concentration before

larvae transfer. For the MARCM experiment (Fig. RES-III 6), 48±4h larvae were heat-shocked for 10 minutes in a water bath at 37°C and allowed to grow for additional 24 hours at 25°C before being transferred to standard food supplemented with Q-VD-Oph at a final concentration of 500μM. After additional 2 days at 25°C, larvae were dissected, and imaginal discs were processed for image analysis.

Disc isolation, dissociation and cell count

192±4h larvae displaying GFP^+ cells were selected under a Nikon SMZ1000 fluorescence stereoscope and dissected at 4°C in PBS1X (Phosphate Buffer Saline, pH 7.5). Tumour discs were isolated from the carcasses, photographed and incubated with gentle agitation for 2.5 hours in 1 ml PBT (4.5 mg/ml porcine trypsin-EDTA-Sigma-Aldrich- in PBS1X) prior to cell count. Cell count was carried out using the Bürker's chamber applying the following equation: [(Average n° cells in 9 squares x 10^4) x Dil. Factor] x ml of cell suspension, obtaining the total number of cells suspended in the initial volume.

Volume analysis

Discs from 192±2 larvae were photographed each day before dissociation. 144±2h discs were also captured as a prior-to-treatment control. Major and minor axes were measured for each wing disc with ImageJ (NIH) and volumes were calculated approximating disc shape to a spheroid with depth=width. For cell volume, four different fields from confocal *z* stacks containing 55 ÷ 80 cells were measured for each sample. Cell perimeter was marked by aPKC staining. GFP^+ and GFP^- cell diameters were measured with ImageJ (NIH) and cell volumes were obtained approximating their shape to a sphere.

Composition of the final masses

Vt=tumour volume, Vg=GFP^+ cell volume; Vb=GFP^- cell volume, Pg=GFP^+ cell percentage, Pb=GFP^- cell percentage. Total number is Ct=Vt(VgxPg+VbxPb), GFP^+ and GFP^- cell number is Cg=CtxPg and Cb=CtxPb. GFP^+ and GFP^- final volumes are: CgxVg and CbxVb. Volumetric values are reported as mean number of voxels.

Immunofluorescence

Tissue isolated from 192±2h larvae were fixed and stained according to standard protocols. Primary antibodies: rabbit α-cleaved Caspase 3 (Cell Signaling #9961, 1:100),

mouse α-MYC (P. Bellosta, 1:5), rabbit α-aPKCζ (Santa Cruz Biotechnology #10800, 1:100). Secondary antibodies: α-mouse 555 Alexa Fluor, 1:500 and α-rabbit Cy5 DyLight (Jackson Laboratories), 1:800. Confocal images were processed as a whole with Adobe Photoshop software. All the images shown represent a single confocal stack. Magnification is 400X, unless otherwise specified.

Statistical analysis

For the experiments as in Figures RES-III 1, 2 and 4, all values are the mean of at least 3 independent experiments where every single count was repeated twice. The number of wing discs analysed was 30÷90 for each sample. For the experiments as in Figure RES-III 6, clone areas (in pixel^2) were measured using ImageJ free software (NIH) on images captured with a Nikon 90i wide-field fluorescence microscope at a magnification of 200x. All error bars are ± standard error of the mean (SEM), if not differently indicated. *p*-values are as follows: $p \leq 0.01$=**, $p \leq 0.001$=***. Mean, Standard Deviation and the t-Student test *p*-value were calculated with GraphPad Prism software, San Diego, California, USA.

CONCLUSIONS AND PERSPECTIVES

Cancer research takes giant steps every day, but many molecular mechanisms that underlie initiation, progression and dissemination of cancer cells are still unknown.

As described in this thesis, cancer mass is composed of different cell types that make the tumour highly heterogeneous, which greatly complicates the understanding of the mechanisms governing it. Each cell type provides the tumour with peculiar properties and is associated with a community where each member, and therefore each group of different cells that composes it, is committed to perform certain tasks.

In particular, during my PhD programme, I developed some *Drosophila* models that may allow studying these intricate relationships *in vivo*.
In *Drosophila*, different genetic tools are available that allow the study of the onset, growth and invasiveness of tumours, and it is precisely on these traits that I focused my attention. MYC is one of the main genes involved in tumour processes, and I have studied its role in the aforementioned traits.

In the first period I focused my attention on the phenomenon of *field cancerisation*, where I managed to show that MYC, contrariwise to other molecules involved in growth, is able to form a (histologically normal) field able to trigger several cell responses (genetic instability, ROS production, apoptosis, increased proliferation) typical of human pre-cancerous fields, which predispose the tissue to the onset of secondary mutations. In particular, through clone induction systems, I allowed the onset of mutations belonging to different pathways, *lgl* and *Rab5*, and I have shown that MYC overexpression was specific and sufficient as to provide these mutant cells with a proliferative advantage, so that they succeeded in triggering tumourigenesis. This model may help further investigate the early molecular events underlying neoplastic transformation.

I subsequently examined MYC's role in tumour *growth* and *migration/tracheogenesis* using clonal systems in *Drosophila*. The two mutations I have induced to trigger tumourigenesis are the LOF of *lgl* and the overexpression of activated Ras (Ras^{V12}). In such mutant clones, we previously observed MAPK/dpERK pathway activation, and it is known to promote MYC stabilisation and accumulation. The Hippo pathway is also

deregulated in these cells and Yorkie moves into the nucleus where it transcribes, among others, MYC. In some groups of *lgl* Ras^{V12} mutant cells, the JNK pathway is also active. Another characteristic of these tumour clones we previously observed is that they are able to form vessel-like structures which mimic both the structure and function of mammalian tumour angiogenesis, and supply the growing mass with oxygen (tumour tracheogenesis).

I have thus tried to dissect the growth and tracheogenic phenotypes to understand what molecules downstream of these pathways may contribute to these central cancer traits. After inhibiting the effectors downstream of the main aforementioned pathways, I concluded that both MAPK and JNK signalling were responsible for the onset of both traits: in fact, their down-regulation rescued both the growth and the tracheogenic phenotypes. Yorkie knockdown downstream of the Hippo pathway was instead found to rescue growth while maintaining tracheogenesis. In these clones, MYC expression was low. Being MYC protein also a target of MAPK, I decided to inhibit its expression in the mutant clones and, as it happened with Yorkie, growth was unbelievably rescued, while the formation of new vessels was amazingly enhanced. Another downstream target of both the MAPK and JNK pathways is *kay* (the *FOS* gene in mammals, Fos-Related Antigen -FRA- the fly protein). Its down-regulation did not provoke any rescue of the primary mass, but I assisted to the disappearance of the tracheogenic trait: the tracheogenic index was much lower than that of the control *lgl* Ras^{V12} clones. These findings allowed me to identify MYC and FRA as the main downstream effectors of these two traits. I hypothesise that these opposite phenotypes may be due to Integrin transcriptional control, which MYC and FRA regulate in opposite manners in mammals. This hypothesis is currently being verified.

In the last, still preliminary, section I analysed the involvement of *non-autonomous cell death in tumour progression*. Both in *Drosophila* and in humans, it has been observed that apoptosis triggered by mechanisms such as cell competition has an important role in promoting tumour growth, due to secretion of pro-mitogenic factors by dying cells. In my laboratory, signs of MYC-Mediated Cell Competition have been observed for the first time in human tumours, and an analysis in cellular models has allowed to confirm that cell competition plays an active role in growth also in humans. To confirm these data *in vivo*, we developed a tumour model of MYC-Mediated Cell Competition. We observed that this mechanism plays an important role not only in the initial stages of a tumour but,

even when the tumour is frankly malignant, MYC-Mediated Cell Competition continues to shape the mass both in size and cell composition. Considering that apoptosis is essential to Cell Competition completion, I investigated its role during the evolution of an expanding tumour. In the same model of MYC-Mediated Cell Competition, I inhibited cell death with a pan-caspase drug and found a decrease in organ size by about 40%. These data were confirmed in the clonal model of *lgl*, Ras^{V12} oncogenic cooperation where, after cell death inhibition, the clonal areas were significantly reduced.

These findings should make us think about the use of current therapies against cancer: when massive death occurs in the tumour mass due to chemotherapeutic agents, will these dying cells possibly secrete factors that make low-proliferating tumour cells reactivate malignant pathways? In *Drosophila* it is known that p35 (Caspase 3 inhibitor from Baculovirus) creates "undead" cells that secrete tumour-promoting factors. My data instead show that inhibition of the whole caspase pathway (the drug acts on both initiator and effector caspases) leads to a decrease of the final cancer mass.

It will be worthwhile to examine and genetically dissect the apoptotic pathways to understand if the inhibition of the cascade at different levels has different effects on cancer evolution.

BIBLIOGRAPHY

1. Weinberg, R. A. The nature of cancer. in *The Biology of Cancer* 31–69 (Garland Science, Taylor & Francis Group, LLC, 2013).
2. Kandoth, C. *et al.* Mutational landscape and significance across 12 major cancer types. *Nature* **503,** 333–339 (2013).
3. Nowell, P. C. The clonal evolution of tumor cell populations. *Science (80-.).* **194,** 23–8 (1976).
4. Hanahan, D. & Weinberg, R. A. The hallmarks of cancer. *Cell* **100,** 57–70 (2000).
5. Bissell, M. J. & Hines, W. C. Why don't we get more cancer? A proposed role of the microenvironment in restraining cancer progression. *Nat. Med.* **17,** 320–9 (2011).
6. Laconi, E., Doratiotto, S. & Vineis, P. The microenvironments of multistage carcinogenesis. *Semin. Cancer Biol.* **18,** 322–329 (2008).
7. Mueller, M. M. & Fusenig, N. E. Friends or foes - bipolar effects of the tumour stroma in cancer. *Nat. Rev. Cancer* **4,** 839–49 (2004).
8. Heppner, G. H. Tumor heterogeneity. *Cancer Res.* **44,** 2259–2265 (1984).
9. Hanahan, D. & Weinberg, R. A. Hallmarks of cancer: The next generation. *Cell* **144,** 646–674 (2011).
10. Witsch, E., Sela, M. & Yarden, Y. Roles for growth factors in cancer progression. *Physiology* **25,** 85–101 (2010).
11. Cheng, N., Chytil, A., Shyr, Y., Joly, A. & Moses, H. L. Transforming growth factor-beta signaling-deficient fibroblasts enhance hepatocyte growth factor signaling in mammary carcinoma cells to promote scattering and invasion. *Mol. cancer Res.* **6,** 1521–33 (2008).
12. Skobe, M. & Fusenig, N. E. Tumorigenic conversion of immortal human keratinocytes through stromal cell activation. *Proc. Natl. Acad. Sci. U. S. A.* **95,** 1050–1055 (1998).
13. Medema, R. H. & Bos, J. L. The Role of p21-Ras Receptor Tyrosine Kinase Signaling. *Crit Rev Oncog* **4,** 615–661 (1993).
14. Harris, C. C. Structure and function of the p53 tumor suppressor gene: clues for rational cancer therapeutic strategies. *J. Natl. Cancer Inst.* **88,** 1442–55 (1996).
15. Evan, G. & Littlewood, T. A matter of life and cell death. *Science (80-.).* **281,** 1317–1322 (1998).
16. Kerr, J. F. R. & Searle, J. A suggested explanation for the paradoxically slow growth rate of basal□ cell carcinomas that contain numerous mitotic figures. *J. Pathol.* **107,** 41–44 (1972).
17. Hayflick, L. Mortality and immortality at the cellular level. A review. *Biochemistry. (Mosc).* **62,** 1180–1190 (1997).
18. Shay, J. W. & Bacchetti, S. A survey of telomerase activity in human cancer. *Eur. J. Cancer* **33,** 787–791 (1997).
19. Bryan, T. M. & Cech, T. R. Telomerase and the maintenance of chromosome ends. *Current Opinion in Cell Biology* **11,** 318–324 (1999).
20. Carmeliet, P. & Jain, R. K. Molecular mechanisms and clinical applications of angiogenesis. *Nature* **473,** 298–307 (2011).
21. De Spiegelaere, W. *et al.* Intussusceptive angiogenesis: A biologically relevant form of

angiogenesis. *J. Vasc. Res.* **49,** 390–404 (2012).

22. Berx, G. & van Roy, F. Involvement of members of the cadherin superfamily in cancer. *Cold Spring Harbor perspectives in biology* **1,** (2009).
23. Cavallaro, U. & Christofori, G. Cell adhesion and signalling by cadherins and Ig-CAMs in cancer. *Nat. Rev. Cancer* **4,** 118–132 (2004).
24. Warburg, O. Injuring of Respiration the Origin of Cancer Cells. *Science (80-.).* **123,** 309–14 (1956).
25. Jones, R. G. & Thompson, C. B. Tumor suppressors and cell metabolism: A recipe for cancer growth. *Genes Dev.* **23,** 537–548 (2009).
26. Feron, O. Pyruvate into lactate and back: From the Warburg effect to symbiotic energy fuel exchange in cancer cells. *Radiotherapy and Oncology* **92,** 329–333 (2009).
27. Semenza, G. L. Tumor metabolism: Cancer cells give and take lactate. *Journal of Clinical Investigation* **118,** 3835–3837 (2008).
28. Vajdic, C. M. & Van Leeuwen, M. T. Cancer incidence and risk factors after solid organ transplantation. *International Journal of Cancer* **125,** 1747–1754 (2009).
29. Kim, J., Eltoum, I. E. A., Roh, M., Wang, J. & Abdulkadir, S. A. Interactions between cells with distinct mutations in c-MYC and Pten in prostate cancer. *PLoS Genet.* **5,** (2009).
30. Teng, M. W. L., Swann, J. B., Koebel, C. M., Schreiber, R. D. & Smyth, M. J. Immune-mediated dormancy: an equilibrium with cancer. *J. Leukoc. Biol.* **84,** 988–993 (2008).
31. Smyth, M. J., Dunn, G. P. & Schreiber, R. D. Cancer Immunosurveillance and Immunoediting: The Roles of Immunity in Suppressing Tumor Development and Shaping Tumor Immunogenicity. *Advances in Immunology* **90,** 1–50 (2006).
32. Strauss, D. C. & Thomas, J. M. Transmission of donor melanoma by organ transplantation. *The Lancet Oncology* **11,** 790–796 (2010).
33. Pagès, F. *et al.* Immune infiltration in human tumors: a prognostic factor that should not be ignored. *Oncogene* **29,** 1093–1102 (2010).
34. Negrini, S., Gorgoulis, V. G. & Halazonetis, T. D. Genomic instability — an evolving hallmark of cancer. *Nat. Rev. Mol. Cell Biol.* **11,** 220–228 (2010).
35. Shen, Z. Genomic instability and cancer: An introduction. *Journal of Molecular Cell Biology* **3,** 1–3 (2011).
36. Abbas, T., Keaton, M. A. & Dutta, A. Genomic Instability in Cancer. *Cold Spring Harb Perspect Biol* **5,** 1–18 (2013).
37. Barnes, D. E. & Lindahl, T. Repair and Genetic Consequences of Endogenous DNA Base Damage in Mammalian Cells. *Annu. Rev. Genet.* **38,** 445–476 (2004).
38. Artandi, S. E. & DePinho, R. A. Telomeres and telomerase in cancer. *Carcinogenesis* **31,** 9–18 (2009).
39. Dvorak, H. F. Tumors: wounds that do not heal. Similarities between tumor stroma generation and wound healing. *N. Engl. J. Med.* **315,** 1650–9 (1986).
40. Grivennikov, S. I., Greten, F. R. & Karin, M. Immunity, Inflammation, and Cancer. *Cell* **140,** 883–899 (2010).

41. Colotta, F., Allavena, P., Sica, A., Garlanda, C. & Mantovani, A. Cancer-related inflammation, the seventh hallmark of cancer: Links to genetic instability. *Carcinogenesis* **30,** 1073–1081 (2009).
42. Herranz, H., Eichenlaub, T. & Cohen, S. M. Cancer in Drosophila: Imaginal Discs as a Model for Epithelial Tumor Formation. in *Current topics in developmental biology* **116,** 181–99 (2016).
43. Sonoshita, M. & Cagan, R. L. Modeling Human Cancers in Drosophila. in *Current topics in developmental biology* **121,** 287–309 (2017).
44. Tapon, N. Modeling transformation and metastasis in Drosophila. *Cancer Cell* **4,** 333–335 (2003).
45. Gateff, E. Malignant neoplasms of genetic origin in Drosophila melanogaster. *Science (80-.).* **200,** 1448–1459 (1978).
46. Bilder, D. Epithelial polarity and proliferation control: Links from the Drosophila neoplastictumor suppressors. *Genes Dev.* **18,** 1909–1925 (2004).
47. Hales, K. G., Korey, C. A., Larracuente, A. M. & Roberts, D. M. Genetics on the fly: A primer on the drosophila model system. *Genetics* **201,** 815–842 (2015).
48. Brumby, A. M. & Richardson, H. E. Using Drosophila melanogaster to map human cancer pathways. *Nat. Rev. Cancer* **5,** 626–639 (2005).
49. Truman, J. W. Metamorphosis of the central nervous system of Drosophila. *J. Neurobiol.* **21,** 1072–1084 (1990).
50. Strausfeld, N. J. *Atlas of an Insect Brain*. *Springer* **52,** (1976).
51. Egger, B., Boone, J. Q., Stevens, N. R., Brand, A. H. & Doe, C. Q. Regulation of spindle orientation and neural stem cell fate in the Drosophila optic lobe. *Neural Dev.* **2,** (2007).
52. Bello, B. C., Izergina, N., Caussinus, E. & Reichert, H. Amplification of neural stem cell proliferation by intermediate progenitor cells in Drosophila brain development. *Neural Dev.* **3,** 5 (2008).
53. Boone, J. Q. & Doe, C. Q. Identification of Drosophila type II neuroblast lineages containing transit amplifying ganglion mother cells. *Dev. Neurobiol.* **68,** 1185–1195 (2008).
54. Brand, A. H. & Livesey, F. J. Neural Stem Cell Biology in Vertebrates and Invertebrates: More Alike than Different? *Neuron* **70,** 719–729 (2011).
55. Bowman, S. K. *et al.* The Tumor Suppressors Brat and Numb Regulate Transit-Amplifying Neuroblast Lineages in Drosophila. *Dev. Cell* **14,** 535–546 (2008).
56. Li, S., Wang, H. & Groth, C. Drosophila neuroblasts as a new model for the study of stem cell self-renewal and tumor formation. *Biosci. Rep.* **34,** 401–414 (2014).
57. Henrique, D. & Bally-Cuif, L. A cross-disciplinary approach to understanding neural stem cells in development and disease. *Development* **137,** 1933–8 (2010).
58. Bonini, N. M. & Fortini, M. E. Human neurodegenerative disease modeling using Drosophila. *Annu. Rev. Neurosci.* **26,** 627–656 (2003).
59. Read, R. D., Cavenee, W. K., Furnari, F. B. & Thomas, J. B. A Drosophila model for EGFR-Ras and PI3K-dependent human glioma. *PLoS Genet.* **5,** (2009).
60. Witte, H. T., Jeibmann, A., Klämbt, C. & Paulus, W. Modeling glioma growth and invasion in Drosophila melanogaster. *Neoplasia* **11,** 882–888 (2009).
61. Gont, A. *et al.* PTEN loss represses glioblastoma tumor initiating cell differentiation via

inactivation of Lgl1. *Oncotarget* **4,** 1266–79 (2013).

62. Gont, A. *et al.* Inhibition of glioblastoma malignancy by Lgl1. *Oncotarget* **5,** 11541–51 (2014).
63. Paglia, S. *et al.* Failure of the PTEN/aPKC/Lgl Axis Primes Formation of Adult Brain Tumours in Drosophila. *BMRI, InPress*
64. Harbecke, R. *et al.* Larval and imaginal pathways in early development of Drosophila. *Int. J. Dev. Biol.* **40,** 197–204 (1996).
65. Baker, N. E. Patterning signals and proliferation in Drosophila imaginal discs. *Curr. Opin. Genet. Dev.* **17,** 287–293 (2007).
66. Bryant, P. J. Pattern formation in the imaginal wing disc of Drosophila melanogaster: Fate map, regeneration and duplication. *J. Exp. Zool.* **193,** 49–77 (1975).
67. Aldaz, S. & Escudero, L. M. Imaginal discs. *Curr. Biol.* **20,** 429–431 (2010).
68. Wodarz, a & Nathke, I. Cell polarity in development and cancer. *Nat. Cell Biol.* **9,** 1016–1024 (2007).
69. Klein, T. Wing disc development in the fly: The early stages. *Curr. Opin. Genet. Dev.* **11,** 470–475 (2001).
70. Cohen, S. M. & Di Nardo, S. Wingless: from embryo to adult. *Trends Genet.* **9,** 189–192 (1993).
71. Cavodeassi, F., Rodríguez, I. & Modolell, J. Dpp signalling is a key effector of the wing-body wall subdivision of the Drosophila mesothorax. *Development* **129,** 3815–3823 (2002).
72. Butler, M. J. *et al.* Discovery of genes with highly restricted expression patterns in the Drosophila wing disc using DNA oligonucleotide microarrays. *Development* **130,** 659–670 (2003).
73. Lawrence, P. A. & Morata, G. Compartments in the wing of Drosophila: A study of the engrailed gene. *Dev. Biol.* **50,** 321–337 (1976).
74. Garcia-Bellido, A., Ripoll, P. & Morata, G. Developmental Compartmentalisation of the Wing Disk of Drosophila. *Nat. New Biol.* **245,** 251–253 (1973).
75. Kim, J. *et al.* Integration of positional signals and regulation of wing formation and identity by Drosophila vestigial gene. *Nature* **382,** 133–138 (1996).
76. Kiecker, C. & Lumsden, A. Compartments and their boundaries in vertebrate brain development. *Nat. Rev. Neurosci.* **6,** 553–564 (2005).
77. Bilder, D., Li, M. & Perrimon, N. Cooperative Regulation of Cell Polarity and Growth by Drosophila Tumor Suppressors. *Science (80-.).* **289,** 113–116 (2000).
78. Grzeschik, N. A., Parsons, L. M. & Richardson, H. E. Lgl, the SWH pathway and tumorigenesis: It's a matter of context & competition! *Cell Cycle* **9,** 3202–3212 (2010).
79. Grifoni, D. *et al.* The human protein Hugl-1 substitutes for Drosophila lethal giant larvae tumour suppressor function in vivo. *Oncogene* **23,** 8688–8694 (2004).
80. Grifoni, D. *et al.* aPKCzeta cortical loading is associated with Lgl cytoplasmic release and tumor growth in Drosophila and human epithelia. *Oncogene* **26,** 5960–5965 (2007).
81. Lelièvre, S. A. Tissue polarity-dependent control of mammary epithelial homeostasis and cancer development: An epigenetic perspective. *Journal of Mammary Gland Biology and Neoplasia* **15,** 49–63 (2010).
82. Etienne-Manneville, S. Polarity proteins in migration and invasion. *Oncogene* **27,** 6970–6980

(2008).

83. Martin-Belmonte, F. & Perez-Moreno, M. Epithelial cell polarity, stem cells and cancer. *Nat. Rev. Cancer* **12,** 23–38 (2012).
84. Cao, F., Miao, Y., Xu, K. & Liu, P. Lethal (2) giant larvae: An indispensable regulator of cell polarity and cancer development. *International Journal of Biological Sciences* **11,** 380–389 (2015).
85. De Lorenzo, C., Strand, D. & Mechler, B. M. Requirement of Drosophila l(2)gl function for survival of the germline cells and organization of the follicle cells in a columnar epithelium during oogenesis. *Int. J. Dev. Biol.* **43,** 207–217 (1999).
86. Lutzelschwab, R. *et al.* A protein product of the Drosophila recessive tumor gene, l (2) gl, potentially has cell adhesion properties. *EMBO J.* **6,** 2856 (1987).
87. Betschinger, J., Eisenhaber, F. & Knoblich, J. A. Phosphorylation-Induced Autoinhibition Regulates the Cytoskeletal Protein Lethal (2) giant larvae. *Curr. Biol.* **15,** 276–282 (2005).
88. Ellenbroek, S. I. J., Iden, S. & Collard, J. G. Cell polarity proteins and cancer. *Semin. Cancer Biol.* **22,** 208–215 (2012).
89. Peng, C. Y., Manning, L., Albertson, R. & Doe, C. Q. The tumour-suppressor genes lgl and dlg regulate basal protein targeting in Drosophila neuroblasts. *Nature* **408,** 596–600 (2000).
90. Wismar, J. *et al.* The Drosophila melanogaster tumor suppressor gene lethal(3)malignant brain tumor encodes a proline-rich protein with a novel zinc finger. *Mech. Dev.* **53,** 141–154 (1995).
91. Woodhouse, E., Hersperger, E. & Shearn, A. Growth, metastasis, and invasiveness of Drosophila tumors caused by mutations in specific tumor suppressor genes. *Dev. Genes Evol.* **207,** 542–550 (1998).
92. Zhang, L., Yue, T. & Jiang, J. Hippo signaling pathway and organ size control. *Fly* **3,** 68–73 (2009).
93. Grzeschik, N. A., Parsons, L. M., Allott, M. L., Harvey, K. F. & Richardson, H. E. Lgl, aPKC, and Crumbs Regulate the Salvador/Warts/Hippo Pathway through Two Distinct Mechanisms. *Curr. Biol.* **20,** 573–581 (2010).
94. Froldi, F. *et al.* Drosophila lethal giant larvae neoplastic mutant as a genetic tool for cancer modeling. *Curr. Genomics* **9,** 147–154 (2008).
95. Sinha, P., Joshi, S., Radhakrishnan, V. & Mishra, A. Developmental effects of l(2)gl4 and l(2)gd recessive oncogenes on imaginal discs of D. melanogaster. *Cell Differ. Dev.* **27,** 175 (1989).
96. Froldi, F. *et al.* The lethal giant larvae tumour suppressor mutation requires dMyc oncoprotein to promote clonal malignancy. *BMC Biol.* **8,** 33 (2010).
97. Morata, G. & Ripoll, P. Minutes: Mutants of Drosophila autonomously affecting cell division rate. *Dev. Biol.* **42,** 211–221 (1975).
98. de la Cova, C., Abril, M., Bellosta, P., Gallant, P. & Johnston, L. A. Drosophila myc regulates organ size by inducing cell competition. *Cell* **117,** 107–116 (2004).
99. Schimanski, C. C. *et al.* Reduced expression of Hugl-1, the human homologue of Drosophila tumour suppressor gene lgl, contributes to progression of colorectal cancer. *Oncogene* **24,** 3100–3109 (2005).
100. Lu, X. *et al.* Aberrant splicing of Hugl-1 is associated with hepatocellular carcinoma progression.

Clin. Cancer Res. **15,** 3287–3296 (2009).

101. Pagliarini, R. A. & Xu, T. A Genetic Screen in Drosophila for Metastatic Behavior. *Science (80-.).* **302,** 1227–1231 (2003).
102. Wu, M., Pastor-Pareja, J. C. & Xu, T. Interaction between RasV12 and scribbled clones induces tumour growth and invasion. *Nature* **463,** 545–548 (2010).
103. Brumby, A. M. & Richardson, H. E. scribble mutants cooperate with oncogenic Ras or Notch to cause neoplastic overgrowth in Drosophila. *EMBO J.* **22,** 5769–5779 (2003).
104. Prober, D. A. & Edgar, B. A. Ras1 Promotes Cellular Growth in the Drosophila Wing. *Cell* **100,** 435–446 (2000).
105. Chen, C.-L., Schroeder, M. C., Kango-Singh, M., Tao, C. & Halder, G. Tumor suppression by cell competition through regulation of the Hippo pathway. *Proc. Natl. Acad. Sci.* **109,** 484–489 (2012).
106. Doggett, K., Grusche, F. A., Richardson, H. E. & Brumby, A. M. Loss of the Drosophila cell polarity regulator Scribbled promotes epithelial tissue overgrowth and cooperation with oncogenic Ras-Raf through impaired Hippo pathway signaling. *BMC Dev. Biol.* **11,** 57 (2011).
107. Menendez, J., Perez-Garijo, A., Calleja, M. & Morata, G. A tumor-suppressing mechanism in Drosophila involving cell competition and the Hippo pathway. *Proc. Natl. Acad. Sci.* **107,** 14651–6 (2010).
108. Elsum, I., Yates, L., Humbert, P. O. & Richardson, H. E. The Scribble–Dlg–Lgl polarity module in development and cancer: from flies to man. *Essays Biochem.* **53,** 141–168 (2012).
109. Fernandez-Medarde, A. & Santos, E. Ras in Cancer and Developmental Diseases. *Genes Cancer* **2,** 344–358 (2011).
110. Di Giacomo, S. *et al.* Human Cancer Cells Signal Their Competitive Fitness Through MYC Activity. *Sci. Rep.* **7,** 12568 (2017).
111. Igaki, T., Pagliarini, R. A. & Xu, T. Loss of Cell Polarity Drives Tumor Growth and Invasion through JNK Activation in Drosophila. *Curr. Biol.* **16,** 1139–1146 (2006).
112. Christofi, T. & Apidianakis, Y. Drosophila and the Hallmarks of Cancer. in *Advances in biochemical engineering/biotechnology* **135,** 79–110 (2013).
113. Hay, B. A. & Guo, M. Coupling cell growth, proliferation, and death: Hippo weighs in. *Dev. Cell* **5,** 361–363 (2003).
114. Martín, F. A., Peréz-Garijo, A. & Morata, G. Apoptosis in Drosophila: Compensatory proliferation and undead cells. *International Journal of Developmental Biology* **53,** 1341–1347 (2009).
115. Brennecke, J., Hipfner, D. R., Stark, A., Russell, R. B. & Cohen, S. M. bantam encodes a developmentally regulated microRNA that controls cell proliferation and regulates the proapoptotic gene hid in Drosophila. *Cell* **113,** 25–36 (2003).
116. Hipfner, D. R., Weigmann, K. & Cohen, S. M. The bantam gene regulates Drosophila growth. *Genetics* **161,** 1527–1537 (2002).
117. Bergmann, A., Agapite, J., McCall, K. & Steller, H. The Drosophila gene hid is a direct molecular target of ras-dependent survival signaling. *Cell* **95,** 331–341 (1998).
118. Herranz, H., Hong, X. & Cohen, S. M. Mutual repression by bantam miRNA and capicua links the EGFR/MAPK and hippo pathways in growth control. *Curr. Biol.* **22,** 651–657 (2012).

119. Uhlirova, M. & Bohmann, D. JNK- and Fos-regulated Mmp1 expression cooperates with Ras to induce invasive tumors in Drosophila. *EMBO J.* **25,** 5294–5304 (2006).

120. Bangi, E., Pitsouli, C., Rahme, L. G., Cagan, R. & Apidianakis, Y. Immune response to bacteria induces dissemination of Ras-activated Drosophila hindgut cells. *EMBO Rep.* **13,** 569–576 (2012).

121. Titen, S. W. A. & Golic, K. G. Telomere loss provokes multiple pathways to apoptosis and produces genomic instability in Drosophila melanogaster. *Genetics* **180,** 1821–1832 (2008).

122. Dekanty, A., Barrio, L., Muzzopappa, M., Auer, H. & Milan, M. Aneuploidy-induced delaminating cells drive tumorigenesis in Drosophila epithelia. *Proc. Natl. Acad. Sci.* **109,** 20549–20554 (2012).

123. Dekanty, A., Barrio, L. & Milán, M. Contributions of DNA repair, cell cycle checkpoints and cell death to suppressing the DNA damage-induced tumorigenic behavior of Drosophila epithelial cells. *Oncogene* **34,** 978–985 (2015).

124. Ohm, J. E. *et al.* A stem cell-like chromatin pattern may predispose tumor suppressor genes to DNA hypermethylation and heritable silencing. *Nat. Genet.* **39,** 237–242 (2007).

125. Zhang, C., Liu, B., Li, G. & Zhou, L. Extra sex combs, chromatin, and cancer: Exploring epigenetic regulation and tumorigenesis in Drosophila. *Journal of Genetics and Genomics* **38,** 453–460 (2011).

126. Oldham, S. & Hafen, E. Insulin/IGF and target of rapamycin signaling : a TOR de force in growth control. *Trends Cell Biol.* **13,** 79–85 (2003).

127. Britton, J. S., Lockwood, W. K., Li, L., Cohen, S. M. & Edgar, B. A. Drosophila's insulin/PI3-kinase pathway coordinates cellular metabolism with nutritional conditions. *Dev. Cell* **2,** 239–249 (2002).

128. Géminard, C., Rulifson, E. J. & Léopold, P. Remote Control of Insulin Secretion by Fat Cells in Drosophila. *Cell Metab.* **10,** 199–207 (2009).

129. Hirabayashi, S., Baranski, T. & Cagan, R. Transformed Drosophila Cells Evade Diet-Mediated Insulin Resistance through Wingless Signaling. *Cell* **154,** 664–675 (2013).

130. del Pozo Martin, Y. *et al.* Mesenchymal Cancer Cell-Stroma Crosstalk Promotes Niche Activation, Epithelial Reversion, and Metastatic Colonization. *Cell Rep.* **13,** 2456–2469 (2015).

131. Herranz, H., Weng, R. & Cohen, S. M. Crosstalk between epithelial and mesenchymal tissues in tumorigenesis and imaginal disc development. *Curr. Biol.* **24,** 1476–1484 (2014).

132. Pastor-Pareja, J. C., Wu, M. & Xu, T. An innate immune response of blood cells to tumors and tissue damage in Drosophila. *Dis. Model. Mech.* **1,** 144–154 (2008).

133. Cordero, J. B. *et al.* Oncogenic ras diverts a host TNF tumor suppressor activity into tumor promoter. *Dev. Cell* **18,** 999–1011 (2010).

134. Diwanji, N. & Bergmann, A. The beneficial role of extracellular reactive oxygen species in apoptosis-induced compensatory proliferation. *Fly* **11,** 46–52 (2017).

135. Muñoz-Chápuli, R. Evolution of angiogenesis. *Int. J. Dev. Biol.* **55,** 345–351 (2011).

136. Grifoni, D., Sollazzo, M., Fontana, E., Froldi, F. & Pession, A. Multiple strategies of oxygen supply in Drosophila malignancies identify tracheogenesis as a novel cancer hallmark. *Sci. Rep.* **5,** 9061 (2015).

137. Calleja, M., Morata, G. & Casanova, J. Tumorigenic Properties of Drosophila Epithelial Cells

Mutant for lethal giant larvae. *Dev. Dyn.* **245,** 834–843 (2016).

138. Di Giacomo, S., Sollazzo, M., Paglia, S. & Grifoni, D. MYC, Cell Competition, and Cell Death in Cancer: The Inseparable Triad. *Genes (Basel)*. **8,** 120 (2017).
139. de la Cova, C. & Johnston, L. A. Myc in model organisms: A view from the flyroom. *Seminars in Cancer Biology* **16,** 303–312 (2006).
140. Conacci-Sorrell, M., McFerrin, L. & Eisenman, R. N. An overview of MYC and its interactome. *Cold Spring Harbor perspectives in medicine* **4,** (2014).
141. Lindsley, D. L. & Zimm, G. G. *The genome of Drosophila melanogaster*. *Annual Review of Genomics and Human Genetics* **4,** (1992).
142. Gallant, P., Shiio, Y., Cheng, P. F., Parkhurst, S. M. & Eisenman, R. N. Myc and Max Homologs in Drosophila. *Science (80-.).* **274,** 1523–1527 (1996).
143. Loo, L. W. M. *et al.* The transcriptional repressor dMnt is a regulator of growth in Drosophila melanogaster. *Mol. Cell. Biol.* **25,** 7078–91 (2005).
144. Trumpp, A. *et al.* C-Myc regulates mammalian body size by controlling cell number but not cell size. *Nature* **414,** 768–773 (2001).
145. Pierce, S. *et al.* dMyc is required for larval growth and endoreplication in Drosophila. *Development* **131,** 2317–2327 (2004).
146. Johnston, L. a, Prober, D. a, Edgar, B. a, Eisenman, R. N. & Gallant, P. Drosophila myc regulates cellular growth during development. *Cell* **98,** 779–90 (1999).
147. Moberg, K. H., Mukherjee, A., Veraksa, A., Artavanis-Tsakonas, S. & Hariharan, I. K. The Drosophila F box protein archipelago regulates dMyc protein levels in vivo. *Curr. Biol.* **14,** 965–974 (2004).
148. Grewal, S. S., Li, L., Orian, A., Eisenman, R. N. & Edgar, B. A. Myc-dependent regulation of ribosomal RNA synthesis during Drosophila development. *Nat. Cell Biol.* **7,** 295–302 (2005).
149. Teleman, A. A., Hietakangas, V., Sayadian, A. C. & Cohen, S. M. Nutritional Control of Protein Biosynthetic Capacity by Insulin via Myc in Drosophila. *Cell Metab.* **7,** 21–32 (2008).
150. Parisi, F. *et al.* Drosophila insulin and target of rapamycin (TOR) pathways regulate GSK3 beta activity to control Myc stability and determine Myc expression in vivo. *BMC Biol.* **9,** 65 (2011).
151. Li, L., Edgar, B. A. & Grewal, S. S. Nutritional control of gene expression in Drosophila larvae via TOR, Myc and a novel cis-regulatory element. *BMC Cell Biol.* **11,** 7 (2010).
152. Delanoue, R., Slaidina, M. & Léopold, P. The steroid hormone ecdysone controls systemic growth by repressing dMyc function in drosophila fat cells. *Dev. Cell* **18,** 1012–1021 (2010).
153. Neto-Silva, R. M., de Beco, S. & Johnston, L. A. Evidence for a Growth-Stabilizing Regulatory Feedback Mechanism between Myc and Yorkie, the Drosophila Homolog of Yap. *Dev. Cell* **19,** 507–520 (2010).
154. Ziosi, M. *et al.* dMyc functions downstream of yorkie to promote the supercompetitive behavior of hippo pathway mutant Cells. *PLoS Genet.* **6,** (2010).
155. Halder, G. & Johnson, R. L. Hippo signaling: growth control and beyond. *Development* **138,** 9–22 (2011).
156. Levens, D. Cellular MYCro economics: Balancing MYC function with MYC expression. *Cold*

Spring Harb. Perspect. Med. **3,** (2013).

157. Montero, L., Müller, N. & Gallant, P. Induction of apoptosis by Drosophila myc. *Genesis* **46,** 104–111 (2008).
158. Yoo, S. J. *et al.* Hid, Rpr and Grim negatively regulate DIAP1 levels through distinct mechanisms. *Nat. Cell Biol.* **4,** 416–424 (2002).
159. Meier, P., Silke, J., Leevers, S. J. & Evan, G. I. The Drosophila caspase DRONC is regulated by DIAP1. *EMBO J.* **19,** 598–611 (2000).
160. Strasser, A., Harris, A. W., Bath, M. L. & Cory, S. Novel primitive lymphoid tumours induced in transgenic mice by cooperation between myc and bcl-2. *Nature* **348,** 331–333 (1990).
161. Knezevich, S. *et al.* Concurrent translocation of BCL2 and MYC with a single immunoglobulin locus in high-grade B-cell lymphomas. *Leukemia* **19,** 659–663 (2005).
162. Zhang, X.-Y. *et al.* Inhibition of the single downstream target BAG1 activates the latent apoptotic potential of MYC. *Mol. Cell. Biol.* **31,** 5037–45 (2011).
163. Marygold, S. J. *et al.* The ribosomal protein genes and Minute loci of Drosophila melanogaster. *Genome Biol.* **8,** R216 (2007).
164. Simpson, P. Parameters of cell competition in the compartments of the wing disc of Drosophila. *Dev. Biol.* **69,** 182–193 (1979).
165. Moreno, E., Basler, K. & Morata, G. Cells compete for Decapentaplegic survival factor to prevent apoptosis in Drosophila wing development. *Nature* **416,** 755–759 (2002).
166. Moreno, E. & Basler, K. dMyc transforms cells into super-competitors. *Cell* **117,** 117–129 (2004).
167. Senoo-Matsuda, N. & Johnston, L. a. Soluble factors mediate competitive and cooperative interactions between cells expressing different levels of Drosophila Myc. *PNAS* **104,** 18543–18548 (2007).
168. Rhiner, C. *et al.* Flower forms an extracellular code that reveals the fitness of a cell to its neighbors in Drosophila. *Dev. Cell* **18,** 985–998 (2010).
169. Portela, M. *et al.* Drosophila SPARC is a self-protective signal expressed by loser cells during cell competition. *Dev. Cell* **19,** 562–573 (2010).
170. Levayer, R., Hauert, B. & Moreno, E. Cell mixing induced by myc is required for competitive tissue invasion and destruction. *Nature* **524,** 476–80 (2015).
171. Li, W. & Baker, N. E. Engulfment Is Required for Cell Competition. *Cell* **129,** 1215–1225 (2007).
172. Lolo, F. N., Casas-Tintó, S. & Moreno, E. Cell Competition Time Line: Winners Kill Losers, which Are Extruded and Engulfed by Hemocytes. *Cell Rep.* **2,** 526–539 (2012).
173. Casas-Tintó, S., Lolo, F.-N. & Moreno, E. Active JNK-dependent secretion of Drosophila Tyrosyl-tRNA synthetase by loser cells recruits haemocytes during cell competition. *Nat. Commun.* **6,** 10022 (2015).
174. Levayer, R., Dupont, C. & Moreno, E. Tissue Crowding Induces Caspase-Dependent Competition for Space. *Curr. Biol.* **26,** 670–677 (2016).
175. Oliver, E., Saunders, T., Tarlé, S. & Glaser, T. Ribosomal protein L24 defect in Belly spot and tail (Bst), a mouse Minute. *Development* **131,** 3907–3920 (2004).
176. Patel, M., Antala, B. & Shrivastava, N. In silico screening of alleged miRNAs associated with cell

competition: An emerging cellular event in cancer. *Cell. Mol. Biol. Lett.* **20,** 798–815 (2015).

177. Rhiner, C. *et al.* Persistent competition among stem cells and their daughters in the Drosophila ovary germline niche. *Development* **136,** 995–1006 (2009).
178. De La Cova, C. *et al.* Supercompetitor status of drosophila Myc cells requires p53 as a Fitness sensor to reprogram metabolism and promote viability. *Cell Metab.* **19,** 470–483 (2014).
179. Merino, M. M. *et al.* Elimination of unfit cells maintains tissue health and prolongs lifespan. *Cell* **160,** 461–476 (2015).
180. Clavería, C., Giovinazzo, G., Sierra, R. & Torres, M. Myc-driven endogenous cell competition in the early mammalian embryo. *Nature* **500,** 39–44 (2013).
181. Villa Del Campo, C. *et al.* Myc overexpression enhances of epicardial contribution to the developing heart and promotes extensive expansion of the cardiomyocyte population. *Sci. Rep.* **6,** 35366 (2016).
182. Villa del Campo, C., Clavería, C., Sierra, R. & Torres, M. Cell competition promotes phenotypically silent cardiomyocyte replacement in the mammalian heart. *Cell Rep.* **8,** 1741–1751 (2014).
183. Slaughter, D. P., Southwick, H. W. & Smejkal, W. Field Cancerization in Oral Stratified Squamous Epithelium: Clinical Implications of Multicentric Origin. *Cancer* **6,** 963–968 (1953).
184. Rhiner, C. & Moreno, E. Super competition as a possible mechanism to pioneer precancerous fields. *Carcinogenesis* **30,** 723–728 (2009).
185. Moreno, E. Is cell competition relevant to cancer? *Nat. Rev. Cancer* **8,** 141–147 (2008).
186. Dakubo, G. D., Jakupciak, J. P., Birch-Machin, M. A. & Parr, R. L. Clinical implications and utility of field cancerization. *Cancer Cell Int.* **7,** 2 (2007).
187. Leemans, C. R., Braakhuis, B. J. & Brakenhoff, R. H. The molecular biology of head and neck cancer. *Nat. Rev. Cancer* **11,** 9–22 (2011).
188. Braakhuis, B. J. M., Tabor, M. P., Kummer, J. A., Leemans, C. R. & Brakenhoff, R. H. A Genetic Explanation of Slaughter's Concept of Field Cancerization: Evidence and Clinical Implications. *Cancer Res.* **63,** 1727–1730 (2003).
189. Mohan, M. & Jagannathan, N. Oral field cancerization: An update on current concepts. *Oncol. Rev.* **8,** 13–19 (2014).
190. Morata, G. & Ballesteros-Arias, L. Cell competition, apoptosis and tumour development. *Int. J. Dev. Biol.* **59,** 79–86 (2015).
191. Tamori, Y. & Deng, W. M. Cell competition and its implications for development and cancer. *J. Genet. Genomics* **38,** 483–495 (2011).
192. Ballesteros-Arias, L., Saavedra, V. & Morata, G. Cell competition may function either as tumour-suppressing or as tumour-stimulating factor in Drosophila. *Oncogene* **33,** 4377–4384 (2014).
193. Shivas, J. M., Morrison, H. A., Bilder, D. & Skop, A. R. Polarity and endocytosis: Reciprocal regulation. *Trends in Cell Biology* **20,** 445–452 (2010).
194. Menut, L. *et al.* A mosaic genetic screen for Drosophila neoplastic tumor suppressor genes based on defective pupation. *Genetics* **177,** 1667–1677 (2007).
195. Spang, A. On the fate of early endosomes. *Biological Chemistry* **390,** 753–759 (2009).

196. Vaccari, T. & Bilder, D. At the crossroads of polarity, proliferation and apoptosis: The use of Drosophila to unravel the multifaceted role of endocytosis in tumor suppression. *Mol. Oncol.* **3,** 354–365 (2009).

197. Perrimon, N. The maternal effect of lethal(1)discs-large-1: A recessive oncogene of Drosophila melanogaster. *Dev. Biol.* **127,** 392–407 (1988).

198. Gateff, E. Tumor suppressor and overgrowth suppressor genes of Drosophila melanogaster: developmental aspects. *Int. J. Dev. Biol.* **38,** 565–90 (1994).

199. Lu, H. & Bilder, D. Endocytic control of epithelial polarity and proliferation in Drosophila. *Nat. Cell Biol.* **7,** 1132–1139 (2005).

200. Wahlström, T. & Henriksson, M. A. Impact of MYC in regulation of tumor cell metabolism. *Biochim. Biophys. Acta* **1849,** 563–569 (2015).

201. Gurel, B. *et al.* Nuclear MYC protein overexpression is an early alteration in human prostate carcinogenesis. *Mod. Pathol.* **21,** 1156–1167 (2008).

202. Xiong, D. *et al.* Bronchial airway gene expression signatures in mouse lung squamous cell carcinoma and thei modulation by cancer chemopreventive agents. *Oncotarget* **8,** 18885–18900 (2016).

203. Kuzyk, A. & Mai, S. c-MYC-induced genomic instability. *Cold Spring Harb. Perspect. Med.* **4,** (2014).

204. Rockwood, L. D. *et al.* Genomic instability in mouse Burkitt lymphoma is dominated by illegitimate genetic recombinations, not point mutations. *Oncogene* **21,** 7235–7240 (2002).

205. Kuttler, F. & Mai, S. c-Myc, Genomic Instability and Disease. *Genome Dyn.* **1,** 171–90 (2006).

206. Huppi, K., Pitt, J., Wahlberg, B. & Caplen, N. J. Genomic instability and mouse microRNAs. *Toxicol. Mech. Methods* **21,** 325–33 (2011).

207. Huppi, K. *et al.* The Identification of MicroRNAs in a Genomically Unstable Region of Human Chromosome 8q24. *Mol. Cancer Res.* **6,** 212–221 (2008).

208. Greer, C. *et al.* Myc-Dependent Genome Instability and Lifespan in Drosophila. *PLoS One* **8,** (2013).

209. Vafa, O. *et al.* c-Myc can induce DNA damage, increase reactive oxygen species, and mitigate p53 function: A mechanism for oncogene-induced genetic instability. *Mol. Cell* **9,** 1031–1044 (2002).

210. Khanna, K. K. & Jackson, S. P. DNA double-strand breaks: Signaling, repair and the cancer connection. *Nat. Genet.* **27,** 247–254 (2001).

211. Dang, C. V. *et al.* The c-Myc target gene network. *Seminars in Cancer Biology* **16,** 253–264 (2006).

212. Wyllie, A. H. *et al.* Rodent fibroblast tumours expressing human myc and ras genes: Growth, metastasis and endogenous oncogene expression. *Br. J. Cancer* **56,** 251–259 (1987).

213. Neiman, P. E., Thomas, S. J. & Loring, G. Induction of apoptosis during normal and neoplastic B-cell development in the bursa of Fabricius. *Proc. Natl. Acad. Sci. U. S. A.* **88,** 5857–61 (1991).

214. McMahon, S. B. MYC and the control of apoptosis. *Cold Spring Harb. Perspect. Med.* **4,** (2014).

215. Baker, N. E. & Li, W. Cell competition and its possible relation to cancer. *Cancer Res.* **68,** 5505–5507 (2008).

216. Eichenlaub, T., Cohen, S. M. & Herranz, H. Cell competition drives the formation of metastatic tumors in a drosophila model of epithelial tumor formation. *Curr. Biol.* **26,** 419–427 (2016).

217. Suijkerbuijk, S. J. E., Kolahgar, G., Kucinski, I. & Piddini, E. Cell competition drives the growth of intestinal adenomas in Drosophila. *Curr. Biol.* **26,** 428–438 (2016).

218. Dotto, G. P. Multifocal epithelial tumors and field cancerization: Stroma as a primary determinant. *J. Clin. Invest.* **124,** 1446–1453 (2014).

219. Sears, R. *et al.* Multiple Ras-dependent phosphorylation pathways regulate Myc protein stability. *Genes Dev.* **14,** 2501–2514 (2000).

220. Gustafson, A. M. *et al.* Airway PI3K pathway activation is an early and reversible event in lung cancer development. *Sci. Transl. Med.* **2,** 26ra25 (2010).

221. Dronamraju, R. & Mason, J. M. MU2 and HP1a regulate the recognition of double strand breaks in Drosophila melanogaster. *PLoS One* **6,** (2011).

222. Sakai, A., Schwartz, B. E., Goldstein, S. & Ahmad, K. Transcriptional and Developmental Functions of the H3.3 Histone Variant in Drosophila. *Curr. Biol.* **19,** 1816–1820 (2009).

223. Kamakaka, R. T. & Biggins, S. Histone variants: Deviants? *Genes and Development* **19,** 295–310 (2005).

224. Leevers, S. J., Weinkove, D., MacDougall, L. K., Hafen, E. & Waterfield, M. D. The Drosophila phosphoinositide 3-kinase Dp110 promotes cell growth. *EMBO J.* **15,** 6584–6594 (1996).

225. Owusu-Ansah, E., Yavari, A. & Banerjee, U. A protocol for in vivo detection of reactive oxygen species. *Protoc. Exch.* (2008). doi:10.1038/nprot.2008.23

226. Hariharan, I. K. & Bilder, D. Regulation of imaginal disc growth by tumor-suppressor genes in Drosophila. *Annu. Rev. Genet.* **40,** 335–361 (2006).

227. Brand, A. H. & Perrimon, N. Targeted gene expression as a means of altering cell fates and generating dominant phenotypes. *Development* **118,** 401–15 (1993).

228. Xu, T. & Rubin, G. M. Analysis of genetic mosaics in developing and adult Drosophila tissues. *Development* **117,** 1223–1237 (1993).

229. Perrimon, N. Creating mosaics in Drosophila. *Int. J. Dev. Biol.* **42,** 243–247 (1998).

230. Ma, X. *et al.* Hippo signaling promotes JNK-dependent cell migration. *Proc. Natl. Acad. Sci. U. S. A.* 201621359 (2017). doi:10.1073/pnas.1621359114

231. Zygulska, A. L., Krzemieniecki, K. & Pierzchalski, P. Hippo pathway - brief overview of its relevance in cancer. *Journal of Physiology and Pharmacology* **68,** 311–335 (2017).

232. Wei, X., Shimizu, T. & Lai, Z. C. Mob as tumor suppressor is activated by Hippo kinase for growth inhibition in Drosophila. *EMBO J.* **26,** 1772–1781 (2007).

233. Wu, S., Huang, J., Dong, J. & Pan, D. hippo encodes a Ste-20 family protein kinase that restricts cell proliferation and promotes apoptosis in conjunction with salvador and warts. *Cell* **114,** 445–456 (2003).

234. Dong, J. *et al.* Elucidation of a Universal Size-Control Mechanism in Drosophila and Mammals. *Cell* **130,** 1120–1133 (2007).

235. Oh, H. & Irvine, K. D. In vivo analysis of Yorkie phosphorylation sites. *Oncogene* **28,** 1916–1927 (2009).

236. Oh, H. & Irvine, K. D. In vivo regulation of Yorkie phosphorylation and localization. *Development* **135,** 1081–1088 (2008).

237. Grusche, F. A., Richardson, H. E. & Harvey, K. F. Upstream regulation of the Hippo size control pathway. *Curr. Biol.* **20,** 574–582 (2010).

238. Sun, S., Reddy, B. V. V. G. & Irvine, K. D. Localization of Hippo signalling complexes and Warts activation in vivo. *Nat. Commun.* **6,** (2015).

239. Sun, G. & Irvine, K. D. Regulation of Hippo signaling by Jun kinase signaling during compensatory cell proliferation and regeneration, and in neoplastic tumors. *Dev. Biol.* **350,** 139–151 (2011).

240. Sun, G. & Irvine, K. D. Ajuba family proteins link JNK to Hippo signaling. *Sci Signal* **6,** ra81 (2013).

241. Grifoni, D., Froldi, F. & Pession, A. Connecting epithelial polarity, proliferation and cancer in Drosophila: The many faces of lgl loss of function. *Int. J. Dev. Biol.* **57,** 677–687 (2013).

242. Creasy, C. L. & Chernoff, J. Cloning and characterization of a member of the MST subfamily of Ste20-like kinases. *Gene* **167,** 303–306 (1995).

243. Tapon, N. *et al.* salvador promotes both cell cycle exit and apoptosis in Drosophila and is mutated in human cancer cell lines. *Cell* **110,** 467–478 (2002).

244. Tao, W. *et al.* Human homologue of the Drosophila melanogaster lats tumour suppressor modulates CDC2 activity. *Nat. Genet.* **21,** 177–181 (1999).

245. Yabuta, N. *et al.* Structure, Expression, and Chromosome Mapping of LATS2, a Mammalian Homologue of the Drosophila Tumor Suppressor Gene lats/warts. *Genomics* **63,** 263–270 (2000).

246. Bichsel, S. J., Tamaskovic, R., Stegert, M. R. & Hemmings, B. A. Mechanism of activation of NDR (nuclear Dbf2-related) protein kinase by the hMOB1 protein. *J. Biol. Chem.* **279,** 35228–35235 (2004).

247. Chow, A., Hao, Y. & Yang, X. Molecular characterization of human homologs of yeast MOB1. *Int. J. Cancer* **126,** 2079–2089 (2010).

248. Stavridi, E. S. *et al.* Crystal structure of a human Mob1 protein: Toward understanding Mob-regulated cell cycle pathways. *Structure* **11,** 1163–1170 (2003).

249. Kanai, F. *et al.* TAZ: A novel transcriptional co-activator regulated by interactions with 14-3-3 and PDZ domain proteins. *EMBO J.* **19,** 6778–6791 (2000).

250. Sudol, M. Yes-associated protein (YAP65) is a proline-rich phosphoprotein that binds to the SH3 domain of the Yes proto-oncogene product. *Oncogene* **9,** 2145–52 (1994).

251. Chan, S. W. *et al.* The hippo pathway in biological control and cancer development. *Journal of Cellular Physiology* **226,** 928–939 (2011).

252. Tumaneng, K., Russell, R. C. & Guan, K. L. Organ size control by Hippo and TOR pathways. *Current Biology* **22,** (2012).

253. Huang, J., Wu, S., Barrera, J., Matthews, K. & Pan, D. The Hippo signaling pathway coordinately regulates cell proliferation and apoptosis by inactivating Yorkie, the Drosophila homolog of YAP. *Cell* **122,** 421–434 (2005).

254. Zhang, N. *et al.* The Merlin/NF2 Tumor Suppressor Functions through the YAP Oncoprotein to Regulate Tissue Homeostasis in Mammals. *Dev. Cell* **19,** 27–38 (2010).

255. Goulev, Y. *et al.* SCALLOPED Interacts with YORKIE, the Nuclear Effector of the Hippo Tumor-Suppressor Pathway in Drosophila. *Curr. Biol.* **18,** 435–441 (2008).

256. Wu, S., Liu, Y., Zheng, Y., Dong, J. & Pan, D. The TEAD/TEF family protein Scalloped mediates transcriptional output of the Hippo growth-regulatory pathway. *Dev. Cell* **14,** 388–398 (2008).

257. Zhao, B. *et al.* TEAD mediates YAP-dependent gene induction and growth control. *Genes Dev.* **22,** 1962–1971 (2008).

258. Zhang, L. *et al.* The TEAD/TEF family of transcription factor Scalloped mediates Hippo signaling in organ size control. *Dev. Cell* **14,** 377–387 (2008).

259. Peng, H. W., Slattery, M. & Mann, R. S. Transcription factor choice in the Hippo signaling pathway: Homothorax and yorkie regulation of the microRNA bantam in the progenitor domain of the Drosophila eye imaginal disc. *Genes Dev.* **23,** 2307–2319 (2009).

260. Oh, H. & Irvine, K. D. Cooperative Regulation of Growth by Yorkie and Mad through bantam. *Dev. Cell* **20,** 109–122 (2011).

261. Pantalacci, S., Tapon, N. & Léopold, P. The salvador partner Hippo promotes apoptosis and cell-cycle exit in Drosophila. *Nat. Cell Biol.* **5,** 921–927 (2003).

262. Harvey, K. F., Pfleger, C. M. & Hariharan, I. K. The Drosophila Mst ortholog, hippo, restricts growth and cell proliferation and promotes apoptosis. *Cell* **114,** 457–467 (2003).

263. Pylayeva-Gupta, Y., Grabocka, E. & Bar-Sagi, D. RAS oncogenes: weaving a tumorigenic web. *Nat. Rev. Cancer* **11,** 761–774 (2011).

264. Neuman-Silberberg, F., Schejter, E., Hoffmann, M. & Shilo, B. Z. The drosophila ras oncogenes: Structure and nucleotide sequence. *Cell* **37,** 1027–1033 (1984).

265. Rajalingam, K., Schreck, R., Rapp, U. R. & Albert, ??tefan. Ras oncogenes and their downstream targets. *Biochimica et Biophysica Acta - Molecular Cell Research* **1773,** 1177–1195 (2007).

266. Repasky, G. A., Chenette, E. J. & Der, C. J. Renewing the conspiracy theory debate: Does Raf function alone to mediate Ras oncogenesis? *Trends in Cell Biology* **14,** 639–647 (2004).

267. Liu, P., Cheng, H., Roberts, T. M. & Zhao, J. J. Targeting the phosphoinositide 3-kinase (PI3K) pathway in cancer. *Nat. Rev. Drug. Discov.* **8,** 627–644 (2009).

268. Sturtevant, M. A., Roark, M. & Bier, E. The Drosophila rhomboid gene mediates the localized formation of wing veins and interacts genetically with components of the EGF-R signaling pathway. *Genes Dev.* **7,** 961–973 (1993).

269. Pascual, J. *et al.* Hippo Reprograms the Transcriptional Response to Ras Signaling. *Dev. Cell* **42,** 667–680.e4 (2017).

270. Karim, F. D. & Rubin, G. M. Ectopic expression of activated Ras1 induces hyperplastic growth and increased cell death in Drosophila imaginal tissues. *Development* **125,** 1–9 (1998).

271. Kurada, P. & White, K. Ras promotes cell survival in Drosophila by downregulating hid expression. *Cell* **95,** 319–329 (1998).

272. Petit, V., Ribeiro, C., Ebner, A. & Affolter, M. Regulation of cell migration during tracheal development in Drosophila melanogaster. *Int. J. Dev. Biol.* **46,** 125–132 (2002).

273. Weston, C. R. & Davis, R. J. The JNK signal transduction pathway. *Current Opinion in Cell Biology* **19,** 142–149 (2007).

274. Stronach, B. Dissecting JNK signaling, one KKKinase at a time. *Developmental Dynamics* **232,** 575–584 (2005).

275. Kockel, L., Homsy, J. G. & Bohmann, D. Drosophila AP-1: Lessons from an invertebrate. *Oncogene* **20,** 2347–2364 (2001).

276. Sluss, H. K. *et al.* A JNK signal transduction pathway that mediates morphogenesis and an immune response in Drosophila. *Genes Dev.* **10,** 2745–2758 (1996).

277. Glise, B., Bourbon, H. & Noselli, S. hemipterous encodes a novel drosophila MAP kinase kinase, required for epithelial cell sheet movement. *Cell* **83,** 451–461 (1995).

278. Holland, P. M., Suzanne, M., Campbell, J. S., Noselli, S. & Cooper, J. A. MKK7 is a stress-activated mitogen-activated protein kinase kinase functionally related to hemipterous. *J. Biol. Chem.* **272,** 24994–24998 (1997).

279. Chen, W., White, M. A. & Cobb, M. H. Stimulus-specific requirements for MAP3 kinases in activating the JNK pathway. *J. Biol. Chem.* **277,** 49105–49110 (2002).

280. Stronach, B. & Perrimon, N. Activation of the JNK pathway during dorsal closure in Drosophila requires the mixed lineage kinase, slipper. *Genes Dev.* **16,** 377–387 (2002).

281. Teramoto, H. *et al.* The small GTP-binding protein Rho activates c-Jun N-terminal kinases/stress-activated protein kinases in human kidney 293T cells. Evidence for a Pak-independent signaling pathway. *J. Biol. Chem.* **271,** 25731–25734 (1996).

282. Su, Y. C., Treisman, J. E. & Skolnik, E. Y. The Drosophila Ste20-related kinase misshapen is required for embryonic dorsal closure and acts through a JNK MAPK module on an evolutionarily conserved signaling pathway. *Genes Dev.* **12,** 2371–2380 (1998).

283. Liu, H., Su, Y. C., Becker, E., Treisman, J. & Skolnik, E. Y. A Drosophila TNF-receptor-associated factor (TRAF) binds the Ste20 kinase Misshapen and activates Jun kinase. *Curr. Biol.* **9,** 101–104 (1999).

284. Martín-Blanco, E. *et al.* puckered encodes a phosphatase that mediates a feedback loop regulating JNK activity during dorsal closure in Drosophila. *Genes Dev.* **12,** 557–670 (1998).

285. White, K. *et al.* Genetic control of programmed cell death in Drosophila. *Science (80-.).* **264,** 677–83 (1994).

286. Martin, S. J. Destabilizing influences in apoptosis: Sowing the seeds of IAP destruction. *Cell* **109,** 793–796 (2002).

287. Kuranaga, E. *et al.* Reaper-mediated inhibition of DIAP1-induced DTRAF1 degradation results in activation of JNK in Drosophila. *Nat. Cell Biol.* **4,** 705–710 (2002).

288. Moreno, E., Yan, M. & Basler, K. Evolution of TNF signaling mechanisms: JNK-dependent apoptosis triggered by Eiger, the Drosophila homolog of the TNF superfamily. *Curr. Biol.* **12,** 1263–1268 (2002).

289. McEwen, D. G. Puckered, a Drosophila MAPK phosphatase, ensures cell viability by antagonizing JNK-induced apoptosis. *Development* **132,** 3935–3946 (2005).

290. Igaki, T. *et al.* Eiger, a TNF superfamily ligand that triggers the Drosophila JNK pathway. *EMBO J.* **21,** 3009–3018 (2002).

291. Lee, J. H. *et al.* JNK pathway mediates apoptotic cell death induced by tumor suppressor LKB1 in

Drosophila. *Cell Death Differ.* **13,** 1110–1122 (2006).

292. Luo, X., Puig, O., Hyun, J., Bohmann, D. & Jasper, H. Foxo and Fos regulate the decision between cell death and survival in response to UV irradiation. *EMBO J.* **26,** 380–390 (2007).

293. Griswold, A. J., Chang, K. T., Runko, A. P., Knight, M. A. & Min, K.-T. Sir2 mediates apoptosis through JNK-dependent pathways in Drosophila. *Proc. Natl. Acad. Sci. U. S. A.* **105,** 8673–8 (2008).

294. Uhlirova, M., Jasper, H. & Bohmann, D. Non-cell-autonomous induction of tissue overgrowth by JNK/Ras cooperation in a Drosophila tumor model. *Proc. Natl. Acad. Sci. U. S. A.* **102,** 13123–13128 (2005).

295. Figueroa-Clarevega, A. & Bilder, D. Malignant drosophila tumors interrupt insulin signaling to induce cachexia-like wasting. *Dev. Cell* **33,** 47–56 (2015).

296. Külshammer, E. *et al.* Interplay among Drosophila transcription factors Ets21c, Fos and Ftz-F1 drives JNK-mediated tumor malignancy. *Dis. Model. Mech.* **8,** 1279–93 (2015).

297. Kulshammer, E. & Uhlirova, M. The actin cross-linker Filamin/Cheerio mediates tumor malignancy downstream of JNK signaling. *J. Cell Sci.* **126,** 927–938 (2013).

298. Ma, X. *et al.* Myc suppresses tumor invasion and cell migration by inhibiting JNK signaling. *Oncogene* **36,** 3159–3167 (2017).

299. Srivastava, A., Pastor-Pareja, J. C., Igaki, T., Pagliarini, R. & Xu, T. Basement membrane remodeling is essential for Drosophila disc eversion and tumor invasion. *Proc. Natl. Acad. Sci.* **104,** 2721–6 (2007).

300. Sun, G. & Irvine, K. D. Regulation of Hippo signaling by Jun kinase signaling during compensatory cell proliferation and regeneration, and in neoplastic tumors. *Dev. Biol.* **350,** 139–151 (2011).

301. Khan, S. J. *et al.* Epithelial neoplasia in Drosophila entails switch to primitive cell states. *Proc. Natl. Acad. Sci. U. S. A.* **110,** E2163-72 (2013).

302. Sollazzo, M. *et al.* Growth and Tracheogenesis are Separable Cancer Traits in Drosophila epithelia. *InPreparation*

303. Enomoto, M., Vaughen, J. & Igaki, T. Non-autonomous overgrowth by oncogenic niche cells: Cellular cooperation and competition in tumorigenesis. *Cancer Sci.* (2015). doi:10.1111/cas.12816

304. Biggs, W. H. *et al.* The Drosophila rolled locus encodes a MAP kinase required in the sevenless signal transduction pathway. *EMBO J.* **13,** 1628–35 (1994).

305. Glasheen, B. M., Robbins, R. M., Piette, C., Beitel, G. J. & Page-McCaw, A. A matrix metalloproteinase mediates airway remodeling in Drosophila. *Dev. Biol.* **344,** 772–783 (2010).

306. Riesgo-Escovar, J. R., Jenni, M., Fritz, A. & Hafen, E. The Drosophila jun-N-terminal kinase is required for cell morphogenesis but not for DJun-dependent cell fate specification in the eye. *Genes Dev.* **10,** 2759–2768 (1996).

307. Pallavi, S. K., Ho, D. M., Hicks, C., Miele, L. & Artavanis-Tsakonas, S. Notch and Mef2 synergize to promote proliferation and metastasis through JNK signal activation in Drosophila. *EMBO J.* **31,** 2895–2907 (2012).

308. Rudrapatna, V. A., Bangi, E. & Cagan, R. L. Caspase signalling in the absence of apoptosis drives Jnk-dependent invasion. *EMBO Rep.* **14,** 172–177 (2013).

309. Meng, Z., Moroishi, T. & Guan, K. Mechanisms of Hippo pathway regulation. *Genes Dev.* **30,** 1–17 (2016).

310. Ehmer, U. & Sage, J. Control of Proliferation and Cancer Growth by the Hippo Signaling Pathway. *Mol. Cancer Res.* **14,** 127–140 (2016).

311. Xiao, W. *et al.* Mutual interaction between YAP and c-Myc is critical for carcinogenesis in liver cancer. *Biochem. Biophys. Res. Commun.* **439,** 167–172 (2013).

312. Reddy, B. V. V. G. & Irvine, K. D. Regulation of Hippo Signaling by EGFR-MAPK Signaling through Ajuba Family Proteins. *Dev. Cell* **24,** 451–471 (2013).

313. Rauskolb, C., Sun, S., Sun, G., Pan, Y. & Irvine, K. D. Cytoskeletal tension inhibits Hippo signaling through an Ajuba-Warts complex. *Cell* **158,** 143–156 (2014).

314. Atkins, M. *et al.* An Ectopic Network of Transcription Factors Regulated by Hippo Signaling Drives Growth and Invasion of a Malignant Tumor Model. *Curr. Biol.* **26,** 2101–2113 (2016).

315. Sears, R., Leone, G., DeGregori, J. & Nevins, J. R. Ras enhances Myc protein stability. *Mol. Cell* **3,** 169–179 (1999).

316. Noguchi, K. *et al.* Regulation of c-Myc through phosphorylation at Ser-62 and Ser-71 by c- Jun N-terminal kinase. *J. Biol. Chem.* **274,** 32580–32587 (1999).

317. Gallant, P. Myc Function in Drosophila. *Cold Spring Harb. Perspect. Med.* **3,** a014324 (2013).

318. Evan, G. I. & Littlewood, T. D. The role of c-myc in cell growth. *Curr. Opin. Genet. Dev.* **3,** 44–49 (1993).

319. Bouchard, C., Staller, P. & Eilers, M. Control of cell proliferation by Myc. *Trends Cell Biol.* **8,** 202–206 (1998).

320. Gabay, M., Li, Y. & Felsher, D. W. MYC Activation Is a Hallmark of Cancer Initiation and Maintenance. *Cold Spring Harb. Perspect Med* **4,** (2014).

321. Li, Y., Casey, S. C. & Felsher, D. W. Inactivation of MYC reverses tumorigenesis. *J. Intern. Med.* **276,** 52–60 (2014).

322. Huang, H., Weng, H., Zhou, H. & Qu, L. Attacking c-Myc: targeted and combined therapies for cancer. *Curr. Pharm. Des.* **20,** 6543–54 (2014).

323. Whitfield, J. R., Beaulieu, M.-E. & Soucek, L. Strategies to Inhibit Myc and Their Clinical Applicability. *Front. Cell Dev. Biol.* **5,** (2017).

324. Ciapponi, L., Jackson, D. B., Mlodzik, M. & Bohmann, D. Drosophila Fos mediates ERK and JNK signals via distinct phosphorylation sites. *Genes Dev.* **15,** 1540–1553 (2001).

325. Zhang, K. *et al.* Oncogenic K-Ras upregulates ITGA6 expression via FOSL1 to induce anoikis resistance and synergizes with αV-Class integrins to promote EMT. *Oncogene* **36,** 5681–5694 (2017).

326. Liu, H. *et al.* MYC suppresses cancer metastasis by direct transcriptional silencing of ?? v and ?? 3 integrin subunits. *Nat. Cell Biol.* **14,** 567–574 (2012).

327. Greaves, M. Cancer's Darwinian dilemma: an evolutionary tale in three acts. *BMJ* **351,** 1–2 (2015).

328. Valastyan, S. & Weinberg, R. A. Tumor metastasis: Molecular insights and evolving paradigms. *Cell* **147,** 275–292 (2011).

329. Farkas, R. & Mechler, B. M. The timing of drosophila salivary gland apoptosis displays an l(2)gl-

dose response. *Cell Death Differ.* **7,** 89–101 (2000).

330. Rolls, M. M., Albertson, R., Shih, H. P., Lee, C. Y. & Doe, C. Q. Drosophila aPKC regulates cell polarity and cell proliferation in neuroblasts and epithelia. *J. Cell Biol.* **163,** 1089–1098 (2003).
331. Lee, T. & Luo, L. Mosaic analysis with a repressible cell marker (MARCM) for Drosophila neural development. *Trends Neurosci.* **24,** 251–254 (2001).
332. Labi, V. & Erlacher, M. How cell death shapes cancer. *Cell Death and Disease* **6,** (2015).
333. Ryoo, H. D., Gorenc, T. & Steller, H. Apoptotic cells can induce compensatory cell proliferation through the JNK and the wingless signaling pathways. *Dev. Cell* **7,** 491–501 (2004).
334. Perez-Garijo, A., Martín, F. & Morata, G. Caspase inhibition during apoptosis causes abnormal signalling and developmental aberrations in Drosophila. *Development* **131,** 5591–5598 (2004).
335. Huh, J. R., Guo, M. & Hay, B. A. Compensatory proliferation induced by cell death in the Drosophila wing disc requires activity of the apical cell death caspase dronc in a nonapoptotic role. *Curr. Biol.* **14,** 1262–1266 (2004).
336. Ford, C. A. *et al.* Oncogenic properties of apoptotic tumor cells in aggressive B cell lymphoma. *Curr. Biol.* **25,** 577–588 (2015).
337. Fulda, S. Targeting apoptosis for anticancer therapy. *Seminars in Cancer Biology* **31,** 84–88 (2015).
338. Egeblad, M., Nakasone, E. S. & Werb, Z. Tumors as organs: Complex tissues that interface with the entire organism. *Dev. Cell* **18,** 884–901 (2010).
339. Pantziarka, P. Emergent properties of a computational model of tumour growth. *PeerJ* **4,** e2176 (2016).
340. Sun, B. *et al.* Extent, relationship and prognostic significance of apoptosis and cell proliferation in synovial sarcoma. *Eur J Cancer Prev* **15,** 258–265 (2006).
341. Jalali Nadoushan, M., Peivareh, H. & Azizzadeh Delshad, A. Correlation between Apoptosis and Histological Grade of Transitional Cell Carcinoma of Urinary Bladder. *Urol. J.* **1,** 177–179 (2004).
342. Naresh, K. N., Lakshminarayanan, K., Pai, S. A. & Borges, A. M. Apoptosis index is a predictor of metastatic phenotype in patients with early stage squamous carcinoma of the tongue: A hypothesis to support this paradoxical association. *Cancer* **91,** 578–584 (2001).
343. Feng, X. *et al.* Dying glioma cells establish a proangiogenic microenvironment through a caspase 3 dependent mechanism. *Cancer Lett.* **385,** 12–20 (2017).
344. Johnston, L. A. Socializing with MYC: Cell competition in development and as a model for premalignant cancer. *Cold Spring Harb. Perspect. Med.* **4,** (2014).
345. Patel, M. S., Shah, H. S. & Shrivastava, N. c-Myc-Dependent Cell Competition in Human Cancer Cells. *J. Cell. Biochem.* **118,** 1782–1791 (2017).
346. Penzo-Méndez, A. I. & Stanger, B. Z. Cell competition in vertebrate organ size regulation. *Wiley Interdisciplinary Reviews: Developmental Biology* **3,** 419–427 (2014).
347. Sancho, M. *et al.* Competitive interactions eliminate unfit embryonic stem cells at the onset of differentiation. *Dev. Cell* **26,** 19–30 (2013).
348. Fuchs, Y. & Steller, H. Live to die another way: Modes of programmed cell death and the signals emanating from dying cells. *Nature Reviews Molecular Cell Biology* **16,** 329–344 (2015).
349. Struhl, G. & Basler, K. Organizing activity of wingless protein in Drosophila. *Cell* **72,** 527–540

(1993).

350. Caserta, T. M., Smith, A. N., Gultice, A. D., Reedy, M. A. & Brown, T. L. Q-VD-OPh, a broad spectrum caspase inhibitor with potent antiapoptotic properties. *Apoptosis* **8,** 345–352 (2003).

351. Schubbert, S., Shannon, K. & Bollag, G. Hyperactive Ras in developmental disorders and cancer. *Nature Reviews Cancer* **7,** 295–308 (2007).

352. Igaki, T. Correcting developmental errors by apoptosis: Lessons from Drosophila JNK signaling. *Apoptosis* **14,** 1021–1028 (2009).